NASA Technical Memorandum 104555

Geopotential Models of the Earth From Satellite Tracking, Altimeter and Surface Gravity Observations: GEM-T3 and GEM-T3S

F.J. Lerch, R.S. Nerem, B.H. Putney, T.L. Felsentreger, B.V. Sanchez, S.M. Klosko, G.B. Patel, R.G. Williamson, D.S. Chinn, J.C. Chan, K.E. Rachlin, N.L. Chandler, J.J. McCarthy, J.A. Marshall, S.B. Luthcke, D.W. Pavlis, J.W. Robbins, S. Kapoor, and E.C. Pavlis

January 1992

NASA

NASA Technical Memorandum 104555

Geopotential Models of the Earth From Satellite Tracking, Altimeter and Surface Gravity Observations: GEM-T3 and GEM-T3S

F.J. Lerch, R.S. Nerem, B.H. Putney, T.L. Felsentreger, B.V. Sanchez
Goddard Space Flight Center
Greenbelt, Maryland

S.M. Klosko, G.B. Patel, R.G. Williamson, D.S. Chinn, J.C. Chan, K.E. Rachlin, N.L. Chandler, J.J. McCarthy, J.A. Marshall, S.B. Luthcke, D.W. Pavlis, J.W. Robbins, S. Kapoor
Hughes STX, Inc.
Lanham, Maryland

E.C. Pavlis,
Astronomy Program
University of Maryland
College Park, Maryland

National Aeronautics and Space Administration

Goddard Space Flight Center
Greenbelt, MD

1992

TABLE OF CONTENTS

LIST OF TABLES

LIST OF ILLUSTRATIONS

ABSTRACT

Improved models of the Earth's gravitational field have been developed from conventional satellite tracking data (GEM-T3S) and from a combination of satellite tracking, satellite altimeter and surface gravimetric data (GEM-T3). This combination model represents a significant improvement in the modeling of the gravity field at half-wavelengths of 350 km and longer. Both models are complete to degree and order 50. The GEM-T3 model provides for more accurate computation of satellite orbital effects as well as giving a superior geoidal representation from that achieved in any previous Goddard Earth Model. A description of the models, their development and an assessment of their accuracy is presented. The GEM-T3 model uses altimeter data from GEOS-3 (1975-76), SEASAT (1978) and GEOSAT (1986-87) to estimate the orbits, geoid, and dynamic height fields. In order to accommodate the non-gravitational signal mapped by these altimeters, spherical harmonic models of the dynamic height of the ocean surface were recovered for each mission simultaneously with the gravitational field. Herein, all of the dynamic height fields are referenced to a common geoid model and are linked to the Conventional Terrestrial Reference System established by Satellite Laser Ranging (SLR).

The tracking data utilized in the solution includes more than 1300 arcs of data encompassing 31 different satellites. The observational data base contains highly precise SLR data, but also includes TRANET Doppler, optical, S-Band average range-rate and satellite-to-satellite tracking acquired between the ATS-6 and GEOS-3 satellites. The tracking data are largely the same as used to develop GEM-T2 with certain important improvements in data treatment and expanded laser coverage.

These models have undergone extensive error calibration and employ an optimal data weighting technique which insures reliable estimates of the models' uncertainties. This method relies on statistical testing using a subset solution technique. The subset solution testing is based on the condition that the expected mean square deviation of a subset gravity solution from the overall solution is predicted by the solutions' error covariances. Data weights are iteratively adjusted until this condition is satisfied. Further gravity field tests were performed where strong satellite data sets were withheld from the solution (thereby insuring their independence) and the performance of the subset models were compared to error projections based on their calibrated error covariances. This testing was made in the space of the observation residuals themselves. These results demonstrate that orbit accuracy projections based on the solution error covariances yield reliable estimates for new satellites which are not in the solution.

1.0 INTRODUCTION

Before the advent of recent space technologies, the nature and relationship of many components of the integrated physical systems on Earth were neither well observed nor well understood. The solid Earth and ocean sciences suffered from incomplete data coverage and poor temporal sampling of global processes. Without the observations provided by satellites, it was difficult to develop a global understanding of the physical systems acting on and within the Earth. Artificial near-Earth satellites introduced dramatic changes within the Earth sciences. In particular, they provided the science of geodesy with a new means of measuring the Earth's gravitational field on global scales. Due to the attenuation of the gravitational field with altitude, the orbital motion evidenced by these satellites provided the means to determine the long-wavelength field to high levels of accuracy. As satellite tracking systems evolved and their deployment improved in geographic distribution, enormous advances were made in modeling this part of the gravitational spectrum. Many research groups have used tracking data to develop spherical harmonic models of the gravity fields since the mid-1960s. This report presents the latest models developed at the NASA/Goddard Space Flight Center.

Another innovation, also fostered by advancing space technologies, has provided the means to determine the oceanic geoid with extremely high accuracy and resolution: spaceborne radar altimeters, from whose measurements the geocentric height of the ocean surface can be deduced on a continuing basis. The oceanic geoid has a ±100m signal which dominates the shape of the mean ocean surface. Satellites have intermittently flown radar altimeters since the 1973 experiment on Skylab. The altimeter ranging acquired by Skylab and, in 1975-78, by GEOS-3, marked the beginning of a new era in physical oceanography and satellite geodesy.

Since Skylab, there have been three "geodetic-class" satellites which have provided global altimeter data. The first, GEOS-3, was placed in a stable orbit; however, it lacked on-board computer memory for data storage, thereby requiring a direct telemetering of the data in near-real time to ground receivers. Telemetry sites were periodically moved so that after approximately a year, a nearly complete mapping of the ocean surface within the latitude bands of the orbital inclination (±65.02 degrees) was achieved. The next NASA altimeter satellite, SEASAT, was launched in 1978. It suffered a catastrophic power failure 3 months into its mission. However, during its short active lifetime, it acquired many complete cycles of altimeter data (between ±72 degrees latitude) as the satellite was in a 17-day followed by a 3-day repeating ground track. The U.S. Navy launched GEOSAT in 1985. This altimeter satellite was maneuvered into a 17-day repeating ground track orbit overflying that of SEASAT (the so-called "Exact Repeat Mission" (ERM)) in November of 1986 which permitted release of subsequent global altimeter data to the civilian science community. More than three years of continuous altimeter observations were acquired by GEOSAT during the ERM phase of its mission before the satellite's failure in early 1990. Altimeter data from each of these geodetic missions have been uniformly processed for inclusion in the GEM-T3 gravity model solution presented in this paper.

Surface gravimetry, a century old method used to measure the local variations in the Earth's gravity field, has also advanced. Measurement modeling, processing, reduction and data verification techniques have improved. The gravity field determined from satellite tracking and altimeter data has provided an independent calibration standard to more fully evaluate these terrestrial observations (Pavlis, 1988). Many of the historic geographic gaps in the data have been filled with newly released data. While these data are characterized by a wide variation in accuracies and coverage, they are becoming more uniform, accurate and better understood with time.

This report describes the next in the series of the Goddard Earth Model (GEM) gravitational models which more fully exploits each of these observational resources. The latest "satellite-only" model, GEM-T3S, is complete to degree and order 50 and uses tracking data acquired on 31

satellites. As will be shown, GEM-T3S is a significant improvement over GEM-T1 and GEM-T2, both for orbit computations and in geoid accuracy. The corresponding comprehensive combination model, GEM-T3, contains the data in GEM-T3S plus satellite altimetry and surface gravimetry. It is also complete to degree and order 50. The "satellite-only" field relies on the earlier GEM-T2 model (Marsh et al., 1990a) with additional periods of tracking for some of the laser satellites and improved environmental correction applied to Doppler data sets. The combination model was developed in a fashion paralleling that of PGS-3337 (Marsh et al., 1990b) which combined GEM-T1 (Marsh et al., 1988) with SEASAT altimeter data and surface gravimetry. The altimeter and surface gravity data treatment issues were previously discussed in the PGS-3337 report and will be reviewed here only as necessary. GEM-T3 combines satellite tracking with altimeter data from GEOS-3, SEASAT and GEOSAT and an advanced set of surface gravity observations.

There is a lingering question which this report will specifically address. Historically there has been a concern as to whether the inclusion of altimeter and surface gravity data in combination models necessitates sacrificing orbital accuracy. There are known unmodeled, non-gravitational long-wavelength signals in the sea surface height mapped by altimeters; the surface gravimetry has irregular data coverage, large regions containing geophysically predicted data and geographically dependent data accuracies. Many of the signals sensed by these data appear to conflict with the more accurate long wavelength gravitational information obtained from tracking data. The proper exploitation of these different types of information in combined solutions is difficult at our current level of modeling. Where common spectral content exists in the data, the competing information of the different data types must be realistically weighted in the combination solution in order to prevent the degradation of otherwise better quality signal.

On the other hand, satellite altimetry and surface gravity data contain a rather direct and unattenuated measure of the short-wavelength geoid. Although they lack complete global coverage and have systematic non-gravitational signals, they represent a source of gravity information which complements that seen in the tracking data. For resolving the gravity model accurately at intermediate and short wavelengths, they are clearly indispensable. This situation is unlikely to change until a dedicated gravitational mission is flown. It will be shown that combination models yield much more accurate global geoid models, especially over areas where these sources of surface information are robust and accurate. Improvements in geoid modeling are a direct result of more accurate global coefficient definition either through the direct contribution of these surface data sources to the definition of the short wavelength gravitational field and through reducing the correlations throughout the whole model (especially within each of its harmonic orders).

Using independent data, we have found that the global improvement in the spherical harmonic coefficients obtained through the inclusion of surface gravimetry and altimeter data in GEM-T3 results in significant orbit determination improvements over those found with the "satellite only" model GEM-T3S. This is notwithstanding the fact that GEM-T3S yields more accurate orbits than those obtained from either GEM-T1 or -T2. Thus, GEM-T3 represents a major advance in the state-of-the-art for orbit modeling from combination gravitational solutions as well as a superior representation of the low- and medium-wavelength geoid. This document sets forth the improvements in our processing which have enabled the computation of this model.

2.0 OBSERVATIONS AND MODELING

2.1 TRACKING OBSERVATION

The GEM-T3S data set is the same as that used for GEM-T2 with a few select changes. It encompasses 31 different satellites which were tracked by optical, TRANET Doppler, laser ranging, satellite-to-satellite range-rate, and S-Band average-range-rate systems (Table 2.1). The observation content of the GEM-T3 solution is shown in Table 2.2. The upgrades made in processing the tracking data since the development of GEM-T2 include:

- The Starlette observations for 1986 were re-analyzed with the data sampled back to match the lower data rate that was used for Starlette during the 1983-4 MERIT Campaign. The normal equations written for Starlette were extended to be complete to degree and order 50.

- An additional year of LAGEOS normal points acquired during 1987 were included.

- Twelve additional Ajisai arcs using data taken during 1987 were generated complete to degree and order 50.

- The S-Band average-range-rate (LANDSAT) and the TRANET Doppler observations (OSCAR-14, GEOSAT, SEASAT, and NOVA-1) were re-analyzed solving for a tropospheric refraction scale parameter for each pass of data. This parameterization significantly reduced the size of the data residuals and gave superior calibration results for these data sets. As a consequence of reducing some of the systematic data errors using these tropospheric scaling parameters, these observations made a more significant contribution to the overall gravity field.

A complete description of the tracking data evaluation which has been employed for the "T" series of the GEM models can be found in Marsh et al., (1987, 1988 and 1990a). A summary of the basic models being applied is presented in Table 2.3, which is reproduced from Marsh et al., (1990a). A typical data reduction strategy is to use data spans of 5-7 days and to adjust one radiation pressure coefficient per arc and one drag coefficient per day in each arc. For Lageos, monthly arcs adjusting two radiation pressure and two along track acceleration parameters are used.

2.2 ALTIMETER DATA

2.2.1 ALTIMETER MODELING

A satellite altimeter maps a complex ocean topography signal. While dominated by the ocean geoid, the sea surface height with respect to a reference ellipsoid also includes the height field due to ocean currents such as geostrophic flow. Furthermore, the ocean surface also exhibits changes in a complex fashion over a large number of wavelengths and timescales, some of which are not well-known or predictable. Nevertheless, the homogeneous mapping of the ocean surface by spaceborne altimeters is an excellent resource for studying the gravity field. Extensive parameterization has been required in the gravity solution to account for and, in some cases, estimate models for these non-gravitational ocean surface signals. The form of this modeling is briefly reviewed.

Table 2.1. Satellite Orbital Characteristics for GEM-T3 Ordered by Inclination

Satellite Name	Semi-major Axis (Km)	Eccentricity	Inclination (Degrees)	Data* Type
ATS-6	41867.	.001	0.9	SST
Peole	7006.	.016	15.0	L,O
Courier 1B	7469.	.016	28.3	O
Vanguard 2	8298.	.164	32.9	O
Vanguard 2RB	8496.	.183	32.9	O
D1-D	7622.	.085	39.5	L,O
D1-C	7341.	.053	40.0	L,O
BE-C	7507.	.026	41.2	L,O
Telestar-1	9669.	.243	44.8	O
Echo-1RB	7966.	.012	47.2	O
Starlette	7331.	.020	49.8	L
Ajisai	7870.	.001	50.0	L
Anna-1B	7501.	.008	50.1	O
GEOS-1	8075.	.072	59.4	L,O
Transit-4A	7322.	.008	66.8	O
Injun-1	7316.	.008	66.8	O
Secor-5	8151.	.079	69.2	O
BE-B	7354.	.014	79.7	O
OGO-2	7341.	.075	87.4	O
OSCAR-7	7440.	.002	89.2	O
OSCAR-14	7448.	.004	89.2	D
5BN-2	7462.	.006	90.0	O
NOVA	7559.	.001	90.0	D
Midas-4	9995.	.011	95.8	O
Landsat-1	7286.	.001	99.1	S
Seasat	7171.	.001	108.0	L,D,A
GEOS-2	7711.	.033	105.8	L,O
Geosat	7169.	.001	108.0	D,A
Lageos	12273.	.001	109.9	L
GEOS-3	7226.	.001	114.9	L,A
OV1-2	8317.	.018	144.3	O

*SST Satellite-to-Satellite Tracking Range Rate
L Laser
O Optical
D TRANET/OPNET Doppler
S S-Band Average Range Rate
A Altimeter

Table 2.2. Tracking Data Summary
GEM T1, T2, T3

Satellite Name	Inclination	Data Type	Number of ARCS GEM-T1	GEM-T2	GEM-T3
ATS-6/GEOS-3	0/115.0	SST	-	26	26
Peole	15.0	L,O	6	6	6
Courier-1B	28.3	O	10	10	10
Vanguard 2	32.9	O	10	10	10
Vanguard 2RB	32.9	O	10	10	10
D1-D	39.5	L,O	15	15	15
D1-C	40.0	L,O	14	14	14
BE-C	41.2	L,O	89	89	89
Telestar-1	44.8	O	30	30	30
Echo-1RB	47.2	O	-	32	32
Starlette	49.8	L	46	157	157
Ajisai	50.0	L	-	36	48
Anna-1B	50.1	O	30	30	30
GEOS-1	59.3	L,O	91	121	121
Transit-4A	66.8	O	-	50	50
Injun-1	66.8	O	-	44	44
Secor-5	69.2	O	-	13	13
BE-B	79.7	O	20	20	20
OGO-2	87.4	O	-	16	16
OSCAR-14	89.2	D	13	13	13
OSCAR-7	89.7	O	-	4	4
5BN-2	90.0	O	-	17	17
NOVA	90.0	D	-	16	16
Midas-4	95.8	O	-	50	50
Landsat-1	98.5	S-B	-	10	10
GEOS-2	105.8	L,O	74	74	74
Seasat	108.0	D,L,A	29	29	39
Geosat	108.0	D,A	-	13	26
Lageos	109.9	L	58	85	97
GEOS-3	114.9	L,A	36	86	162
OV1-2	144.3	O	-	4	4
TOTAL			581	1130	1243

*SST Satellite-to-Satellite Tracking
L Laser ranging
O Optical
D Doppler
S-B United S-Band average range rate
A Altimeter

Table 2.3. Reference Frame Parameters and Constants for GEM-T3 and GEM-T3S

Astronomical Constants	
Speed of Light	299792458 m/s
Equatorial radius of the Earth	6378137 m
Flattening of the Earth	1/298.257
Mean spin rate of Earth	0.00007292115 rad/s
Geocentric Gravitational Constant	398600.436 km^3/s^2
Moon-Earth mass ratio	0.012300034
Astronomical unit	149597870660 m
Sun-Earth mass ratio	332946.038
Dynamical Models	
Static Geopotential	Adjusted, GEM-T1, GEM-T2 and PGS-3520 a priori
Solid Earth Tides	Wahr (1979)
Ocean Tides	GEM-T1 background model with 90 adjusting coefficients
Radiation pressure at 1 AU	0.0000045783 $kg/m/s^2$
• radiation pressure coefficient	adjusted
Atmospheric Drag	Jacchia (1971) and Barlier et al., (1977) with values of F10.7 and Kp flux
• atmospheric drag coefficient	adjusted; nominally once/day
Measurement Models	
Optical Data	
parallactic refraction	Hotter (1968)
annual aberration	"
diurnal aberration	"
precession/nutation of images	Wahr/Lieske
proper motions	Hotter (1968)
satellite clock corrections for active satellites	APL provided values
TRANET Doppler Data	
Time tag correction from WWV	O'Toole (1976)
Tropospheric refraction	Modified Hopfield Model of Goad (Eddy et al., 1989)
Ionospheric refraction	First-order correction obtained from difference of 150- and 400-Mhz freq.
Frequency bias correction	pass-by-pass bias adjustment

Table 2.3. Reference Frame Parameters and Constants for GEM-T3 and GEM-T3S (Continued)

Laser Range Data	
Pre- and post-pass range calibrations	Figgatte and Polesco (1982)
Tropospheric refraction	Marini and Murray (1973)
S-band Average Range-rate Data	
Tropospheric refraction	Modified Hopfield Model of Goad (Eddy et al., 1989)
Ionospheric refraction	none
Antenna axis offset correction for non-az/el mounts	Gross (1968)/Eddy et al., (1989)
Reference System	
CIRS	J2000.0
Planetary Ephemeris	JPL DE200
Terrestrial time scale	UTC (USNO)
Precession	IAU 1976 (Lieske, 1976)
Nutation	IAU 1980 (Wahr, 1979)
CTRS	Lageos global solution SL6 rotated to "zero-mean" system

Within the GEM-T3 solution, the altimeter range is represented by:

$$O = R - (SSH + \Delta R + \varepsilon) + B \qquad \text{(eq. 2.1)}$$

where:

- O is the observed altimeter range corrected for instrument offsets to the satellite center-of-mass.
- R is the distance from the satellite center-of-mass to the surface of the Earth's reference ellipsoid, defined through the orbit determination process.
- SSH is the sea surface height above the reference ellipsoid.
- ΔR are corrections to the measurements which include sea state, atmospheric propagation delay (ionospheric and tropospheric) and attitude induced pointing errors. In several instances we have improved upon the information distributed with the altimeter data on the respective Geophysical Data Records (GDR) for these corrections. For the sea state correction, we employed a linear scaling algorithm based on the significant waveheight value given on the GDR which is satellite-specific. The media correction represents an additional modeling problem affecting GEOSAT. The wet term in the tropospheric refraction correction is difficult to determine since GEOSAT, unlike SEASAT, lacked an onboard radiometer to measure the columnar water vapor content of the atmosphere directly. The sub-satellite relative humidity provided by the FNOC hindcast models on the GDR have been found to be inadequate (e.g., Fu, 1987) especially in the tropics. The wet delay we computed was based on the analysis of the SMMI data by Emery et al., (1990). We substituted interpolated satellite radiometric estimates of atmospheric water vapor content for the FNOC values. These measurements were obtained by other satellite missions coincident with GEOSAT.
- B is a term which accommodates both the invariant bias in the altimeter instrument and an error in the adopted value of the Earth's semi-major axis (a_e = 6378137m). An altimeter bias for each arc of data was estimated.
- ε is observation noise in the altimeter measurement.

The sea surface height (SSH) in (eq. 2.1) is represented by:

$$SSH = \zeta + T_g + N_{ref} + \Delta N + T + A \qquad \text{(eq. 2.2)}$$

where

- ζ is the quasi-stationary sea surface topography (QSST) model used to approximate the mean dynamic height of the ocean during a given altimeter mission. In the GEM-T3 solution, three spherical harmonic models of the QSST field were simultaneously estimated, one for each altimeter mission (e.g., GEOS-3, SEASAT and GEOSAT). These models are complete to degree and order 15. An evaluation of these models is presented in Section 6.

T_g is the geocentric body tide. In the GEM-T3 solution, the standards adopted by the MERIT Campaign (Melbourne et al., 1983) were employed for the solid body tides. This required using a frequency-independent model of the response of the solid-Earth to tidal forces through the use of constant Love and Shida numbers (h_2 =.609, l_2 =.0852). A correction term is then applied for the sidereal resonance at the K_1 frequency.

N_{ref} is the geoid height from the estimated long wavelength gravity field through degree and order 50, which is the size of the GEM-T3 model recovery.

ΔN is a correction which has been applied to the altimeter data to reduce errors and aliasing of the gravity field due to its omission of higher degree terms. An estimate of the gravitational signal from the field above the truncation limits of GEM-T3 is computed. Herein, we employed the high degree gravity model, OSU89B (Rapp and Pavlis, 1990) to calculate the contribution of the terms from degree 51 to 360. The altimeter data were then "corrected" for these geoidal contributions.

T is the ocean tide. We have applied a uniform set of tidal corrections with respect to the sea floor which in all cases required recomputation of the values provided on the GDR for each of the altimeter missions. We used the Schwiderski models for M_m, M_f, O_1, K_1, P_1, Q_1, S_2, N_2, M_2 and K_2. The tidal contribution for S_{sa} was not used since this tide is likely contaminated by thermal effects. To bring these tidal corrections into the geocentric frame of the altimeter measurement, an ocean loading correction was applied accounting for all of these tides using an algorithm developed by Ray and Sanchez (1989).

A is the atmospheric load computed using NMC pressure and an inverted barometer assumption.

The altimeter data which were employed in the GEM-T3 solution were also extensively edited by (a) masking out regions with high geoid gradients and/or large contributions (>2.5m) to the geoid height computations arising from harmonic terms between degree 51 to 360; (b) eliminating data over ocean areas shallower than 2250 m; (c) excluding data south of -60 degrees latitude; (d) editing data with high Automatic Gain Control; and (e) editing data with undefined ocean tidal corrections. These masking operations are fully reviewed in Marsh et al., (1990b).

2.2.2. ALTIMETER DATA ANALYSIS OVERVIEW

The altimeter data utilized in GEM-T3 was uniformly processed with consistent models. The altimeter data were treated as tracking data and fully modeled in the orbit definition process (i.e. the altimeter range observations were utilized directly in the analysis). The preliminary gravity solution, PGS-3520 (Marsh and Lerch, 1989) was used to define the a priori geoid, QSST and orbit field for the reduction of the data for all three satellites. We also introduced 1 cycle/revolution satellite accelerations which were adjusted within each orbital arc to improve the radial modeling from non-conservative force model effects. The altimeter data reduction by satellite is summarized below:

- GEOS-3: The GEOS-3 satellite lacked an on-board tape recorder to support storage of the altimeter data. Consequently, the data which were acquired were immediately transmitted to ground sites. This altimetry consists of a large number of short segments in time gathered around the ground sites. Some of these sites were moved over the duration of the mission so that within approximately 14 months of launch, a good global data set was available. However, some regions, like the north-eastern Atlantic which

was designated as an altimeter calibration area, were continuously supported by telemetry sites. Consequently, there is a considerable geographic imbalance in the GEOS-3 altimeter data distribution. We developed an algorithm which sampled the GEOS-3 passes acquired from May 1975 to July 1976 producing an optimal distribution of data satisfying a 3 degree grid over the ocean surface. Approximately 70 5-day arcs were required for this global data distribution in GEM-T3. This yielded the 142,503 altimeter observations from GEOS-3 used in GEM-T3.

In the reduction of the orbits used for GEOS-3, laser tracking from NASA and SAO systems were included. However, the laser data were down weighted especially for the SAO systems. All of the SAO data of this era are believed to be biased, therefore range biases per pass were adjusted in the orbital reduction for the SAO sites. (The SAO laser systems were substantially upgraded in 1979.) More accurate third generation laser data from GEOS-3 acquired during 1980 were utilized in the GEM-T3 solution. These data, while not coincident with GEOS-3 altimeter data, received considerably greater weight in the solution to better represent the orbit dynamics of this important satellite.

- SEASAT: The altimeter data acquired by SEASAT spanning July 27 through October 10, 1978 were used in GEM-T3. The data were reduced in 6-day arcs which were interrupted at the times of maneuvers. However, due to high solar activity and less than satisfactory drag modeling, the data acquired from September 28-30 were eliminated from the solution. In total, there were 14 arcs containing 85,700 altimeter observations. The orbits were defined using a combination of the laser, TRANET Doppler and altimeter data (see Marsh et al., 1990b for a more complete discussion of the SEASAT data analysis).

- GEOSAT: The GEOSAT altimeter data acquired at the beginning of the Exact Repeat Mission were incorporated in GEM-T3. The orbit definition for these data included tracking provided by the entire TRANET Network. In total, there were 13 6-day arcs which spanned the time period of November 11, 1986 through January 25, 1987. The orbital maneuvers which occurred on the 7th of December, 1986 and the 7th of January, 1987 caused two of the arcs to be of shorter duration than the nominal 6-day interval. This is the only time period where the complete TRANET data set was available. There was a total of 145,000 altimeter and 547,000 TRANET observations from GEOSAT included in GEM-T3. The TRANET stations supporting GEOSAT were tied to the TRANET stations which tracked SEASAT through survey ties which were made available to us from three sites. In doing so, and given the laser data acquired on SEASAT, we were able to bring both TRANET station networks into the Earth-fixed frame defined by SLR (cf. Smith et al., 1990).

2.3 SURFACE GRAVIMETRY

The analysis of the surface gravity data was performed by N. Pavlis at the Ohio State University under the supervision of Prof. Richard Rapp. These observations were developed into normal equations for incorporation into the GEM-T3 solution. The analysis of the surface gravimetry was done in parallel and concert with the processing utilized for the satellite altimetry. This work is summarized in Appendix A.

3.0 METHOD OF ESTIMATION

A modified least squares method of solution is used in developing recent GEM models. Primary considerations of the modeling is twofold: (a) to optimally combine the diverse observation data sets available for gravitational field recovery; and (b) to produce a reliable estimate of the resulting model's uncertainty. Both of these objectives hinge on establishing an optimal set of data weights for each of the major data types which include numerous satellite tracking systems, satellite altimetry and surface gravimetry. Normal equations are formed from a reduction of the data in a least squares estimation process. Weights are then assigned to each of the data normals before they are combined. To objectively derive these weights, a method employing subset solutions has been developed (Lerch, 1991) which iteratively converges on an optimal weighting from each data set's contribution to the gravitational solution. This method requires the error covariance matrix of the gravity parameters to be calibrated with the change observed in the parameters themselves across these subset solutions. The data weighting method also yields a realistic error calibration of the gravity parameters. This is deemed necessary since all contemporary gravitational models in the presence of standard ancillary environmental and non-conservative force models are presently unable to fit precise tracking data (like those provided by satellite laser ranging systems) at their true noise level. The a posteriori tracking residuals display systematic offsets and trends within each pass of data due to mismodeled and unmodeled effects. These trended residuals prevent gravity recovery at the noise level of the data and must be accounted for in the determination of the gravitational model and its accuracy estimate.

To illustrate the importance of the weighting process, we give a simplified example of the nature of the problem. The unmodeled systematic error in the observation residuals for a pass of tracking data causes the data to be repetitious in a statistical sense with non-random systematic residuals. Hence the error calibration process must properly account for this redundancy of information through appropriate down weighting of the data to accommodate these effects. For instance, if a pass of highly accurate tracking data (σ_o = 1 cm) had n = 100 points in the pass with a offset bias, b = 10 cm, then the effective (i.e. realistic) accuracy for each data point is essentially

$$\sigma = b\,n = 100\,\sigma_o \qquad \text{(cm)}$$

Hence, a 1 cm observation is down weighted in accuracy by a factor of 100, which in terms of weight is a factor of 10,000 since

$$w = 1/\sigma^2 \qquad (\text{cm}^{-2})$$

While this level of down weighting of data is severe, it does represent current experience when SLR data from low earth satellites are utilized in the GEM model recovery.

The remainder of this section explains our method of forming the modified least squares normal equations and our iterative process for deriving adjusted data weights for the solution.

3.1 MODIFIED LEAST SQUARES NORMALS IN THE ESTIMATION OF GEM-T3S AND GEM-T3

The method of solution for GEM-T3S for a given set of data weights is a modified least squares process (Lerch et al., 1979) which we have shown (Marsh et al., 1988) to be equivalent to a special

case of least squares collocation as presented in Moritz, (1980: Eq. 21.38). Herein, we minimize the sum (Q) of signal and noise as follows:

$$Q = \sum_{\ell,m} \frac{C^2_{\ell,m} + S^2_{\ell,m}}{\sigma^2_\ell} + \sum_{t} \sum_{obs\ i} f_t \frac{r^2_{it}}{\sigma^2_t} \qquad \text{(eq. 3.0)}$$

where the signal is given by

$C_{\ell,m}$, $S_{\ell,m}$: spherical harmonics comprising the solution coefficients; and

$\sigma_\ell : \frac{1}{\sqrt{2}} \times \frac{10^{-5}}{\ell^2}$ is the RMS of the coefficients of degree ℓ (a priori constraint based on Kaula's rule). Kaula's rule has been obtained from gravimetry and is used here to represent the observed power within the geopotential.

and the noise is given by

r_{it} : observation residual (observed minus computed) for the ith observation of satellite tracking data set (type) t and for the combination models it is generalized to include all data types t; and

σ_t : RMS of observation residuals (generally significantly greater than a priori data precision because of unmodeled effects)

f_t : down weighting factor to compensate for the non-random character of the unmodeled error effects in the data (ideally f=1)

f_t / σ_t^2 is the combined weight (w_i) for the least squares normal equations for each data set t.

With the standard least squares approach (noise-only minimization), there is a problem in determining realistic values for all of the high-degree coefficients due to their strong correlation with one another. An absence of collocation (i.e. neglecting the first term in eq. 3.0) results in excessively large power in the adjustment of the potential coefficients. Poor performance of an unconstrained high-degree field is normally circumvented in the noise-only least squares method by solving for a smaller sized field. Unfortunately, restricting the size of the field causes the higher degree terms above the field's maximum degree to be exactly zero. The disadvantage of this approach is the aliasing of the coefficients due to the part of the model which is now not adjusted. We have found that the best approach is with the least squares collocation (or constrained) solution [Lerch et al., (1991b)].

The a priori constraint matrix (the first term in 3.0) contains only diagonal terms. A comparison of the relative size of their contribution to the overall data normals shows that the satellite normal equations have considerably larger diagonal terms than the collocation matrix. At lowest degree, the ratio of the two contributions indicates that the collocation contribution is barely visible. It is only at highest degree that the collocation contributions become a significant percent of the diagonal terms. Collocation stabilizes the entire solution by indirectly controlling ill-conditioning due to correlation within the system of observation equations.

In the present solution, t = 0 represents the constraint matrix with weights $(1/\sigma_t^2)$. These weights are fixed since the spectrum of the Earth's gravitational field is well known and the power of 100% uncertainty in the gravity coefficients is defined in this way.

3.2 LINEARIZATION OF MODEL FOR THE GENERAL DATA SET T

Returning to (3.0), when minimizing Q using the least squares method, the normal matrix equation and error covariance are described below. The optimal weighting algorithm is based on subset gravitational solutions which are also discussed. First we express the observation residuals r of the solution X as a first order Taylor series expanding about X_o (using a linearity assumption):

$$r = o - c = o - c_o - (c - c_o)$$

$$= r_o - A\,x \qquad \text{(eq. 3.1)}$$

where

- o is the observation
- r_o is $o - c_o$, the initial residuals with c_o evaluated from the initial parameters, X_o
- x is the adjustment $X - X_o$ from the initial parameters X_o
- A is the matrix of observation partials with respect to the modeled parameters evaluated at X_o

As indicated, this linearization enables us to represent r in terms of the solution X in the neighborhood of X_o. For each data subset t

$$r = (r_t) = (o_t - c_t)$$

$$r_t = o_t - c_{ot} - (c_t - c_{ot})$$

$$= r_{ot} - A_t\,x \qquad \text{(eq 3.2)}$$

Let t = 0 represent the data set of constraints for the gravity harmonics. They represent zero estimates of the coefficient values with uncertainties obtained from the expected rms power of the coefficients of a given degree, ℓ given by Kaula's rule; thus, the t = 0 data is treated as observations although they are clearly biased toward zero.

Denoting the errors in the unmodelled part of the observations by:

$$e = o - \bar{c} \qquad \text{(eq 3.3)}$$

where $\bar{c}$ is based upon the true values of $\bar{X}$ of the modeled parameters, then we again have through the assumption of linearity

$$r = o - c = (o - \bar{c}) - (c - \bar{c})$$

$$= e - A x_e$$

$$r_t = e_t - A_t x_e \qquad \text{(eq 3.4)}$$

where

$x_e = X - \bar{X}$ are the errors in the solution X.

3.3 LEAST SQUARES (LS) MATRIX NORMAL SOLUTION AND ERROR MATRIX

The normality condition from minimizing Q by least squares, with $W = (W_t)$ being a diagonal weight matrix, is

$$A^T W r = \sum_t A_t^T w_t r_t = 0 \qquad \text{(eq 3.5)}$$

using r at the solution X from the linearized equations (3.1) and (3.2). Thus the normal equations are:

$$(A^T W A) r = A^T W r_o$$

or rather

$$Nx = R$$

where

$$N = A^T W A$$

$$R = A^T W r_o \qquad \text{(eq 3.6)}$$

The nature of W_t has not been specified, other than noting that it is diagonal. Mixed data weights within a data set or group of data sets where it is desirable to hold the relative data weights fixed must be allowed. The Kaula's rule constraint is an example of this situation. It is also desirable to specify a scalar weighting factor for each data set t, which is required for the determination of relative data set weighting. We define:

$$W_t = w_t W_t'$$

where W_t' is often the identity matrix, but may be the Kaula constraint matrix (t=0 with w_o=1 held fixed) or other such a priori fixed relative weighting. We wish to keep the w_t explicitly in our equations. Thus it is convenient to consider the normal matrices as:

$$N = \sum_t w_t N_t$$

$$R = \sum_t w_t R_t \qquad \text{(eq 3.7)}$$

where

$$N_t = A_t^T W_t' A_t$$

$$R_t = A^T W_t' r_{ot} \qquad \text{(eq 3.8)}$$

3.4 THE SIMPLIFIED LS ERROR MATRIX

Using (3.4), the errors in the solution X are given by:

$$x_e = (A^T W A)^{-1} A^T W e$$

$$= N^{-1} A^T W e \qquad \text{(eq 3.9)}$$

and thus the error matrix for X is:

$$E(x_e x_e^T) = N^{-1} A^T W E(e e^T) W A N^{-1} \qquad \text{(eq 3.10)}$$

where E denotes the statistically expected value.

Under certain assumptions, the error matrix in (3.10) will simplify to:

$$E(x_e x_e^T) = (A^T W A)^{-1} \equiv N^{-1} \equiv V(x) \qquad \text{(eq 3.11)}$$

which is generally used for the LS estimator. The usual assumption for the LS estimator is to let the error e be a random and uncorrelated error, where:

$$W^{-1} = E(e e^T) \qquad \text{(eq 3.12)}$$

resulting in (3.11). A less stringent condition on the data and their errors is:

$$A^T W E(e e^T) W A = A^T W A = N \qquad \text{(eq 3.13)}$$

will also result in (3.11). A simple example of this case is seen when a constant estimator is applied when using a series of independent data sets with random noise which also contain different biases within segments of the data. In Lerch (1991) it is shown that (3.12) is approximately "true" for the satellite determined gravitational model based upon certain properties of the mismodeled signal seen over each individual pass of tracking data. However, there is a severe penalty in the weighting for (3.13) because not only does the size of the "bias" influence the data weight, but so does the fact that this bias is seen throughout each data segment/subset. Within the tracking environment, this segment is usually one pass of data over a tracking site. The repetition of the biases within each pass of data produces a fully correlated data error which requires significant down weighting of the data relative to its nominal accuracy as indicated in the introduction of this section.

For convenience in the remainder of this report, we employ the simplified error matrix (3.11):

$$N^{-1} = [\sum_{t} (w_t N_t)]^{-1} = V(x) \equiv E(x_e\, x_e^T)$$

(eq 3.14)

which is referred to as the error covariance matrix V(x), but with the understanding that realistic weights, w_t, are determined for each of the major data sets. The weights are determined from the optimum weighting system based upon a calibration of subset solutions with the complete solution. This calibration is introduced below; its application for the GEM-T3S and GEM-T3 solutions are described in the next section.

3.5 CALIBRATION AND OPTIMIZATION OF DATA WEIGHTS USING SOLUTION SUBSETS

The automatic data weighting algorithm as developed by Lerch (1991) compares a complete and subset solution. The complete solution from (3.6) and (3.7) containing all data sets is given as:

$$x = (\sum_{j} w_j N_j)^{-1} (\sum_{j} w_j R_j)$$

(eq 3.15)

where the error covariance from (3.14) is:

$$V(x) = N^{-1} = (\sum_{j} w_j N_j)^{-1}$$

A subset solution x_t with errors x_{te}, which lacks data set t is given as:

$$x_t = (\sum_{j\neq t} w_j N_j)^{-1} (\sum_{j\neq t} w_j R_j)$$

(eq 3.16)

with the error covariance for the data employed being:

$$V(x_t) = (\sum_{j\neq t} w_j N_j)^{-1} \equiv E(x_{te}\, x_{te}^T)$$

The difference between the subset and full solutions should be predicted by their respective covariances. This difference largely reflects the unmodeled errors in data set t, since the error effects to first order subtract out for the data sets common to both solutions. This difference from (3.15) and (3.16) is:

$$x_t - x = V(x_t)\, R(x_t) - V(x)\, R(x)$$

(eq 3.17)

where

$$R(x) = \Sigma\, w_j\, R_j$$

$$R(x_t) = \Sigma_{j \neq t}\, w_j\, R_j$$

If E is used to express the expected value, then the differences in these models are predicted by the error covariances of the solution differences (Lerch, 1991) given as:

$$E[(x_t - x)(x_t - x)^T] = E(x_{te}\, x_{te}^T) - 2\, E(x_{te}\, x_e^T) + E(x_e\, x_e^T)$$

$$= E(x_{te}\, x_{te}^T) - E(x_e\, x_e^T)$$

$$= V(x_t) - V(x)$$

$$= V(x_t - x)$$

(eq 3.18)

from (3.15) and (3.16) where:

$$x_t - x = x_{te} - x_e = (X_t - \bar{X}) - (X - \bar{X}) = X_t - X$$

It should be noted that the variances would be added if the data in the two solutions (x and x_t) were independent. However, here the data in the subset solution is wholly contained in the complete solution resulting in the above difference of variances. Equation (3.18) serves as the basis for the subset solution calibration method described in the next section which is used to both determine the optimal data weights and provide a reliable error estimate of the resulting solutions.

4.0 WEIGHTING, CALIBRATION AND ACCURACY ASSESSMENT

4.1 CALIBRATION APPROACH

An optimal data weighting technique which automatically calibrates the errors for the estimated gravity field (Lerch, 1991a) was first applied in the GEM-T2 solution (Marsh et al., 1990a). This technique is applied herein for the development of GEM-T3 and GEM-T3S. This data weighting technique is now an integral part of the solution design. However, certain refinements were required for the calibration of combination models where data have very different bandwidths of gravitational signal.

Briefly, the method determines the weights for the data subsets across the different satellite tracking systems on different orbits in order to automatically obtain an optimal least squares solution and an error calibration of the adjusted parameters. It is based on the simple concept that the expected mean square deviation of a subset gravity solution from the overall solution is predicted by the solution covariances. Consider the ratio of the observed deviation to the expected deviation:

$$k = \Delta C / E(\Delta C) = [\Sigma(C'-C)^2 \; / \; \Sigma(\sigma'^2-\sigma^2)]^{1/2} \qquad \text{(eq 4.1)}$$

where C' is a subset solution, C the complete model, their differences are denoted ΔC, and E is the expected value of the model differences based on the solution covariances, σ' and σ. This quantity, k, is ideally equal to 1 and is the calibration factor required for the prediction to hold.

The weighting system is primarily designed to produce realistic error estimates. The data receive optimal weight according to their individual contributions to the model's accuracy. The method employs data subset solutions in comparison with the complete solution and uses an algorithm to adjust the data weights to satisfy (4.1). With the adjusted weights, the process provides for an automatic calibration of the solution's error estimates. The data weights which are obtained are generally much smaller than the weights expected when considering the accuracies of the observations (noise-only) themselves. The observations and ancillary models suffer from problems which need to be accounted for if an optimal gravitational model is to result. As was observed in the introduction to Section 3, our solution a posteriori can only fit our most precise data sets to a factor of 3 to 10 worse than their noise-only expectation of system performance and hence, these data require down weighting. Optimization of data weighting and field calibration is a major undertaking requiring assessment for each data subset.

The optimal weighting algorithm based on (4.1) is briefly described below. The method is discussed in Marsh et al., (1990a) with a full development found in Lerch (1991a). The principle behind the method is that the squared difference of the corrections to the parameter estimates of a solution from a proper subset of that solution should be predicted by the formal uncertainties of the associated covariance matrix. In other words, the actual differences observed in the solution need to be consistent with the formal uncertainties derived from the normal matrix. Let x be the full solution adjustment vector, x_t be the subset solution adjustment vector, and $V(x_t-x)$ the covariance matrix of the solution difference. Then, using just the time invariant gravity parameters:

$$(x_t - x)^T (x_t - x) = k_t \, Tr \, [V(x_t - x)] \qquad \text{(eq 4.2)}$$

provides the defining relationship for the calibration factor k_t. When the weights are correct, k_t is unity. The difference between the solutions as discussed earlier largely reflects the unmodeled data errors (e_t) within data set t since the errors common to both solutions (e_j, $j \neq t$) largely cancel out when comparing the solutions. Hence, scaling the original data weight for a given data subset by the inverse of k_t, namely:

$$w_t^* = w_t / k_t \qquad \text{(eq 4.3)}$$

provides for k_t to be nearer to unity. However, because the subset and complete solution alike change when the weight on a subset data set is altered, these weights require iteration.

Section 3 shows that the covariance of the solution difference when subset and complete solutions are used is given by the differences:

$$V(x_t - x) = V(x_t) - V(x)$$

$$Tr[V(x_t - x)] = k_t \, Tr\,[\, V(x_t) - V(x)]$$

$$= k_t \, (\sigma_{xt}^2 - \sigma_x^2) \qquad \text{(eq 4.4)}$$

Some major assumptions behind this method are considered. The most important assumption in the above relationship is seen from (3.18) where the simplified covariance result

$$E(x_{te} \, x_e^T) = E(x_e \, x_e^T) \qquad \text{(eq 4.5)}$$

requires that the different data sets t and t' (Lerch, 1991) have independent data errors producing:

$$E(e_t \, e_{t'}) = 0 \qquad \text{(eq 4.6)}$$

Since the source of the errors e are unknown this assumption may not be true and solutions may have common errors which inadvertently cancel when forming the difference in (4.4). The effect of this cancellation on the calibration would tend to give an optimistic error assessment and incorrect data weighting. We have found that this effect can easily happen in the calibration when the excluded data subset is similar in character to a data set maintained in the subset solution. This is especially noticeable when only part of a data set (e.g., recent SLR data acquired on Lageos) is eliminated in forming the subset solution. In this example, while the withheld Lageos data is independent and no longer shared across subset and complete solutions, it is highly similar in its information content to the other Lageos data kept in the subset solution. Distinct satellite orbits, even those tracked by different tracking instruments, still may require simultaneous elimination from the complete solution for a good calibration to result if the orbit characteristics between them are too similar. To avoid these problems, we combine similar data sets into "groups" which strengthened the independence of the data being tested and produced more conservative and realistic calibration results. Furthermore, we have introduced additional tests to evaluate the resulting solution error estimates as will be presented in Section 4.4.

Other considerations are that the parameters being calibrated are restricted to the static gravitational field so that the trace is consistent with units of normalized gravity. The use of the trace implies a certain neglecting of possible high correlations in adjusted parameters, and thus a possible overstating of the formal error contribution to the squared differences. The calibration factor is presumed to apply to all of the normal equations in the difference set equally. The

analyst must classify the data into groups, which is an act of intuition as indicated above. This is especially difficult for data sets which vary over time or have suspected or known modeling errors. Furthermore, when data types are mixed, such as altimetry and conventional tracking data, the information bandwidth of the data in terms of the gravity parameters barely overlap. Clearly, the method also requires the covariance matrices to be distinct, so that the differences are well defined in the computer implementation. Results showing this latter effect are given below.

4.2 OPTIMAL WEIGHTS FOR GEM-T3S AND GEM-T3

The Earth's gravitational field is globally sensed by the precise tracking data taken on numerous near-Earth orbiting satellites. However, the attenuation of the gravitational field with altitude restricts the bandwidth of the model which is resolvable using these data. An emphasis has been placed on fully exploiting the gravitational signal sensed by tracking data to exhaust the signal in the data. To do so, "satellite-only" models have been estimated to high degree and order. However, many of the highest degree coefficients are not well resolved. This has been the general trend seen in recent Goddard Earth Models (GEM) with GEM-T1 (Marsh et al., 1988a) solved to degree and order 36 followed by GEM-T2 (Marsh et al., 1990a) which, in addition, recovered harmonics for resonance and low order terms to degree 50. GEM-T3S presented here, is complete to degree and order 50. Least squares collocation has been used in the development of these models to ensure that coefficients which are not resolvable yield near zero values. These poorly resolved coefficients all have error estimates which approach 100% of the expected power of the terms. The "satellite-only" model is biased toward zero for the high degree terms (see Figure 4.1) with a smooth transition to the model's truncation limits where the coefficients are defined to be zero and not solved for. While many high degree coefficients display this behavior, many orders in the harmonic expansion of the field have detectable orbital perturbations for geodetic class satellites out to degree 50, and for certain resonance orders even beyond. The advantages of extending the "satellite-only" models to these limits are:

(a) By solving for a model to the limits of tracking data sensitivity, there is little aliasing resulting from the truncation limits of the models. This is a necessary condition for the successful combination of these "satellite-only" models with surface data and altimetry which sees the unattenuated gravitational field to very high degree and order.

(b) The calibration of these models is robust since all of the signal in the data attributable to gravitational sources is represented in the solution parameter space. This avoids the spurious calibration results which were seen in GEM-T1 for certain resonance orders due to the truncation of the model at degree and order 36 (see Lerch et al., 1991b). The calibration of more complete fields, even though many of the terms are 100% in error, yields a better insight into the systematic errors contained within individual data sets.

(c) Since a wide range of geodetic class satellites are sampled, these "satellite-only" models yield excellent orbit determination capabilities. A sufficient number of coefficients are adjusted to model the "lumped-harmonics" sensed by the different orbits involved. The orbit determination performance of "satellite-only" models can then be compared with that achieved using combination models to locate data and modeling incompatibilities.

Figure 4.1

Coefficient RMS per Degree

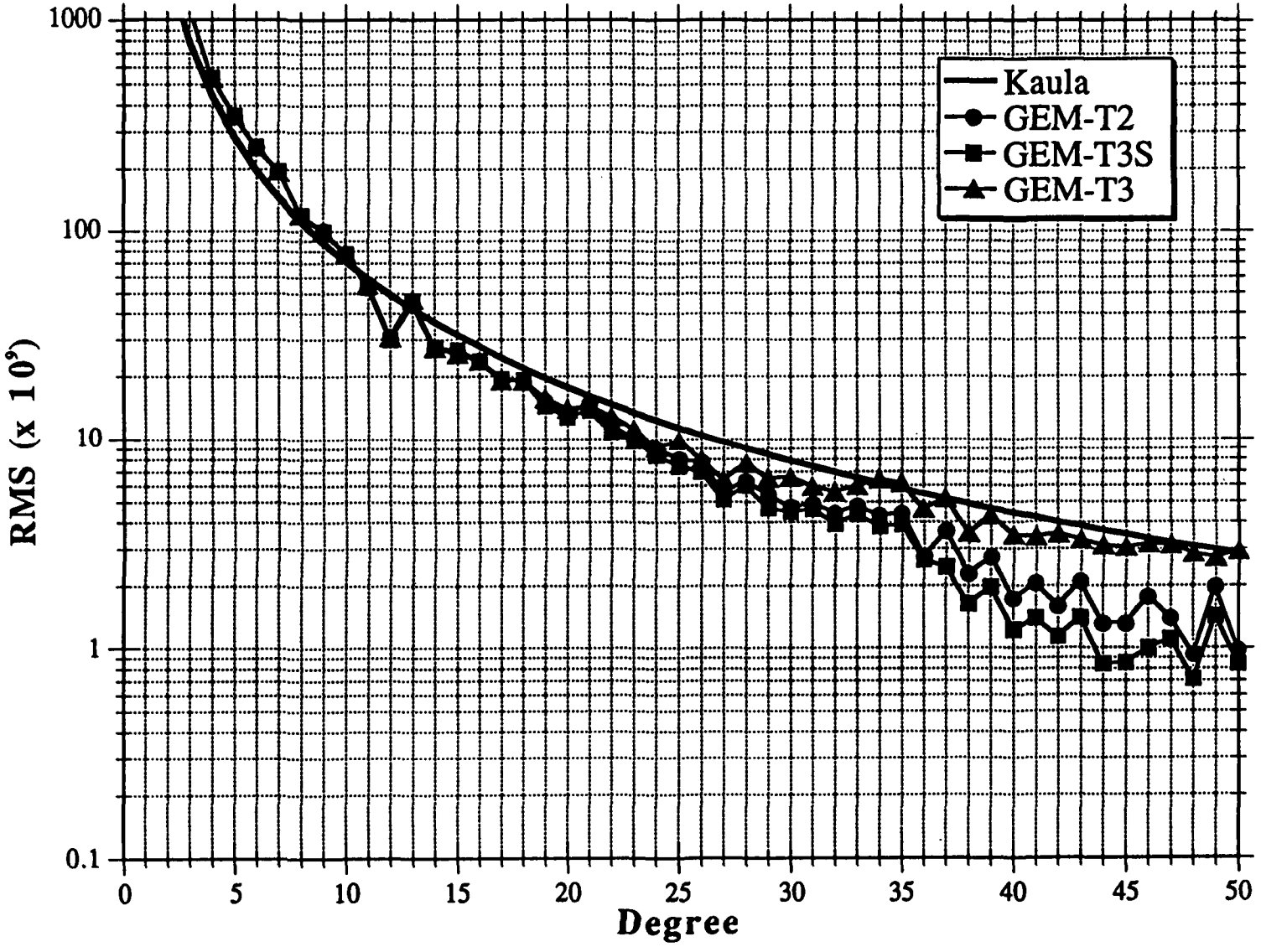

Using this optimal weighting algorithms (eqs 4.2 and 4.3) we first calibrated the GEM-T3S "satellite-only" model. A set of subset solutions was computed for GEM-T3S where each of the major data sets was omitted from preliminary versions of the solution. The final set of calibration factors, K_t, which were obtained are listed in Table 4.1a. In Table 4.1a, the calibration factor (K_t) scales the errors of the gravity parameters instead of the variances of these errors as given by k_t. Hence, the values shown are:

$$K_t = k_t^{1/2} \qquad \text{(eq 4.7)}$$

The calibration factors obtained from grouping observation subsets with common characteristics show much more conservative behavior than those obtained for individual data sets within the group. This tends to support the concept that similar data sets, particularly those obtained on the same satellite, have common errors which inadvertently cancel when the fields are differenced. Grouping the data sets after determining their relative weight and then calibrating the entire group was found to be a much better approach.

While the calibration of the "satellite-only" GEM-T3S model was reasonably straight forward and in large measure paralleled that of GEM-T2, there are some other notable differences besides the use of group calibration factors. GEM-T3S solved for a complete set of station coordinates while GEM-T2 held all the non-Doppler stations fixed. The presence of these adjusting station parameters were accounted for in the calibration. To do so, we prevented the station position uncertainties from degrading unreasonably as data set weights were altered. Although improvements are seen in the geopotential field when the station coordinates are adjusted, the calibration factors and weights are not greatly affected. A comparison of the final weights and data employed in GEM-T2 and GEM-T3S are shown in Table 4.1b.

The calibration of GEM-T3S required some additional fine tuning. The calibration method as shown above, is based on the detection of systematic errors in individual data sets which should be independent and adversely affect the gravity recovery. Improving data models (e.g., the introduction of tropospheric refraction scaling parameters for TRANET data in GEM-T3S) and including more accurate data (e.g., upgrading Lageos and Ajisai data sets in GEM-T3S beyond those used in GEM-T2) are ongoing efforts. It is important to investigate new relative weighting factors for these augmented and improved data sets. For example, the new Ajisai data was composed of laser "normal points" which yielded better relative weights compared to the older full-rate (sampled) Ajisai data common between GEM-T2 and GEM-T3S. However, since both data sets of Ajisai would tend to have common systematic errors either coming from unmodeled orbit effects or possible common inaccurate measurement corrections, calibrating the old versus the new Ajisai data as separate subsets yields calibration results which are too optimistic. These optimistic results appear by obtaining a value of σ_0 for these data which is too small (i.e. w_t is too large). The calibration is better performed if all Ajisai data is included within a single group being tested; this requires establishing relative weights between the original and "normal point" Ajisai data sets. A similar picture is seen with Lageos, where the observations included in the gravity models have been upgraded twice; GEM-T1 used data spanning 1980 through late 1984; GEM-T2 extended the Lageos data set through February of 1987; and finally, GEM-T3S contains Lageos data through the end of 1987. Calibration factors were optimistic (.62 on average) for individual segments of the Lageos data and .93 for the grouped data set.

Two data sets, shown in Table 4.1a were held to have conservative data weighting: Ajisai and the GEOS-3/ATS-6 satellite-to-satellite tracking. This was done to insure maximum signal coming from Lageos in the definition of the long wavelength gravitational field.

Table 4.1a

DATA WEIGHTS AND CALIBRATION OF GEM-T3S

Subset Solution Dataset	GEM-T3S Weights σ'_o *	GEM-T3S Individual Calibration Factors K^1	GEM-T3S Group Calibration Factors K^1
Geos-1 Las '77-'78	816 cm	.99	
Geos-1 Las '80	353 cm	.94	
Geos-2 Las '75-'77	913 cm	.99	.96
Geos-3 Las '75-'78	1000 cm	.90	
Geos-3 Las '80	224 cm	.84	
DI-C,DI-D,Peole Las	745 cm	.92	.92
Optical	6.7 arcsec	.97	.97
BE-C Las '79-'82	577 cm	.90	
Starlette '83-'84	182 cm	.86	
Starlette '86	182 cm	.86	
Lageos'80-'84	112 cm	.93	
Lageos'84-'86	112 cm	.93	.96
Lageos'87	105 cm	.93	
Ajisai '86-feb '87	387 cm	.66	
Ajisai mar-apr '87	182 cm	.66	
Geos-3:ATS Las	816 cm	.60	
Geos-3:ATS SST	3.2 cm/sec	.60	
Geos-3:ATS SST	7.1 cm/sec	.60	
Oscar-14	10.0 cm/sec	.67	
Nova	2.9 cm/sec	.71	.86
Landsat	10.5 cm/sec	.76	
Geosat Dop	7.1 cm/sec	.86	
Seasat Las	707 cm	.86	
Seasat Dop	5.0 cm/sec	.86	

[1] Individual data set calibration factors indicate weights are conservative, however, group calibration factors (more independent) show weights are calibrated

$$K = \sqrt{\left(\frac{\sum(c-\bar{c})^2}{\sum(\bar{\sigma}^2 - \sigma^2)}\right)} \qquad w' = \frac{w}{K^2} \qquad * \sigma_o = \frac{1}{\sqrt{w}} \qquad * \sigma'_o = \frac{1}{\sqrt{w'}}$$

Table 4.1b

DATA WEIGHTS AND OBSERVATIONS

Dataset	GEM-T3S Obs.	GEM-T3S Number of arcs	GEM-T3S Weights σ'_0 *	GEM-T3 Obs.	GEM-T3 Number of arcs	GEM-T3 Weights σ'_0 *	GEM-T2 Obs.	GEM-T2 Number of arcs	GEM-T2 Weights σ'_0 *
Geos-1 Las '77-'78	62417	48	816 cm	62417	48	816 cm	62417	48	667 cm
Geos-1 Las '80	54129	30	353 cm	54129	30	353 cm	54129	30	258 cm
Geos-2 Las '75-'77	26613	28	913 cm	26613	28	913 cm	26613	28	816 cm
Geos-3 Las '75-'78	53270	48	1000 cm	53270	48	1000 cm	53270	48	816 cm
Geos-3 Las '80	54526	50	224 cm	54526	50	224 cm	54526	50	224 cm
BE-C Las '79-'82	64240	39	577 cm	64240	39	577 cm	64240	39	577 cm
Starlette '83-'84	97397	84	182 cm	97397	84	182 cm	97397	157	224 cm
Starlette '86	93287	72	182 cm	93287	72	182 cm	411102	73	500 cm
Lageos '80-'86	278620	86	112 cm	278620	86	112 cm	278620	86	112 cm
Lageos '87	55360	11	112 cm	55360	11	112 cm			
Ajisai '86-feb '87	161390	36	387 cm	156021	36	387 cm	156021	36	316 cm
Ajisai mar-apr '87	5369	12	182 cm	5369	12	182 cm			
DI-C,DI-D,Peole Las	23398	16	745 cm	23398	16	1000 cm	23398	16	816 cm
Geos-3:ATS Las	17027	26	816 cm	17027	26	976 cm	17027	26	816 cm
Geos-3:ATS SST	19074	9	3.2 cm/sec	19074	9	3.8 cm/sec	19074	9	3.2 cm/sec
Geos-3:ATS SST	8326	17	7.1 cm/sec	8326	17	8.5 cm/sec	8326	17	7.1 cm/sec
Optical	202093	498	6.7 arcsec	202093	498	11.2 arcsec	202093	498	6.7 arcsec
Oscar-14	62685	13	10. cm/sec	62685	13	14.1 cm/sec	63098	13	8. cm/sec
Nova	73186	16	2.9 cm/sec	73186	16	4.5 cm/sec	73238	16	2.6 cm/sec
Landsat	26287	10	10.5 cm/sec	26287	10	10.5 cm/sec	26426	10	10.5 cm/sec
Geos-3 Las+Alt				195006	64	577 cm			
Geosat Dop	550263	13	7.1 cm/sec	550263	13	7.1 cm/sec	549141	13	4.5 cm/sec
Geosat Alt.				145024	13	353 cm			
Seasat Las	12428	13	707 cm	12428	13	707 cm	14923	14	707 cm
Seasat Dop	115093	13	5.0 cm/sec	115093	13	5.0 cm/sec	138042	14	7. cm/sec
Seasat Alt				85679	13	353 cm			
Surface Gravity				54048	1	3.2mgals			

In the GEM-T3S calibration, we observed in subset solutions that the elimination of certain data sets (as was done for GEM-T2's calibration) gave rise to calibration factors as in (4.1) where both the change in the model and the expected change in the model were small. This causes some concern for numerical stability. Examples of the differences for subset solutions lacking Lageos data are presented in Figure 4.1.1 for GEM-T3S and Figure 4.1.2 for GEM-T3. The results are quite consistent for each degree which indicates we have not yet reached the point of instability especially for the complete calibration factors which sum over all of the observed model changes and over all of the predicted errors. It is remarkable that significant effects are seen as high as degree 20 just due to the Lageos data. This is likely due to the decoupling of the correlation between high and low degree terms provided by the high altitude Lageos data. Lageos provides virtually no direct sensitivity to these high degree terms because of its altitude. Figure 4.1.3 shows the effects due only to high and low degree decoupling.

Before discussing the GEM-T3 weights and calibration, we show a comparison of calibration factors in Table 4.1.c between individual data sets and grouped data sets. The results show that the grouped calibration factors, particularly those obtained for altimeter data are significantly larger than the individual factors. All data sets used the same weighting for the altimeter data within the respective solutions. If the data sets are evaluated individually, for example, using Seasat, then the weight obtained based upon the individual calibration factor should be increased by over a factor of 5, (i.e. $[.75/.33]^2$), over that for the group calibration factor. Such an increase would yield not only very optimistic error estimates for the resulting gravity field but would cause the altimeter signal to excessively dominate the solution. We know that all altimeter data contain common, difficult to model, non-geoidal signals; imperfect modeling and estimation of these effects cause systematic errors to be present in altimetry when these data are employed for geopotential recovery. Therefore, altimeter data forms an ideal data group and while data from different missions are contained therein, calibrating these data in this fashion yields a more conservative and realistic solution error covariance.

Grouped calibration factors were employed for the GEM-T3 calibration which are shown in Table 4.2. One important group was the entire altimeter data set and all tracking data coincident with these data. Merging the tracking data into these groups was desirable since altimeter data alone is incapable of defining the out-of-plane components of the orbit. Since altimeter and surface gravity data are capable of directly resolving the geoid over the entire bandwidth of these GEM solutions, all tracking data takes on a redundant quality for defining the gravitational harmonics when these data are utilized. The entire set of tracking data in GEM-T3 is somewhat downweighted as a result, yet we see from Figure 4.2 that the lowest degree terms ($\ell < 8$) are still significantly improved in GEM-T3 over GEM-T3S. Further, we see that the subset solution containing surface gravity and altimetry alone contributes very little in itself to the overall accurate definition of these low degree terms. Hence, the improvement GEM-T3 is achieving over GEM-T3S for the low degree terms comes from the indirect effect of reducing the correlations throughout the entire gravity model, and especially those found within each of the harmonic orders in "satellite-only" solutions. This can further be demonstrated by comparing GEM-T3S with a solution which largely reduces this correlation. GEM-T3S is solved only to degree 10 and its errors (showing phenomenal improvement) are compared to those obtained from the complete model in Figure 4.2. From this figure it is clear that correlation within the "satellite-only" model is a serious limitation with the population of satellites we have available for study. This problem is greatly reduced when surface gravity and altimeter data are added to the solution. The decreased weighting for the satellite data in GEM-T3 versus GEM-T3S also compensates for the exaggerated improvement for the low degree terms which would otherwise result. Examination of the satellite laser ranging residuals between these models indicates only slight improvements for GEM-T3 (Section 7). However, using a new calibration procedure presented at the end of this section, one finds that significant improvement in the low degree model has been achieved using GEM-T3.

Figure 4.1.1

Spectral Content by Degree l of Gravity Calibration for GEM-T3S vs. GEM-T3S without Lageos

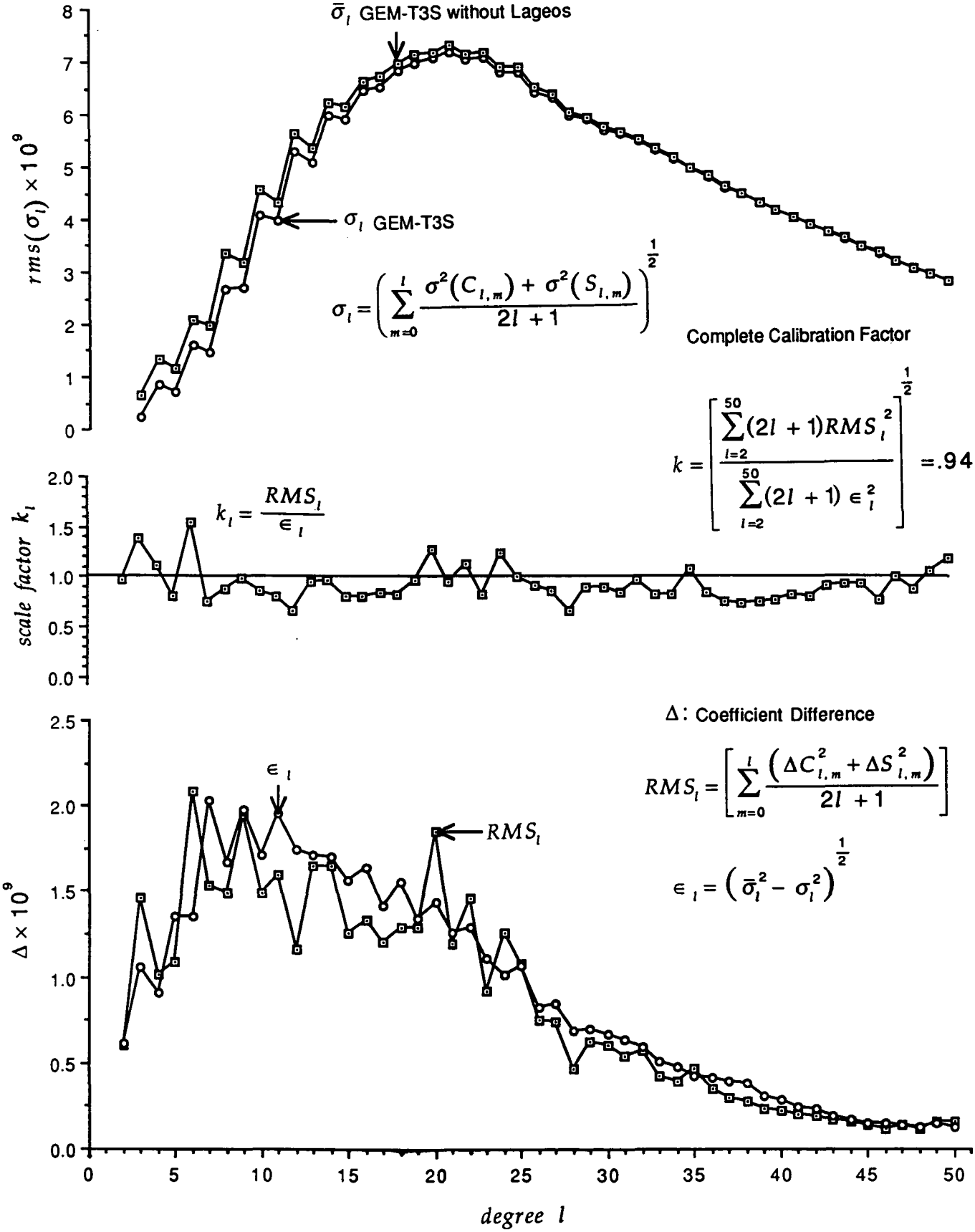

Figure 4.1.2

Spectral Content by Degree l of Gravity Calibration for
GEM-T3 vs. GEM-T3 without Lageos

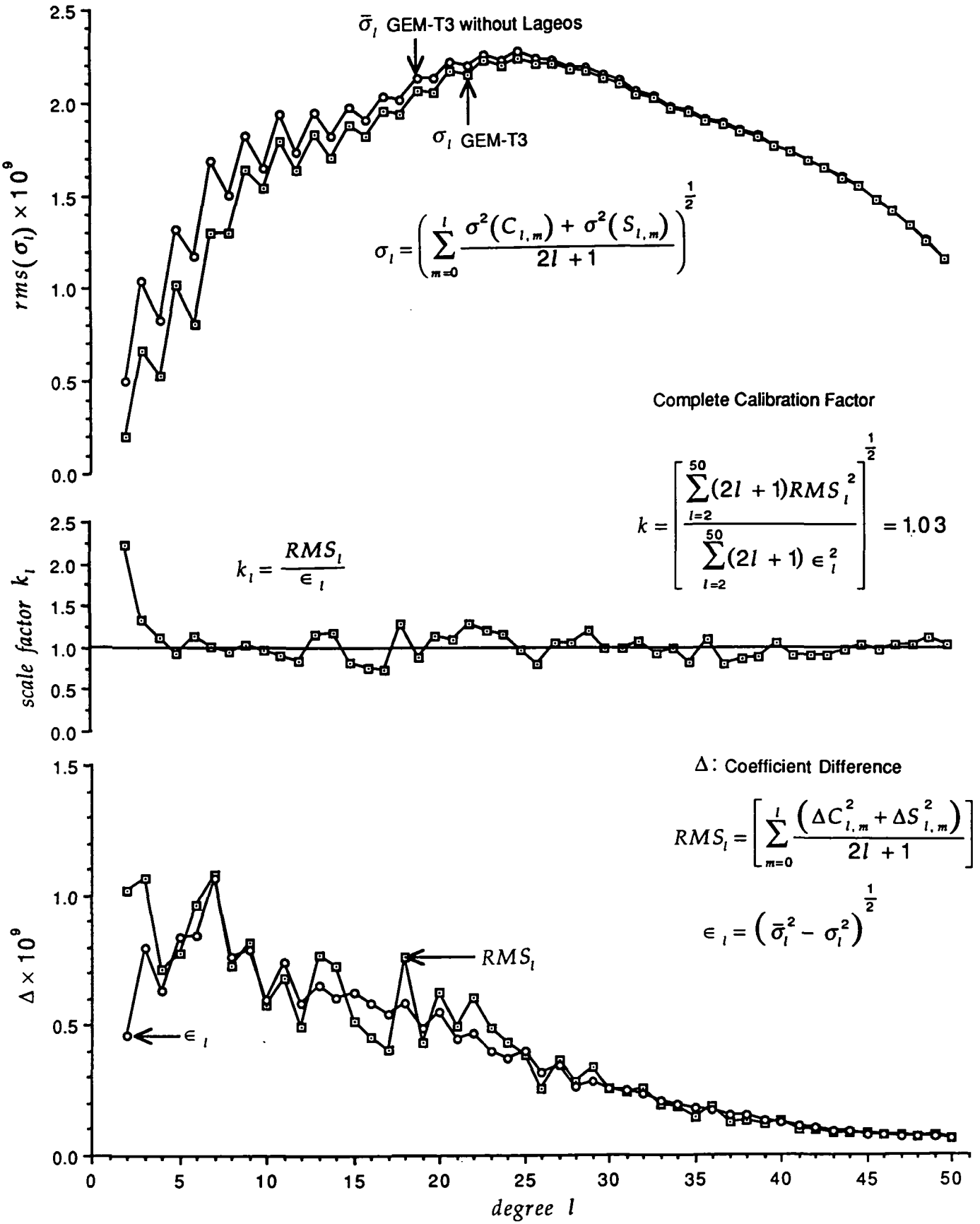

Figure 4.1.3

Rms of Coefficient Errors per Degree for GEM-T3 vs. Subset Solution

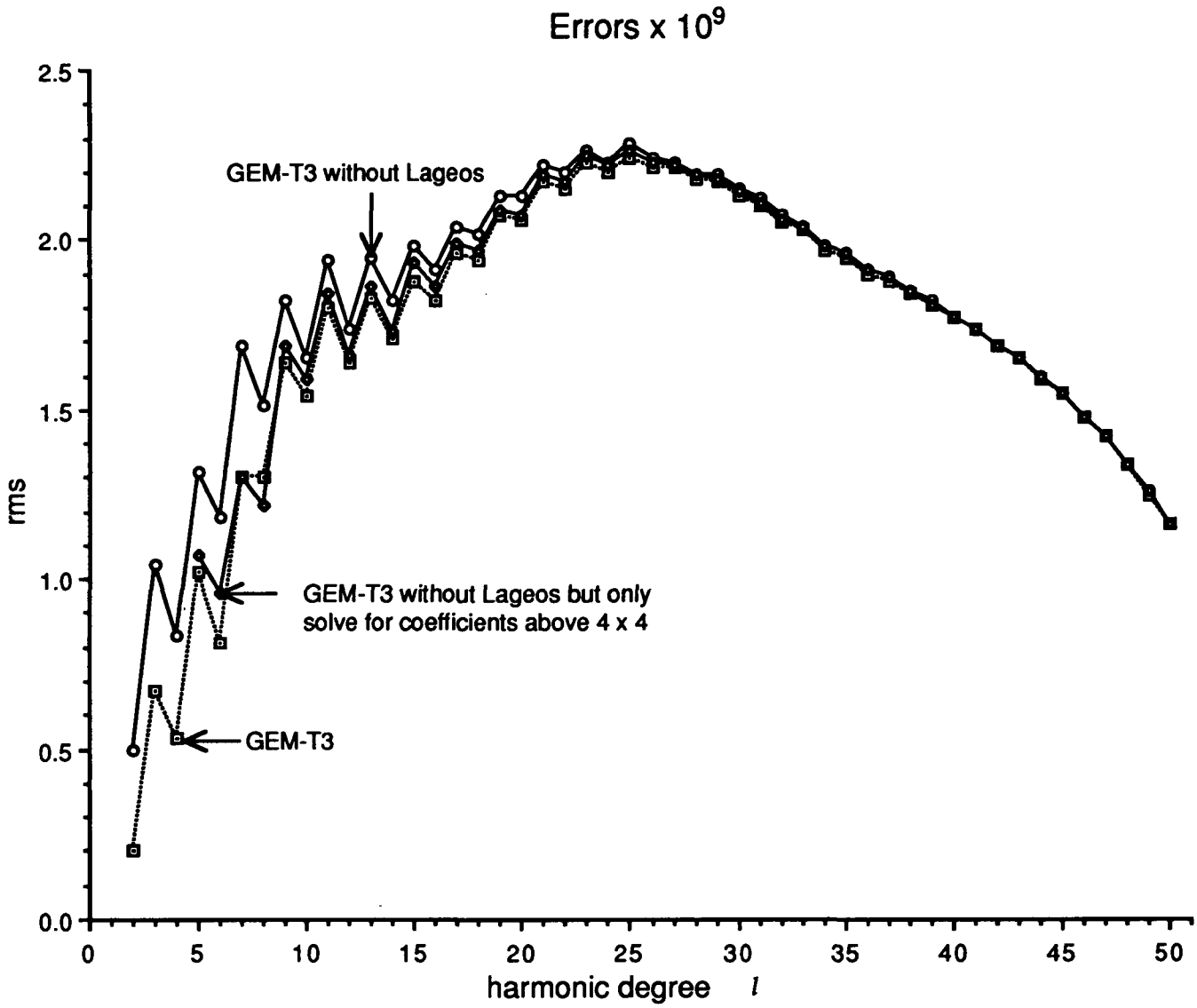

Table 4.1.c

CALIBRATION TESTS OF GEM-T3

Subset Solution Dataset	GEM-T3 Individual Calibration Factors *K*	GEM-T3 Sub group Calibration Factors *K*	GEM-T3 Group Calibration Factors *K*
Lageos'80 -'84 Lageos'84 -'86 Lageos'87	.57 .89 .43	1.03	1.03
Geos-3 Las+Alt	.43	.43	.75
Geosat Dop Geosat Alt	.66 .41	.43	
Seasat Las+ Dop Seasat Alt	.54 .33	.38	

Table 4.2

DATA WEIGHTS AND CALIBRATION OF GEM-T3

Subset Solution Dataset	GEM-T3 Weights σ_0' *	GEM-T3 Calibration Factors k
Geos-1 Las '77-'78	816 cm	.79
Geos-1 Las '80	353 cm	
Geos-2 Las '75-'77	913 cm	
Geos-3 Las '75-'78	1000 cm	
Geos-3 Las '80	224 cm	
BE-C Las '79-'82	577 cm	.96
Ajisai '86-feb '87	387 cm	1.14
Ajisai mar-apr '87	182 cm	
Starlette '83-'84	182 cm	
Starlette '86	182 cm	
Lageos'80-'84	112 cm	1.03
Lageos'84-'86	112 cm	
Lageos'87	112 cm	
DI-C,DI-D,Peole Las	1000 cm	1.00
Optical	11.2 arcsec	1.10
Geos-3:ATS Las	976 cm	.66
Geos-3:ATS SST	3.8 cm/sec	
Geos-3:ATS SST	8.5 cm/sec	
Landsat	10.5 cm/sec	
Oscar-14	14.1 cm/sec	1.11
Nova	4.5 cm/sec	
Geos-3 Las+Alt	577 cm	.75
Geosat Dop	7.1 cm/sec	
Geosat Alt.	353 cm	
Seasat Las	707 cm	
Seasat Dop	5.0 cm/sec	
Seasat Alt	353 cm	
Surface Gravity	3.2 mgals	.94

Figure 4.2

Rms of Coefficient Errors per Degree for GEM-T3S vs. GEM-T3

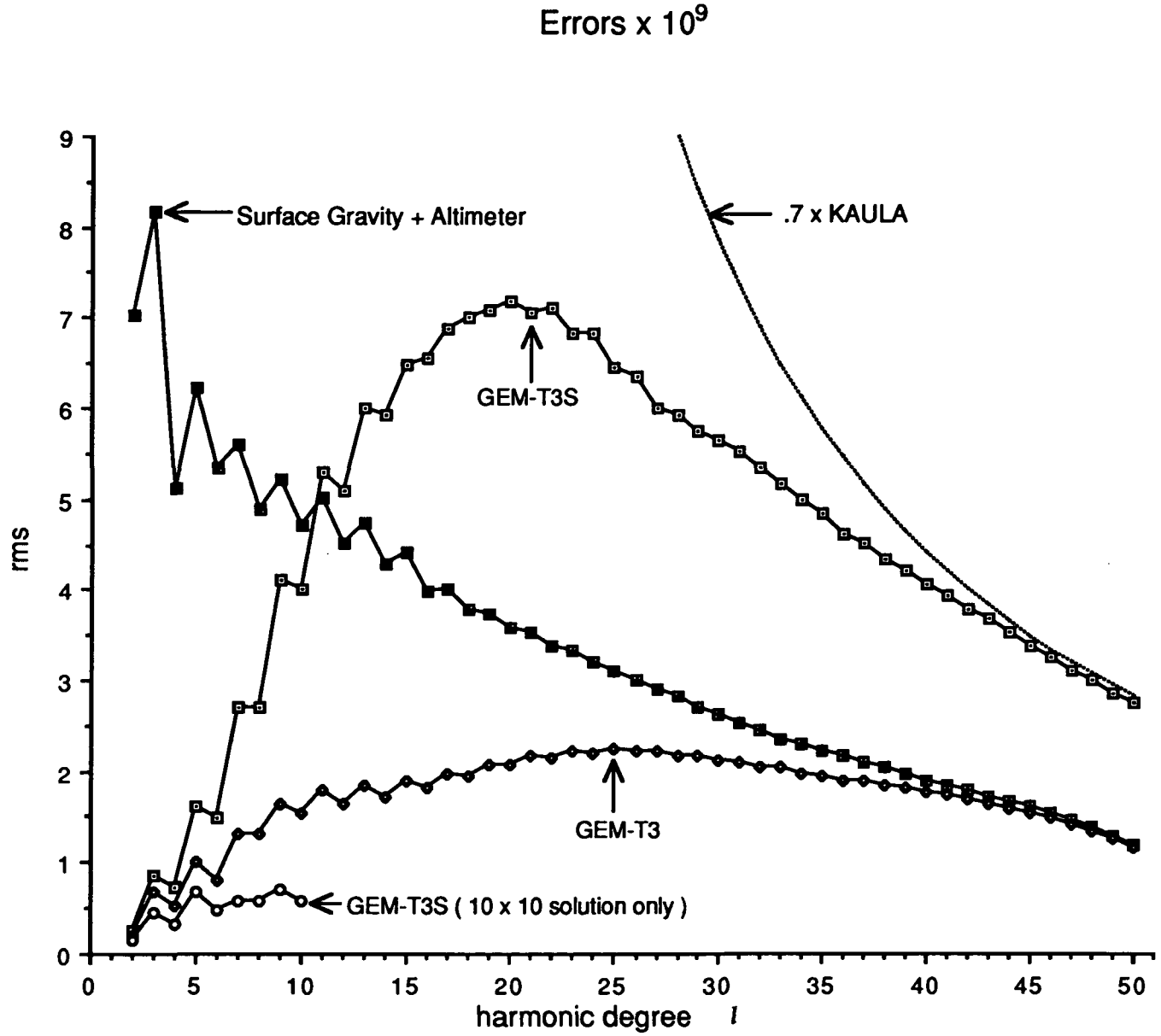

The need to employ data set groups in the weighting procedure is even more evident when combination models undergo calibration. In models like GEM-T3, the unattenuated gravitational signal provided by the altimeter and surface gravimetry observations alone are capable of strongly defining the entire intermediate and short wavelength field which makes the formerly unique satellite tracking data contributions at these wavelengths somewhat redundant statistically. Therefore, while it was attempted, removal of single data sets from GEM-T3 did not yield satisfactory calibration results. Hence, the relative weights established for the tracking data in GEM-T3S were largely maintained in forming GEM-T3. The contribution of GEM-T3S to GEM-T3 did undergo some down weighting, but this was accomplished with minimal change to the relative tracking data weights previously established. The only exceptions were for the tracking data used coincident with the altimeter data to define these orbits. These data were calibrated along with the altimeter data. This was done to avoid constraining unresolvable orbit parameters if altimeter data alone would have been used.

The down weighting of the satellite data in the combination model was modest. Further down weighting of the tracking data can have a negative impact on the solution's accuracy because the best signal at longer wavelength comes from tracking data as shown in Figure 4.2. Since the non-gravitational/systematic error contained in the altimeter and surface data lacks proper representation in the normal equations, this non-gravitational signal appears to the solution as strong gravity field information. We know that this is an incorrect characterization of these observations. Therefore, we must down weight the altimeter and surface gravity data to ensure that better quality signal coming from the laser tracking data, especially at long wavelength, controls the model definition.

When evaluating GEM-T3 in terms of its largest data groupings, the subset solution worked well when the complete GEM-T3 model was calibrated against models which eliminated either altimetry (e.g., GEM-T3 versus GEM-T3S plus surface gravity) or that eliminating surface gravimetry, e.g., GEM-T3 versus GEM-T3S plus altimetry. However, reliable results were not obtained with GEM-T3 versus a solution based on altimetry plus surface gravimetry, since this later subset yielded a significantly degraded model especially at long wavelength (Figure 4.2). This is largely because the spectral content of the satellite tracking data and the reliable part of the surface gravity/altimeter combination barely overlap. As will be described later, a new method to validate the weight and calibration of the combination model was developed.

4.3 CALIBRATION OF GEM-T3S WITH 5° x 5° MEAN GRAVITY ANOMALIES FROM ALTIMETRY

Altimeter-derived gravity anomalies were also used to calibrate GEM-T3S. Since the previous methods indirectly test a field by comparing it internally to its data contributions, a possible concern is that both the full and subset solutions share a common systematic error which would be untested using this method. The direct calibration of the model with independent and globally distributed altimeter gravity anomalies was undertaken to avoid this problem.

Mean 5° x 5° gravity anomalies are somewhat commensurate in field resolution with the harmonic model of GEM-T3S. The values we are using here were computed from the 1° x 1° values developed from the SEASAT and GEOS-3 Missions which were kindly provided to us by Rapp (1986). The gravity anomaly calibration was performed using the method given in Lerch et al., (1991a) for GEM-T1. We also corrected these altimeter anomalies using the high degree and order gravitational field of Rapp and Cruz (1986) to remove contributions to the Δg values for all terms

above degree 50 extending to degree 300 which are neglected from the GEM-T3S solution. The calibration factor obtained from this comparison is given as:

$$k = \left(\frac{\Sigma k_i^2}{1071} \right)^{1/2}$$

(eq 4.8)

where k_i is an individual calibration factor computed for each of the 1071 5° blocks as:

$$k_i = \frac{| \Delta g - \Delta g_c |_i}{[\sigma (\Delta g) + \sigma (\Delta g_c)]^{1/2}}$$

(eq 4.9)

and Δg and Δg_c are the observed and GEM-T3S -computed gravity anomalies. When computing the gravity anomalies from GEM-T3S we used the spectral smoothing operator of Pellinen (Jekeli and Rapp, 1980). The gravity anomaly uncertainties are obtained from the altimeter analysis of Rapp (1986) and GEM-T3S models respectively. The global calibration factor obtained for GEM-T3S from this analysis is:

$$k = 0.96$$

which indicated a high level of calibration consistency and gives an independent demonstration of the values of the calibration/data weighting approach.

4.4 CALIBRATION OF GEM-T3 AND GEM-T3S THROUGH PROJECTION ON DATA RESIDUALS

As noted earlier, the a posteriori orbit fit of the most precise data used in forming GEM-T3 is not close to the inherent noise level of these data. This is a vexing problem, for there are many error sources which contribute to this post-solution fit. We have some evidence that the error attributable to the static or tidal gravitational field is no longer the major contributing factor to the observation residuals. This conclusion is reached by taking individual satellite data sets like the laser data acquired on Ajisai, and giving these data extremely high weight in test solutions. When such solutions are then tested, there is little improvement in the orbital fit. This indicates that the static and tidal gravity signals in the laser observations are being well accommodated in the current GEM solutions. A second issue is the prediction of model accuracy on satellites yet to reach orbit like TOPEX. If we cannot fit data in the solution to their expected accuracy, can we reliably predict the model's performance on an independent satellite's orbit? While we can use the solution covariance to make accuracy predictions, these predictions are not easily testable.

To address both of these issues, we have adopted an additional calibration approach where we construct solutions which have our most accurate observation sets removed. These accurate data sets are then used to test the solution and its covariance. This testing is accomplished by projecting the gravitational, tide, station coordinate and polar motion uncertainties on the observation residuals and compare the results with the actual fit obtained with these data. This calibration did not include the effect of the orbital state parameters arising from data noise. However, these effects are much smaller than commission error made in modeling the various forces perturbing the satellite orbit and do not contribute significantly to the projection of errors on the data residuals. Since we have not calibrated the uncertainties for the non-gravitational parameters in the solution, cases which are dominated by the error in the gravitational field are

the most meaningful. For example, a subset version of GEM-T3S is developed which omits all Starlette data. This model predicts more than 1 meter RMS from gravity model errors on the Starlette range data. This model is then used to fit the Starlette data and the prediction of the observation residuals is compared to the actual fits which are obtained.

These experiments have been extended to evaluate the contribution of satellite altimeter data and surface gravimetry on the orbit determination performance of the models. For example, the GEM-T3S subset solution which lacks Starlette range data is combined with surface gravimetry (at the weight it is given in GEM-T3). This new model is tested using the Starlette data for its accuracy prediction. The same experiment is repeated using all of the altimeter data, and lastly for a model which combines both altimeter data and surface gravimetry in these test satellite solutions. This later subset model is GEM-T3 without Starlette data.

Such tests have been performed using Starlette, Lageos, Ajisai, and the GEOSAT altimeter data. These experiments provided two important insights into model performance: (a) by using accurate observation subsets and adopting a procedure where gravity error is the dominant error source, we can test our general field optimization approach and our gravity model accuracy estimates; and (b) we can assess the contribution, aliasing and treatment of the non-gravitational signal within the satellite altimeter and surface gravity data sets. While the contribution of these data to the field's geoid definition is rather well understood by this approach, herein we are able to detect any orbit determination problems resulting from the incorporation of these data in the gravity solution.

In addition, a calibration test was performed using the precise DORIS average range-rate data acquired on the SPOT-2 satellite which is independent of GEM-T3 and GEM-T3S.

The results of these tests for Starlette are presented in Table 4.3. A series of special models was developed which omitted all Starlette data. PGS-4214 is one such model and predicts a RMS residual for the Starlette range data of 131.8 cm. When this projection was studied, it was discovered that a disproportionate amount of this error contribution was due to the orbital resonance effects. To prevent a few select orders in the gravity model from overwhelming this test, two additional models were produced where the Starlette normals were allowed to contribute to the solution for (a) the order m = 13, 14, 15, 27 and 28, and (b) only the order m=14 and 27 resonance terms. The resonance error was greatly reduced in these latter models, and a more balanced test of the contribution of the entire gravity field that Starlette senses quite well was achieved. For example, when all 5 resonance orders have Starlette data contributions, the predicted RMS range error on the Starlette observations was reduced to 44.0 cm RMS. This result displays a reasonable agreement with the fit obtained using the data (31.8 cm) although the actual performance of the model was found to be significantly better than predicted. Therefore, our procedures for GEM-T3S gave an accurate although conservative estimate of the Starlette orbit error if Starlette was unavailable for inclusion in the model.

Table 4.3 also shows the contribution of surface gravity and altimeter data on the Starlette predictions and data fits. While predicted improvement in the fit to Starlette data may be expected when the gravity field includes surface gravity and/or altimeter observations, it is gratifying that the performance of the model actually does improve when these data are used in the solution. This indicates that our data processing and calibration of the surface gravity and altimeter data has largely reduced modeling inconsistencies which otherwise could arise from these data. It also shows significant improvement in orbit modeling coming from combination models over "satellite-only" models. The excellent agreement between the actual RMS of fit and the error projections for the combination model lacking Starlette shows that GEM-T3 will give accurate error projections on orbits not contained in the solution.

Table 4.4 presents the results obtained using the Ajisai laser data. However, since Ajisai and Starlette have similar orbit inclinations, tests solutions were also developed withholding both of these satellite data sets. These results are shown in Table 4.5. The gravity models which exclude

Table 4.3. Comparison of Predicted and Actual Starlette Data Fits When Starlette is Independent of the Gravity Solutions

Field (PGS-) Name	Contents:	Resonance Orders with Starlette Contributions	Actual RMS of fit (cm)	Predicted Errors RMS (cm) Total*	Gravity Only
GEM-T3S	T3S	___	11.4	8.4	7.1
PGS-4214	T3S-Starl	none	123.3	131.8	131.6
PGS-4394	T3S-Starl	13,14,15, 27,28	**31.8**	**44.0**	**43.8**
PGS-4431	T3S-Starl	14,27	59.9	55.1	55.0
PGS-4401	T3-Starl-Alt	13,14,15, 27,28	28.5	37.4	37.1
PGS-4434	T3-Starl-Alt	14,27	41.6	46.6	46.4
PGS-4400	T3-Starl-SGr	13,14,15, 27,28	23.4	23.1	22.6
PGS-4433	T3-Starl-SGr	14,27	35.3	29.1	29.0
PGS-4396	T3-Starl	13,14,15, 27,28	**20.2**	**20.6**	**20.1**
PGS-4432	T3-Starl	14,27	28.0	26.0	25.6

* Total = [gravity^2 + tides^2 + polar motion^2 + stations^2]$^{1/2}$ where each error source is derived from the range error projection from the covariance matrix of the solutions

Table 4.4. Comparison of Predicted and Actual Ajisai Data Fits When Ajisai is Independent of the Gravity Solutions

Field (PGS-) Name	Contents:	Resonance Orders with Ajisai Contributions	Actual RMS of fit (cm)	Predicted Errors RMS (cm) Total*	Gravity Only
GEM-T3S	T3S	____	8.6	6.7	4.0
PGS-4215	T3S-Aji	none	10.2	9.1	6.7

Table 4.5. Comparison of Predicted and Actual Ajisai Data Fits When Ajisai/Starlette are Independent of the Gravity Solutions

Field (PGS-) Name	Contents:	Resonance Orders with Starlette Contributions	Actual RMS of fit (cm)	Predicted Errors RMS (cm) Total*	Gravity Only
PGS-4312	T3S-Aji-Starl	none	26.1	43.6	42.7
PGS-4395	T3S-Aji-Starl	13,14,15, 27,28	**23.8**	**41.6**	**41.1**
PGS-4399	T3-Aji-Starl -Alt	13,14,15 27,28	23.8	38.9	38.4
PGS-4398	T3-Aji-Starl -SGr	13,14,15 27,28	23.8	27.1	26.3
PGS-4397	T3-Aji-Starl	13,14,15, 27,28	**24.2**	**24.9**	**24.0**

* Total = [gravity^2 + tides^2 + polar motion^2 + stations^2]$^{1/2}$ where each error source is derived from the range error projection from the covariance matrix of the solutions

only Ajisai data still perform well on Ajisai due to Starlette's contribution to the solution. However, with the additional elimination of the Starlette observations in the solution, both the fit to the Ajisai data and the range error projections increase considerably. When Starlette is excluded, gravity modeling is again found to be the dominant contributing error source within the Ajisai tests. The Ajisai calibrations are quite reasonable, and the projected errors are in good agreement with the actual fit to these data in all cases. However, the Ajisai orbital fits do not improve with the inclusion of surface gravimetry and altimetry although the error projections do improve. Nevertheless, in only one case was a slight degradation detected. This result can be explained by comparing the characteristics of the Ajisai and Starlette orbits. Ajisai is in a higher orbit than Starlette. The improvement in Starlette's orbital fits when including altimeter and/or surface gravimetry is likely a result of improvement in the definition of many high degree and order terms to which Starlette is sensitive. Ajisai is less sensitive to the shorter wavelength model, and is thereby testing the longer wavelength contributions to the models from altimeter and surface gravimetry. While the improvement predicted by the respective solution covariances through the inclusion of surface gravity and altimetry is not confirmed by the Ajisai data fits, the RMS of fit achieved using the GEM-T3-type solution does agree well with the prediction. It is the GEM-T3S-type models which are doing much better than their predictions.

The testing of the Lageos data is presented in Table 4.6. Lageos is in a high altitude orbit whose semi-major axis is nearly two Earth radii. Due to attenuation, the Lageos orbit is only sensitive to the lower degree terms in the gravitational model. This part of the model is best determined for it gives rise to the largest orbital perturbations and is sensed strongly by all satellites included in the solution. In Table 4.6, it is evident that gravitational models which include Lageos have small gravity error projections on Lageos range data. In the GEM-T3 and GEM-T3S projections, while the predicted error seems to agree with the actual fit obtained in the Lageos test arcs, these results are largely fortuitous. The projected errors coming from station and polar motion sources are likely over-estimated. For example, a typical polar motion parameter in the GEM-T3S solution has an estimated uncertainty of 3-4 mas. In reality, the pole parameters are better determined than this estimate indicates since they agree with those independently measured using VLBI at about 2 mas. Since these non-gravitational parameters are not directly calibrated, their error projections are not reliable. Moreover, there are also a host of other error sources which are not addressed in this experiment which contribute to the mismodeling of the Lageos range data within our orbital solutions. However, after excluding the Lageos data from the solutions, gravity model error again dominates. In these cases, the projected range error is in good agreement with the actual fit achieved using these test models. Furthermore, it is encouraging to see that the combination GEM-T3 model again outperforms the GEM-T3S "satellite-only" test solution and does so at the level predicted by the covariance matrices.

In the context of altimetry mission support, such as for TOPEX/Poseidon, we are most concerned with the radial orbital accuracy achieved using the GEM models. To test the prediction of radial orbit accuracy, test solutions were developed where SEASAT and GEOSAT tracking data were excluded from GEM-T3S. The covariance matrix from this test solution was then used to project the radial orbit error on the altimeter range data coincident with the GEOSAT tracking data. In this test, we sought to treat the geoid and orbit errors as separate issues and concentrate on the radial modeling provided by these test subset solutions. A GEOSAT tracking interval was selected to perform this test which is not part of the GEM-T3 solution. The geoid calculated from "satellite-only" models lacks good definition of the short wavelength gravitational signals. Therefore, in these computations, the geoid and dynamic height models from GEM-T3 were used when fitting the actual altimeter ranges. Hence, the projected altimeter range errors must consider two contributions: (1) the radial orbit error from the test gravity solution which is a dynamic error source and is the quantity which we are attempting to verify and calibrate; and (2) the commission error in the GEM-T3 geoid (as shown in Figure 5.4b) plus the GEM-T3 dynamic height model for GEOSAT (shown in Figure 6.5) which are obtained from the GEM-T3 covariance matrix. The geoid and dynamic height modeling uncertainties projected into the altimeter range data represents the

Table 4.6. Comparison of Predicted and Actual Lageos Data Fits When Lageos is Independent of the Gravity Solutions

Field (PGS-) Name	Contents:	Resonance Orders with Lageos Contributions	Actual RMS of fit (cm)	Predicted Errors RMS (cm) Total*	Gravity Only
GEM-T3S	T3S	___	7.5	7.5	0.8
PGS-4374	T3S-Lag	none	**14.2**	**12.3**	**9.4**
GEM-T3	T3	___	7.5	7.8	0.8
PGS-4427	T3-Lag	none	**10.2**	**10.0**	**6.2**

* Total = [gravity^2 + tides^2 + polar motion^2 + stations^2]$^{1/2}$ where each error source is derived from the range error projection from the covariance matrix of the solutions

error in defining the geometric shape of the overflown ocean surface and is satellite-independent, being strictly a function of latitude and longitude.

Table 4.7 compares the RMS of fit obtained using the GEOSAT altimetry compared to the projected error of the same quantity. The experiment was repeated with a test gravity solution which included surface gravimetry. Again, the GEM-T3 geoid and dynamic height models were used to define the geometric shape of the ocean surface and this error projection remains unchanged. With surface gravimetry included, the model predicts better GEOSAT radial accuracies, which is borne out by the improved fit it provides to the altimeter ranging. However, the improvement seen is smaller than projected. Lastly, Table 4.7 presents the altimeter fit and projection using the complete set of GEM-T3 models. Since this time period of GEOSAT altimeter data is not employed in the GEM-T3 solution, this is a further independent confirmation that the radial accuracy predicted by the calibrated covariance matrices yield reliable estimates of orbit accuracies.

The results of a calibration test for the complete GEM-T3 model using independent Doppler data acquired by the DORIS system on SPOT-2 is shown in Table 4.8. Herein we see excellent agreement between the predicted observation residuals and those obtained using GEM-T3.

Table 4.7. Calibration Test for GEM-T3 With GEOSAT Altimeter Data Using Models Independent of the Data

RMS of Altimeter (ALT) Residuals vs. Model Error Projections on Data

Projected Error (Note: GEM-T3 is used for geoid and SST projections)

Satellite Arc	Test Model	Dynamic	Geometric≠	(A) Total Error	(B) ALT Residuals	(B)÷(A) Calibration Factor
GEOSAT (870510) 6-days)	T3-ALT-SG*	159.8	23.8	161.6	139.4	.86
	T3-ALT**	114.1	23.8	116.6	124.4	1.06
	T3	12.1	23.8	29.6	25.6	.86

* GEOSAT, SEASAT, and GEOS-3 altimeter and ground track data along with surface gravity data removed from GEM-T3

** same as * with surface gravity data included in the model

≠ computed from GEM-T3 error covariance matrix for geoid and dynamic height fields

Table 4.8. Calibration Test for GEM-T3 With 50 French Stations of DORIS Data on SPOT-2

(Data Independent of Solution)

5-Day Arc RMS Residuals	Projected Error
.35 cm/sec	.35 cm/sec

5.0 RESULTS

5.1 GRAVITATIONAL FIELDS

The spherical harmonic coefficients for the GEM-T3 and GEM-T3S models are given in Tables 5.1 and 5.2. Figures 5.1 and 5.2 present the respective calibrated harmonic coefficient uncertainties for each of these fields. Because of the sometimes large correlations between harmonics in the solution, the full error covariance is required for a realistic definition of the errors in the model. The calibration of these solutions and a detailed discussion of their accuracy is found in Section 4. The global geoid computed for GEM-T3 is shown in Figure 5.3 and the corresponding free air gravity anomalies for the field are shown in Figure 5.3a.

In the GEM models, we use a frequency-independent computation in the time domain for the solid earth tidal deformation (Marsh et al., 1988). This implicitly removes the indirect tidal contribution from the second degree zonal harmonic, C(2,0) based on the adopted Love number, which for GEM-T3 and GEM-T3S, is $k_2 = 0.30$. To be consistent with the most recent International Association of Geodesy Resolution 16, adopted in 1983, the indirect tidal effect should be included in the reported value for C(2,0). While this has not been done in Tables 5.1 and 5.2, it is accomplished using the following correction (Rapp et al., 1991) yielding the so-called "zero-value of C(2,0)":

$$C(2,0)_{zero} = C(2,0)_{GEM} - 4.17357 \times 10^{-9}$$

The geoid uncertainty obtained from the solution covariance for the GEM-T3 model through degree 10 and the complete 50x50 model is displayed in Figures 5.4a and 5.4b. It is evident from these figures that at long wavelength, the satellite dynamics control the model definition. Therefore, the global geoid at these wavelengths is uniformly well determined. However, when the full spectral content of GEM-T3 is considered, one can clearly see the geographic distribution of the altimeter data which has been employed, with a large model uncertainty seen in ocean regions lacking this coverage. Likewise, the continents have quite different levels of estimated uncertainty depending on the quality and geographic distribution of the surface gravimetry. Presently, significant lack of coverage is found within the USSR, parts of South America and Africa and over the polar regions. Figure 5.5 presents the growth in geoidal uncertainty as a function of field truncation for typical ocean and continental locations. In the later case, we include United States and Asian locations to contrast the effect of good versus poor knowledge of the surface gravimetry. In general, the ocean geoid is known with an uncertainty of 20 to 25 cm for the spatial wavelengths contained in GEM-T3 (approximately 300 km and longer) for regions mapped by the altimeters. Knowledge over the best continental regions is at the 50-60 cm uncertainty level.

The geoid uncertainty due to commission errors complete to degree and order 50 for GEM-T3S is estimated to be 158 cm RMS while GEM-T3 is assessed to be 59 cm RMS. This RMS uncertainty for GEM-T3S is higher than that quoted for GEM-T2 in Marsh et al., (1990a): This is a result of a recalibration of the model using a modified approach which we believe to be more realistic. The details of this calibration were discussed in Section 4. We believe that GEM-T3S is a significant improvement over GEM-T2 and this discrepancy merely reflects the fact that the calibration of the errors is one of the difficult areas where improvement was required.

Figure 5.6 shows a comparison of the RMS coefficient error by degree for these models. Figure 5.7 shows the ability of the models at different levels of truncation to predict the values of the 5° x 5° gravity anomaly blocks obtained from SEASAT/GEOS-3 altimetry. GEM-T3S outperforms GEM-T2 whereas the error spectrum shown in Figure 5.6 might have indicated otherwise. Again, the calibration for GEM-T3S was more conservative than that previously done on GEM-T2.

TABLE 5.1 GEM-T3S Normalized Coefficients for Zonals
Units of 10^{-6}

Index n	m	Value C	Index n	m	Value C	Index n	m	Value C	Index n	m	Value C	Index n	m	Value C
2	0	-484.1648853	3	0	0.9570928	4	0	0.5388446	5	0	0.0685727	6	0	-0.1483014
7	0	0.0903888	8	0	0.0467358	9	0	0.0281079	10	0	0.0560775	11	0	-0.0513932
12	0	0.0332468	13	0	0.0423347	14	0	-0.0208865	15	0	0.0015621	16	0	-0.0077271
17	0	0.0201231	18	0	0.0095858	19	0	-0.0042338	20	0	0.0171279	21	0	0.0085040
22	0	-0.0075970	23	0	-0.0243201	24	0	-0.0016892	25	0	0.0065304	26	0	0.0020972
27	0	0.0012812	28	0	-0.0063334	29	0	-0.0026965	30	0	-0.0011753	31	0	0.0055504
32	0	-0.0010348	33	0	0.0015261	34	0	-0.0053579	35	0	0.0047667	36	0	-0.0033053
37	0	0.0004951	38	0	0.0014386	39	0	-0.0020201	40	0	0.0012413	41	0	0.0000954
42	0	0.0004031	43	0	0.0012005	44	0	-0.0001962	45	0	0.0012613	46	0	-0.0004856
47	0	0.0000966	48	0	0.0000508	49	0	-0.0003145	50	0	0.0004076			

TABLE 5.1 GEM-T3S Normalized Coefficients for Sectorials and Tesserals
Units of 10^{-6}

Index n	m	Value C	S	Index n	m	Value C	S	Index n	m	Value C	S
2	2	2.4392873	-1.4002539								
3	1	2.0285919	0.2492488	3	2	0.9035734	-0.6185702	3	3	0.7204805	1.4137526
4	1	-0.5360650	-0.4732505	4	2	0.3490773	0.6640277	4	3	0.9909801	-0.2006774
4	4	-0.1884629	0.3092360								
5	1	-0.0614086	-0.0956433	5	2	0.6549359	-0.3250473	5	3	-0.4523091	-0.2170083
5	4	-0.2959269	0.0500421	5	5	0.1745230	-0.6676291				
6	1	-0.0763592	0.0260724	6	2	0.0516966	-0.3761426	6	3	0.0574756	0.0089625
6	4	-0.0877032	-0.4716446	6	5	-0.2671762	-0.5362968	6	6	0.0097783	-0.2373639
7	1	0.2796031	0.0961554	7	2	0.3226442	0.0956056	7	3	0.2508335	-0.2115686
7	4	-0.2745535	-0.1257550	7	5	0.0021601	0.0193125	7	6	-0.3587597	0.1516096
7	7	0.0006206	0.0240072								
8	1	0.0227424	0.0597255	8	2	0.0727149	0.0688168	8	3	-0.0175659	-0.0866821
8	4	-0.2436470	0.0678796	8	5	-0.0245565	0.0884404	8	6	-0.0649028	0.3085013
8	7	0.0685744	0.0756640	8	8	-0.1231599	0.1216877				
9	1	0.1377340	0.0229788	9	2	0.0287114	-0.0360008	9	3	-0.1608155	-0.0847757
9	4	-0.0147058	0.0222450	9	5	-0.0189594	-0.0540296	9	6	0.0656089	0.2224804
9	7	-0.1194414	-0.0973529	9	8	0.1880592	-0.0032998	9	9	-0.0517649	0.0965484
10	1	0.0826226	-0.1314502	10	2	-0.0852370	-0.0535415	10	3	-0.0067776	-0.1539927
10	4	-0.0918192	-0.0761173	10	5	-0.0526750	-0.0452151	10	6	-0.0358302	-0.0789713
10	7	0.0090063	-0.0029436	10	8	0.0402578	-0.0917715	10	9	0.1248145	-0.0375152
10	10	0.0977682	-0.0187361								
11	1	0.0207172	-0.0305824	11	2	0.0099889	-0.0972582	11	3	-0.0305625	-0.1360325
11	4	-0.0346340	-0.0701708	11	5	0.0421022	0.0511969	11	6	-0.0012124	0.0320558
11	7	0.0053099	-0.0884769	11	8	-0.0060857	0.0247920	11	9	-0.0326476	0.0422627
11	10	-0.0524372	-0.0182421	11	11	0.0440720	-0.0656116				
12	1	-0.0533018	-0.0445791	12	2	0.0074436	0.0318592	12	3	0.0409301	0.0181622
12	4	-0.0631943	-0.0021721	12	5	0.0373449	0.0027699	12	6	0.0013501	0.0369868
12	7	-0.0164938	0.0350736	12	8	-0.0230986	0.0158669	12	9	0.0429353	0.0252072
12	10	-0.0072315	0.0318605	12	11	0.0106799	-0.0074979	12	12	-0.0040254	-0.0102479

TABLE 5.1 (continued)

Index		Value		Index		Value		Index		Value	
n	m	C	S	n	m	C	S	n	m	C	S
13	1	-0.0630221	0.0413113	13	2	0.0626114	-0.0635043	13	3	-0.0192898	0.0852221
13	4	-0.0122844	-0.0098290	13	5	0.0566290	0.0635707	13	6	-0.0276448	-0.0042989
13	7	0.0011957	-0.0073920	13	8	-0.0111519	-0.0091786	13	9	0.0248576	0.0446411
13	10	0.0400965	-0.0377824	13	11	-0.0445239	-0.0017651	13	12	-0.0311282	0.0861914
13	13	-0.0613859	0.0676584								
14	1	-0.0223408	0.0346869	14	2	-0.0348109	-0.0012663	14	3	0.0351679	0.0291629
14	4	-0.0086355	-0.0163999	14	5	0.0203927	-0.0072605	14	6	-0.0125213	0.0048436
14	7	0.0379390	-0.0057317	14	8	-0.0342699	-0.0167959	14	9	0.0353406	0.0300656
14	10	0.0378384	-0.0021328	14	11	0.0150813	-0.0394437	14	12	0.0084481	-0.0314408
14	13	0.0318272	0.0456078	14	14	-0.0517960	-0.0054900				
15	1	0.0102621	0.0087396	15	2	-0.0327824	-0.0339060	15	3	0.0518443	0.0210674
15	4	-0.0439912	0.0136448	15	5	0.0125111	0.0093185	15	6	0.0277011	-0.0422275
15	7	0.0624039	0.0134916	15	8	-0.0355526	0.0227401	15	9	0.0145953	0.0395405
15	10	0.0098007	0.0151404	15	11	0.0003139	0.0206892	15	12	-0.0318919	0.0121071
15	13	-0.0289726	-0.0045711	15	14	0.0072234	-0.0241312	15	15	-0.0193349	-0.0051955
16	1	0.0303027	0.0249945	16	2	-0.0220231	0.0226844	16	3	-0.0337939	-0.0404625
16	4	0.0432058	0.0470238	16	5	-0.0075090	-0.0046881	16	6	0.0084376	-0.0354765
16	7	-0.0000404	-0.0084670	16	8	-0.0150240	0.0056183	16	9	-0.0216707	-0.0344097
16	10	-0.0111558	0.0101025	16	11	0.0188631	-0.0031692	16	12	0.0203800	0.0054428
16	13	0.0136027	0.0014073	16	14	-0.0198840	-0.0383619	16	15	-0.0138939	-0.0315300
16	16	-0.0332765	0.0000283								
17	1	-0.0281134	-0.0376986	17	2	-0.0012070	0.0082543	17	3	0.0036428	0.0063070
17	4	0.0146804	0.0130315	17	5	-0.0111053	0.0000079	17	6	-0.0038057	-0.0230899
17	7	0.0244679	-0.0104317	17	8	0.0408311	0.0036507	17	9	0.0035342	-0.0352295
17	10	-0.0032920	0.0178248	17	11	-0.0141001	0.0125103	17	12	0.0300389	0.0164678
17	13	0.0162396	0.0205034	17	14	-0.0127178	0.0118335	17	15	0.0049091	0.0053751
17	16	-0.0307827	0.0021174	17	17	-0.0361056	-0.0221918				
18	1	-0.0022145	-0.0294727	18	2	0.0127338	0.0192491	18	3	-0.0050029	0.0061514
18	4	0.0485858	-0.0096583	18	5	0.0042638	0.0307928	18	6	0.0276421	-0.0145890
18	7	-0.0034728	0.0025243	18	8	0.0349791	-0.0034549	18	9	-0.0157496	0.0320922
18	10	0.0047029	-0.0101995	18	11	-0.0079630	0.0026507	18	12	-0.0278175	-0.0184398
18	13	-0.0063341	-0.0346908	18	14	-0.0091839	-0.0121414	18	15	-0.0398011	-0.0191650
18	16	0.0093834	0.0069556	18	17	0.0006902	0.0030919	18	18	-0.0018122	-0.0103516
19	1	-0.0167510	0.0002376	19	2	0.0119416	-0.0034015	19	3	0.0057655	0.0081235
19	4	0.0008283	0.0095902	19	5	-0.0026880	0.0286305	19	6	-0.0073234	0.0118612
19	7	0.0073034	-0.0002442	19	8	0.0200104	-0.0131394	19	9	0.0059931	0.0114506
19	10	-0.0356164	-0.0052417	19	11	0.0166678	0.0087057	19	12	-0.0005331	0.0044061
19	13	-0.0073410	-0.0282896	19	14	-0.0046531	-0.0128418	19	15	-0.0176620	-0.0133092
19	16	-0.0216271	-0.0083312	19	17	0.0280173	-0.0141824	19	18	0.0274804	-0.0077287
19	19	0.0020157	0.0036999								
20	1	0.0097453	-0.0019054	20	2	0.0129207	0.0099662	20	3	0.0003898	0.0240557
20	4	0.0023750	-0.0077399	20	5	-0.0142637	0.0030745	20	6	0.0017966	0.0014834
20	7	-0.0077675	0.0020434	20	8	-0.0024087	0.0052519	20	9	0.0188316	0.0120476
20	10	-0.0288688	-0.0091512	20	11	0.0158380	-0.0220435	20	12	-0.0053187	0.0149111
20	13	0.0278595	0.0064126	20	14	0.0105452	-0.0126071	20	15	-0.0247261	0.0006718
20	16	-0.0145261	-0.0000486	20	17	0.0017167	-0.0141816	20	18	0.0137934	0.0002385
20	19	-0.0101916	0.0092466	20	20	0.0056531	-0.0099809				
21	1	-0.0182109	0.0253697	21	2	0.0016251	-0.0011025	21	3	0.0057172	0.0173366
21	4	-0.0058591	0.0052956	21	5	0.0119098	-0.0072890	21	6	-0.0103662	0.0026451
21	7	-0.0068152	-0.0028738	21	8	-0.0135148	0.0017134	21	9	0.0244601	-0.0051934
21	10	-0.0060758	-0.0015837	21	11	0.0099976	-0.0375982	21	12	-0.0018323	0.0127422

TABLE 5.1 (continued)

Index		Value		Index		Value		Index		Value	
n	m	C	S	n	m	C	S	n	m	C	S
21	13	-0.0188783	0.0131923	21	14	0.0190823	0.0083995	21	15	0.0178574	0.0123625
21	16	0.0084478	-0.0058667	21	17	-0.0088444	-0.0029433	21	18	0.0216122	-0.0082306
21	19	-0.0245660	0.0121487	21	20	-0.0207621	0.0151894	21	21	0.0082560	-0.0063060
22	1	0.0100046	0.0033244	22	2	-0.0167598	0.0027580	22	3	-0.0002956	0.0041006
22	4	-0.0055637	0.0072957	22	5	-0.0001824	-0.0002202	22	6	0.0149424	-0.0023625
22	7	0.0066312	-0.0047588	22	8	-0.0091616	-0.0089349	22	9	0.0125285	-0.0038326
22	10	0.0076447	0.0174648	22	11	-0.0043675	-0.0133607	22	12	0.0052799	-0.0103255
22	13	-0.0173446	0.0194963	22	14	0.0103590	0.0080531	22	15	0.0259420	0.0045503
22	16	-0.0027703	-0.0060237	22	17	0.0072403	-0.0158220	22	18	0.0091064	-0.0130804
22	19	0.0084750	-0.0047278	22	20	-0.0138905	0.0187579	22	21	-0.0182926	0.0135550
22	22	-0.0035963	0.0016030								
23	1	0.0043055	0.0060830	23	2	-0.0066360	-0.0000534	23	3	-0.0098085	-0.0112061
23	4	-0.0127253	-0.0005352	23	5	-0.0089032	-0.0040374	23	6	-0.0037522	0.0129563
23	7	0.0005591	-0.0032105	23	8	0.0027498	-0.0004122	23	9	-0.0013889	-0.0089614
23	10	0.0129162	-0.0048380	23	11	0.0068416	0.0152227	23	12	0.0193387	-0.0191634
23	13	-0.0127078	-0.0051519	23	14	0.0029376	-0.0033319	23	15	0.0172998	-0.0026718
23	16	0.0076245	0.0134392	23	17	-0.0061091	-0.0101141	23	18	0.0026614	-0.0119902
23	19	-0.0075980	0.0066297	23	20	0.0145378	-0.0073123	23	21	0.0137992	0.0092344
23	22	-0.0060183	-0.0033685	23	23	-0.0023135	-0.0067952				
24	1	-0.0018256	-0.0120959	24	2	-0.0066492	0.0153892	24	3	0.0074812	-0.0068395
24	4	0.0046572	0.0062334	24	5	-0.0048869	-0.0088808	24	6	-0.0015168	-0.0059003
24	7	-0.0039312	0.0012144	24	8	0.0026645	0.0011374	24	9	-0.0039742	0.0031546
24	10	0.0136231	0.0099044	24	11	0.0177005	0.0131962	24	12	0.0129780	-0.0096400
24	13	-0.0011945	0.0019464	24	14	-0.0198269	0.0013194	24	15	0.0076059	-0.0140641
24	16	0.0024913	0.0068800	24	17	-0.0129594	-0.0072180	24	18	0.0015058	-0.0072364
24	19	-0.0050151	-0.0145294	24	20	-0.0038941	0.0039075	24	21	0.0105027	0.0051094
24	22	0.0029288	0.0003989	24	23	-0.0027817	-0.0092027	24	24	0.0037301	-0.0070748
25	1	0.0022276	-0.0016416	25	2	0.0032506	0.0052408	25	3	-0.0055189	-0.0043409
25	4	-0.0002769	0.0027232	25	5	0.0009251	-0.0012909	25	6	0.0096135	-0.0051520
25	7	0.0000591	-0.0060547	25	8	-0.0009791	-0.0014490	25	9	-0.0113758	0.0113100
25	10	0.0054615	-0.0033282	25	11	0.0070222	-0.0006241	25	12	-0.0094026	0.0127072
25	13	0.0076194	-0.0130502	25	14	-0.0243784	0.0100381	25	15	-0.0008903	-0.0032057
25	16	0.0045998	-0.0099141	25	17	-0.0138377	-0.0026518	25	18	-0.0013145	-0.0125280
25	19	0.0066293	0.0044974	25	20	-0.0017730	-0.0058322	25	21	0.0086463	0.0038440
25	22	-0.0044280	-0.0002217	25	23	0.0060622	-0.0054142	25	24	0.0051582	-0.0076870
25	25	0.0038311	0.0068059								
26	1	-0.0045729	-0.0011970	26	2	-0.0042336	0.0095605	26	3	0.0006878	-0.0002273
26	4	0.0115140	-0.0006681	26	5	0.0060911	0.0069675	26	6	0.0068451	0.0014339
26	7	0.0038680	-0.0024482	26	8	0.0067550	-0.0038484	26	9	-0.0002574	-0.0000819
26	10	-0.0090482	0.0037283	26	11	0.0004584	0.0040528	26	12	-0.0198829	0.0034978
26	13	-0.0010962	0.0015779	26	14	0.0078289	0.0043732	26	15	-0.0132121	0.0049938
26	16	0.0008237	-0.0054789	26	17	-0.0080006	0.0085201	26	18	-0.0096749	0.0110645
26	19	0.0015892	-0.0000865	26	20	0.0087362	-0.0130603	26	21	-0.0019513	-0.0043608
26	22	0.0125747	0.0066492	26	23	-0.0005275	0.0113276	26	24	-0.0009315	0.0131171
26	25	-0.0037714	0.0067698	26	26	0.0058188	0.0033006				
27	1	-0.0044894	0.0006423	27	2	0.0102227	0.0000576	27	3	0.0024345	-0.0053014
27	4	-0.0052389	-0.0018476	27	5	0.0037849	0.0035433	27	6	0.0077426	0.0037616
27	7	0.0014440	-0.0041880	27	8	-0.0016868	-0.0042890	27	9	-0.0031437	0.0011824
27	10	-0.0079587	0.0042484	27	11	-0.0004129	-0.0043314	27	12	-0.0071959	-0.0085109
27	13	-0.0070741	-0.0032111	27	14	0.0094295	0.0072591	27	15	-0.0044133	0.0005139
27	16	0.0063224	-0.0005542	27	17	0.0026463	-0.0008430	27	18	-0.0042326	0.0096213
27	19	0.0035165	-0.0065741	27	20	0.0040977	-0.0026627	27	21	0.0016034	-0.0088020
27	22	0.0008340	0.0060683	27	23	-0.0047486	-0.0008390	27	24	-0.0011170	-0.0004258

TABLE 5.1 (continued)

Index		Value		Index		Value		Index		Value	
n	m	C	S	n	m	C	S	n	m	C	S
27	25	0.0124629	0.0018754	27	26	-0.0047816	0.0046491	27	27	0.0073463	0.0043961
28	1	-0.0011112	0.0011171	28	2	-0.0097782	-0.0047845	28	3	0.0000365	0.0024808
28	4	0.0074792	-0.0025102	28	5	0.0002267	-0.0051544	28	6	-0.0083557	0.0006604
28	7	-0.0049382	0.0005254	28	8	0.0006685	-0.0020984	28	9	0.0055473	-0.0053615
28	10	-0.0032817	0.0008581	28	11	-0.0040450	0.0002559	28	12	0.0085219	0.0041469
28	13	0.0045966	0.0038743	28	14	-0.0032712	-0.0076352	28	15	-0.0108277	0.0024656
28	16	-0.0097629	-0.0099686	28	17	0.0096665	-0.0061770	28	18	0.0011124	-0.0002070
28	19	0.0023955	0.0194746	28	20	-0.0006179	0.0050410	28	21	0.0091114	0.0006105
28	22	-0.0033787	-0.0029365	28	23	0.0017825	0.0061758	28	24	0.0050867	-0.0120753
28	25	0.0038720	-0.0056010	28	26	0.0064546	0.0030284	28	27	-0.0084055	-0.0010571
28	28	0.0055871	0.0002380								
29	1	0.0027058	-0.0020187	29	2	0.0052774	-0.0015470	29	3	0.0039038	-0.0027338
29	4	-0.0060015	-0.0023035	29	5	0.0016863	0.0009801	29	6	0.0006187	0.0011967
29	7	-0.0027230	-0.0048083	29	8	-0.0053579	0.0027935	29	9	0.0021908	0.0006240
29	10	0.0023472	0.0034358	29	11	-0.0055338	0.0004176	29	12	-0.0015734	-0.0041025
29	13	-0.0009236	-0.0024275	29	14	-0.0080848	-0.0013380	29	15	-0.0011606	-0.0000159
29	16	0.0002742	-0.0070127	29	17	0.0011455	-0.0037321	29	18	0.0027636	-0.0001661
29	19	-0.0065290	0.0002918	29	20	-0.0048165	0.0043288	29	21	-0.0079954	-0.0065886
29	22	0.0157233	0.0040280	29	23	-0.0031612	0.0018809	29	24	-0.0021737	0.0005084
29	25	0.0089099	0.0045437	29	26	0.0084085	-0.0058707	29	27	-0.0072176	-0.0043119
29	28	0.0044831	-0.0068938	29	29	0.0038798	-0.0059998				
30	1	-0.0035407	0.0010481	30	2	-0.0104353	-0.0028708	30	3	-0.0003412	0.0019743
30	4	-0.0017454	-0.0000347	30	5	-0.0002917	-0.0042734	30	6	-0.0022676	0.0027807
30	7	-0.0008155	0.0023325	30	8	0.0011208	0.0006422	30	9	0.0006710	-0.0042463
30	10	0.0045205	-0.0022049	30	11	-0.0042910	0.0036716	30	12	-0.0007401	-0.0034243
30	13	0.0118244	0.0013426	30	14	0.0034672	-0.0004765	30	15	0.0014355	-0.0078076
30	16	-0.0048955	0.0040340	30	17	0.0014195	-0.0018802	30	18	-0.0007603	-0.0035421
30	19	-0.0058826	-0.0020043	30	20	-0.0030024	0.0078491	30	21	-0.0111651	-0.0063089
30	22	-0.0006811	-0.0022230	30	23	-0.0017849	-0.0037852	30	24	-0.0024228	0.0004950
30	25	0.0059361	-0.0038833	30	26	-0.0042099	0.0076368	30	27	-0.0060304	0.0133533
30	28	-0.0025454	-0.0023611	30	29	0.0000203	0.0044943	30	30	-0.0000520	-0.0002800
31	1	0.0048275	-0.0004363	31	2	0.0033100	0.0008955	31	3	-0.0003665	-0.0011844
31	4	-0.0007412	-0.0025412	31	5	-0.0041822	-0.0016758	31	6	-0.0021885	-0.0006402
31	7	0.0003298	0.0015657	31	8	-0.0012425	0.0006831	31	9	0.0012694	-0.0033781
31	10	0.0055107	-0.0039057	31	11	-0.0011746	0.0066644	31	12	0.0007187	0.0020519
31	13	0.0094826	0.0040923	31	14	-0.0112968	0.0022535	31	15	0.0000728	-0.0052464
31	16	-0.0033476	0.0014392	31	17	-0.0065968	0.0055273	31	18	0.0016482	0.0019801
31	19	0.0033864	0.0035899	31	20	-0.0014756	0.0044439	31	21	-0.0042204	0.0048509
31	22	-0.0057416	-0.0079308	31	23	0.0092540	0.0073943	31	24	-0.0041604	-0.0004030
31	25	-0.0128434	-0.0017347	31	26	-0.0111655	-0.0018416	31	27	0.0003879	0.0055092
31	28	0.0040120	0.0030630	31	29	-0.0021454	-0.0044115	31	30	-0.0001579	0.0061550
31	31	-0.0019940	-0.0017525								
32	1	-0.0052653	0.0016644	32	2	-0.0023372	0.0014425	32	3	0.0026744	0.0023805
32	4	0.0009487	-0.0015711	32	5	-0.0007603	-0.0025170	32	6	-0.0048240	-0.0012326
32	7	-0.0017812	0.0027595	32	8	-0.0001485	0.0034913	32	9	-0.0008088	0.0012446
32	10	0.0011115	-0.0022674	32	11	-0.0032513	-0.0006601	32	12	-0.0031747	0.0042104
32	13	0.0072572	0.0007097	32	14	0.0066424	0.0075456	32	15	0.0028732	-0.0043837
32	16	0.0054708	0.0031500	32	17	-0.0088448	0.0047501	32	18	0.0039755	-0.0012921
32	19	0.0024080	-0.0045938	32	20	0.0024743	-0.0016833	32	21	-0.0027024	0.0100339
32	22	-0.0041395	-0.0016909	32	23	0.0023387	0.0009106	32	24	-0.0037651	0.0027305
32	25	-0.0137712	0.0038092	32	26	-0.0004611	-0.0020303	32	27	-0.0035905	-0.0040263
32	28	0.0054298	0.0017479	32	29	-0.0001078	0.0048806	32	30	0.0039288	-0.0004130
32	31	0.0005348	-0.0006292	32	32	0.0006960	-0.0005170				

TABLE 5.1 (continued)

Index		Value		Index		Value		Index		Value	
n	m	C	S	n	m	C	S	n	m	C	S
33	1	-0.0006868	0.0029869	33	2	-0.0029025	0.0002111	33	3	-0.0025903	0.0013273
33	4	0.0020108	0.0026021	33	5	-0.0024197	0.0007226	33	6	0.0015634	-0.0039492
33	7	0.0002932	0.0010432	33	8	-0.0020655	0.0017881	33	9	0.0003700	0.0018257
33	10	0.0008956	0.0000743	33	11	0.0025819	-0.0004309	33	12	0.0025620	0.0035914
33	13	0.0008388	0.0082076	33	14	0.0029131	0.0022904	33	15	-0.0038857	0.0020012
33	16	-0.0001531	0.0003349	33	17	0.0005473	0.0056021	33	18	-0.0043099	-0.0020967
33	19	0.0052299	-0.0007223	33	20	0.0032559	-0.0013749	33	21	0.0028703	0.0012618
33	22	-0.0126709	-0.0040476	33	23	0.0013913	-0.0039592	33	24	0.0057516	-0.0012315
33	25	0.0013059	-0.0081458	33	26	0.0091841	-0.0005956	33	27	-0.0027992	0.0023171
33	28	-0.0038147	0.0033365	33	29	-0.0158185	0.0030330	33	30	0.0034280	-0.0148811
33	31	0.0019222	-0.0016037	33	32	0.0039558	0.0012118	33	33	-0.0009125	-0.0010679
34	1	0.0012616	-0.0003407	34	2	0.0027234	0.0019685	34	3	0.0003260	0.0005015
34	4	0.0030223	-0.0017356	34	5	-0.0000472	0.0024276	34	6	-0.0005232	-0.0006637
34	7	0.0026429	0.0003473	34	8	0.0005067	-0.0005414	34	9	-0.0006070	0.0011092
34	10	-0.0019152	-0.0003422	34	11	0.0029709	-0.0025228	34	12	0.0018740	0.0026275
34	13	-0.0046838	0.0046244	34	14	-0.0030911	0.0009245	34	15	0.0018740	0.0024590
34	16	0.0049590	-0.0018916	34	17	-0.0015371	0.0032500	34	18	-0.0014679	-0.0000324
34	19	0.0039867	-0.0008542	34	20	0.0025303	-0.0021047	34	21	0.0005549	-0.0013593
34	22	0.0035270	0.0013138	34	23	-0.0001281	-0.0037702	34	24	0.0057252	0.0025883
34	25	0.0088163	-0.0050854	34	26	0.0008241	-0.0107665	34	27	0.0117278	-0.0034130
34	28	0.0025202	-0.0143562	34	29	0.0008691	-0.0036429	34	30	-0.0092588	-0.0015334
34	31	0.0014202	0.0020567	34	32	-0.0015349	-0.0007826	34	33	0.0010213	0.0017048
34	34	-0.0000027	-0.0003232								
35	1	-0.0024448	0.0023994	35	2	-0.0031238	0.0000240	35	3	0.0008937	0.0023475
35	4	0.0025070	0.0022923	35	5	0.0012361	-0.0011199	35	6	0.0014452	-0.0016492
35	7	0.0003714	0.0001637	35	8	0.0005564	-0.0000846	35	9	-0.0004608	-0.0013740
35	10	-0.0019131	-0.0005219	35	11	-0.0007858	-0.0045579	35	12	0.0009083	-0.0017266
35	13	-0.0015558	0.0043626	35	14	-0.0045855	-0.0036079	35	15	-0.0025462	0.0043774
35	16	0.0024175	0.0013225	35	17	0.0049446	-0.0037347	35	18	0.0005858	-0.0019592
35	19	-0.0039319	-0.0000469	35	20	-0.0008673	-0.0001351	35	21	0.0045253	0.0024338
35	22	0.0024294	0.0027000	35	23	-0.0060217	-0.0017672	35	24	0.0044361	0.0038735
35	25	0.0016224	0.0041906	35	26	-0.0071940	-0.0032118	35	27	0.0106395	-0.0107112
35	28	0.0020982	-0.0130018	35	29	0.0095701	-0.0002859	35	30	0.0010445	-0.0024920
35	31	0.0022863	0.0033530	35	32	-0.0075272	-0.0032116	35	33	0.0022872	0.0059087
35	34	-0.0011744	-0.0004966	35	35	-0.0001432	0.0000997				
36	1	0.0038684	-0.0002626	36	2	0.0012013	0.0004159	36	3	-0.0020581	-0.0017981
36	4	0.0016029	-0.0002355	36	5	0.0000790	0.0017166	36	6	-0.0000199	-0.0009966
36	7	-0.0002275	-0.0010441	36	8	-0.0009510	-0.0007338	36	9	0.0000784	-0.0001418
36	10	-0.0012864	-0.0000700	36	11	0.0010054	0.0000570	36	12	-0.0012282	-0.0016080
36	13	-0.0027775	0.0033650	36	14	-0.0026673	-0.0048211	36	15	0.0021082	0.0002744
36	16	0.0011377	-0.0000163	36	17	0.0037861	-0.0017233	36	18	-0.0009892	-0.0001876
36	19	-0.0000283	0.0000999	36	20	-0.0021325	-0.0006982	36	21	0.0024136	-0.0045793
36	22	0.0002061	0.0021050	36	23	-0.0022370	-0.0008671	36	24	0.0002301	-0.0035470
36	25	0.0002676	0.0091052	36	26	0.0021661	0.0064223	36	27	-0.0078363	0.0043773
36	28	0.0014853	-0.0017752	36	29	-0.0003350	-0.0005930	36	30	-0.0055006	0.0017589
36	31	-0.0046938	0.0004249	36	32	-0.0008515	0.0025834	36	33	-0.0005408	-0.0056214
36	34	-0.0010749	0.0027601	36	35	0.0003238	-0.0015217	36	36	-0.0002161	0.0003154
37	1	0.0019761	0.0002567	37	2	-0.0006295	-0.0007260	37	3	-0.0006264	-0.0001379
37	4	-0.0000038	-0.0005495	37	5	0.0014014	-0.0007934	37	6	0.0000002	0.0001000
37	7	0.0003444	0.0003100	37	8	-0.0006309	0.0004709	37	9	-0.0003597	-0.0005134
37	10	-0.0001661	-0.0007892	37	11	0.0003363	0.0002772	37	12	-0.0035300	-0.0023768
37	13	-0.0020151	-0.0043063	37	14	-0.0039976	-0.0021303	37	15	0.0022282	0.0004775
37	16	-0.0000154	-0.0005844	37	17	0.0000288	-0.0005662	37	18	0.0013172	-0.0003409
37	19	-0.0012449	0.0006396	37	20	-0.0002401	-0.0022930	37	21	0.0000354	-0.0003067
37	22	0.0011147	0.0006460	37	23	-0.0009803	-0.0002122	37	24	-0.0037861	-0.0018059

TABLE 5.1 (*continued*)

Index		Value		Index		Value		Index		Value	
n	m	C	S	n	m	C	S	n	m	C	S
37	25	0.0035858	0.0024162	37	26	0.0037998	0.0050984	37	27	-0.0022770	0.0043656
37	28	0.0085177	0.0059619	37	29	0.0090416	0.0025426	37	30	-0.0020266	0.0058474
37	31	0.0000230	-0.0008018	37	32	0.0002299	0.0000572	37	33	-0.0022409	-0.0029887
37	34	0.0014673	-0.0002428	37	35	-0.0004774	-0.0005485	37	36	-0.0000771	-0.0005497
37	37	-0.0000614	-0.0000048								
38	1	0.0017556	-0.0005730	38	2	0.0005163	-0.0003801	38	3	0.0017170	0.0008501
38	4	-0.0012239	0.0010915	38	5	-0.0001639	-0.0000248	38	6	0.0009266	0.0001095
38	7	-0.0006279	-0.0005581	38	8	0.0002098	-0.0001610	38	9	0.0003968	0.0006367
38	10	0.0007987	-0.0002158	38	11	-0.0002650	0.0013298	38	12	-0.0006152	-0.0014731
38	13	-0.0007283	-0.0030525	38	14	-0.0002379	-0.0004698	38	15	-0.0007748	-0.0017872
38	16	-0.0013625	-0.0001665	38	17	-0.0003385	-0.0018986	38	18	-0.0001917	0.0005431
38	19	-0.0008782	-0.0007612	38	20	-0.0009285	0.0007748	38	21	0.0010069	0.0000537
38	22	0.0005776	-0.0004151	38	23	0.0005521	0.0047155	38	24	-0.0034301	-0.0015110
38	25	-0.0016049	-0.0046784	38	26	-0.0034191	0.0020501	38	27	-0.0018291	0.0024037
38	28	-0.0044494	-0.0025509	38	29	0.0034921	0.0010620	38	30	0.0024619	-0.0003820
38	31	0.0016541	-0.0018681	38	32	0.0015461	0.0006767	38	33	0.0009313	0.0011179
38	34	-0.0003426	-0.0017146	38	35	-0.0002789	0.0035545	38	36	0.0001324	-0.0015416
38	37	0.0007782	-0.0002085	38	38	-0.0000100	-0.0000195				
39	1	0.0005515	0.0001224	39	2	0.0006132	-0.0004435	39	3	-0.0006074	-0.0004503
39	4	-0.0000708	0.0004222	39	5	0.0001161	0.0001566	39	6	-0.0003794	0.0002988
39	7	0.0004966	0.0002377	39	8	0.0003670	-0.0008140	39	9	-0.0004722	0.0003327
39	10	-0.0000226	0.0006548	39	11	0.0016062	0.0010678	39	12	-0.0004437	0.0015767
39	13	-0.0010778	-0.0027453	39	14	0.0001588	-0.0001917	39	15	0.0024662	-0.0027370
39	16	-0.0011026	-0.0014208	39	17	-0.0007934	0.0000349	39	18	-0.0003069	0.0000045
39	19	-0.0003038	0.0004803	39	20	0.0000653	0.0001400	39	21	-0.0007890	-0.0003803
39	22	-0.0004852	0.0001737	39	23	0.0006211	0.0008404	39	24	-0.0034715	0.0000675
39	25	-0.0009455	-0.0029885	39	26	-0.0030737	0.0041816	39	27	-0.0066818	-0.0014588
39	28	-0.0037722	-0.0080576	39	29	-0.0055720	-0.0042680	39	30	0.0023502	-0.0046533
39	31	-0.0009265	-0.0008372	39	32	0.0020082	0.0002817	39	33	0.0007992	-0.0001184
39	34	-0.0008523	0.0005878	39	35	0.0003890	0.0002616	39	36	-0.0001721	0.0009778
39	37	-0.0001019	0.0002765	39	38	0.0001176	0.0000172	39	39	-0.0005810	-0.0004588
40	1	-0.0001654	0.0000015	40	2	0.0001575	-0.0002112	40	3	0.0001921	0.0005345
40	4	-0.0003259	-0.0002407	40	5	0.0000030	-0.0001243	40	6	0.0009929	-0.0006715
40	7	-0.0000938	-0.0001797	40	8	-0.0003616	0.0000837	40	9	0.0001661	0.0000776
40	10	0.0002065	0.0005138	40	11	-0.0004812	0.0001615	40	12	0.0010156	0.0013554
40	13	-0.0007498	-0.0023428	40	14	0.0009566	0.0014781	40	15	0.0002075	0.0012845
40	16	-0.0000922	-0.0003119	40	17	0.0003769	0.0004840	40	18	-0.0001172	0.0005854
40	19	0.0001341	0.0002727	40	20	-0.0000486	-0.0005648	40	21	-0.0002220	0.0007654
40	22	0.0005631	-0.0005670	40	23	0.0004545	-0.0028186	40	24	0.0014030	0.0020647
40	25	-0.0012415	-0.0025770	40	26	0.0055099	0.0005127	40	27	-0.0006233	-0.0005807
40	28	0.0019450	0.0027580	40	29	0.0018413	-0.0000899	40	30	-0.0003199	0.0005065
40	31	-0.0014235	0.0012509	40	32	-0.0018343	-0.0013605	40	33	-0.0008781	-0.0019627
40	34	0.0005470	-0.0001754	40	35	0.0011815	-0.0029420	40	36	-0.0003305	0.0016334
40	37	-0.0016504	0.0005276	40	38	-0.0004711	0.0001833	40	39	0.0006081	-0.0002920
40	40	-0.0003001	-0.0001841								
41	1	-0.0009287	0.0001297	41	2	0.0005710	0.0001227	41	3	-0.0000712	0.0000675
41	4	-0.0000655	0.0004143	41	5	-0.0002771	0.0002868	41	6	-0.0003591	0.0002920
41	7	-0.0000466	0.0001142	41	8	0.0006168	-0.0005152	41	9	0.0002459	0.0002943
41	10	0.0000266	0.0004729	41	11	0.0006099	0.0005391	41	12	0.0017031	0.0015074
41	13	0.0009212	0.0028448	41	14	0.0018852	0.0015432	41	15	0.0006760	-0.0012332
41	16	-0.0005471	-0.0004563	41	17	-0.0002821	0.0001330	41	18	-0.0002560	0.0003585
41	19	0.0004612	-0.0004497	41	20	0.0001009	0.0007784	41	21	-0.0001544	-0.0001346
41	22	0.0000956	0.0000255	41	23	0.0004374	0.0010142	41	24	0.0023253	-0.0008096
41	25	-0.0009379	0.0009570	41	26	0.0042544	-0.0079559	41	27	0.0005764	0.0008604
41	28	-0.0035305	-0.0019717	41	29	0.0001297	0.0021131	41	30	-0.0001028	-0.0025183

TABLE 5.1 (continued)

Index		Value		Index		Value		Index		Value	
n	m	C	S	n	m	C	S	n	m	C	S
41	31	0.0017765	0.0019098	41	32	-0.0004862	0.0009066	41	33	-0.0009264	0.0012366
41	34	-0.0007600	-0.0002381	41	35	0.0006198	0.0001476	41	36	-0.0002968	-0.0000369
41	37	-0.0001178	-0.0005404	41	38	-0.0005443	-0.0000112	41	39	-0.0002965	-0.0005058
41	40	0.0002047	-0.0007063	41	41	-0.0001307	0.0004896				
42	1	-0.0004694	-0.0001465	42	2	0.0004058	-0.0002145	42	3	-0.0005675	-0.0001036
42	4	-0.0000764	-0.0002910	42	5	0.0000153	-0.0000369	42	6	0.0004634	-0.0002822
42	7	0.0002324	0.0000795	42	8	-0.0002171	-0.0000101	42	9	-0.0000736	-0.0002462
42	10	-0.0002219	0.0004336	42	11	0.0006416	-0.0005518	42	12	0.0009634	-0.0003521
42	13	0.0007663	0.0003422	42	14	-0.0001790	-0.0005149	42	15	-0.0014332	0.0011161
42	16	0.0003372	-0.0001715	42	17	0.0000232	0.0005883	42	18	-0.0000345	-0.0000887
42	19	0.0004227	0.0007347	42	20	0.0003235	-0.0000967	42	21	-0.0005410	-0.0002223
42	22	-0.0001293	-0.0000251	42	23	0.0001102	-0.0014030	42	24	0.0004831	0.0002415
42	25	0.0012002	0.0027064	42	26	-0.0044055	-0.0037923	42	27	0.0017820	-0.0000040
42	28	0.0002041	0.0044317	42	29	-0.0025589	-0.0005135	42	30	0.0012852	0.0006132
42	31	0.0007646	-0.0006384	42	32	-0.0001851	0.0018980	42	33	0.0015510	0.0021801
42	34	-0.0003699	0.0008343	42	35	-0.0016261	0.0013550	42	36	0.0008033	0.0001417
42	37	0.0005386	-0.0005869	42	38	0.0007931	-0.0002435	42	39	-0.0002134	0.0012068
42	40	0.0003190	-0.0010664	42	41	-0.0002983	0.0005233	42	42	-0.0000290	0.0001247
43	1	-0.0003296	-0.0001613	43	2	-0.0002484	0.0000324	43	3	0.0001336	0.0001213
43	4	-0.0000223	-0.0000957	43	5	-0.0000419	0.0000686	43	6	-0.0001120	0.0001444
43	7	-0.0001792	-0.0000646	43	8	0.0001343	0.0001244	43	9	0.0002167	-0.0000850
43	10	0.0000727	-0.0001672	43	11	-0.0010050	-0.0003301	43	12	0.0004771	-0.0002685
43	13	0.0019833	0.0004343	43	14	-0.0011388	0.0007134	43	15	-0.0010133	-0.0000683
43	16	0.0000625	0.0000282	43	17	0.0001438	0.0000828	43	18	0.0001915	0.0002173
43	19	0.0001774	-0.0003741	43	20	-0.0000727	-0.0000462	43	21	0.0001550	0.0000802
43	22	0.0003254	-0.0000535	43	23	0.0003687	-0.0005048	43	24	0.0014525	0.0007611
43	25	-0.0001826	0.0000435	43	26	-0.0038955	0.0013003	43	27	0.0048705	0.0040429
43	28	-0.0005103	0.0086710	43	29	-0.0033143	-0.0002913	43	30	-0.0005848	-0.0008414
43	31	-0.0006833	-0.0003933	43	32	-0.0003783	-0.0006339	43	33	0.0013381	-0.0002956
43	34	0.0007339	-0.0001837	43	35	-0.0006831	-0.0003629	43	36	0.0010044	-0.0015032
43	37	0.0008469	0.0001497	43	38	0.0007125	0.0000950	43	39	0.0001973	0.0007811
43	40	0.0002444	-0.0002978	43	41	-0.0001301	0.0009476	43	42	0.0003903	0.0009204
43	43	0.0001135	0.0000012								
44	1	-0.0002100	-0.0002573	44	2	0.0000804	0.0002054	44	3	-0.0000992	-0.0001521
44	4	-0.0001081	0.0000772	44	5	-0.0000233	-0.0000093	44	6	0.0000034	0.0001419
44	7	0.0000018	0.0000862	44	8	0.0000464	-0.0000601	44	9	0.0000201	-0.0000801
44	10	0.0000167	0.0000299	44	11	-0.0000767	-0.0003205	44	12	-0.0004764	-0.0005327
44	13	0.0009189	0.0009443	44	14	0.0002347	-0.0015381	44	15	0.0003330	0.0000297
44	16	0.0002092	-0.0000511	44	17	-0.0002967	-0.0002477	44	18	-0.0001188	-0.0001983
44	19	0.0000625	0.0001821	44	20	0.0001254	0.0003489	44	21	-0.0001911	-0.0003508
44	22	-0.0002442	0.0000870	44	23	-0.0003400	0.0016189	44	24	-0.0000015	-0.0006788
44	25	-0.0003167	0.0013656	44	26	0.0006282	0.0004601	44	27	0.0038711	-0.0027597
44	28	-0.0011077	0.0001258	44	29	-0.0010555	0.0009471	44	30	0.0001490	-0.0001846
44	31	-0.0001763	0.0002153	44	32	-0.0004754	-0.0009182	44	33	-0.0012754	-0.0016144
44	34	0.0001884	-0.0003401	44	35	0.0007975	-0.0014334	44	36	-0.0006169	-0.0007959
44	37	0.0011542	0.0005463	44	38	-0.0004023	-0.0000367	44	39	0.0005398	-0.0006026
44	40	-0.0009693	0.0021188	44	41	0.0005214	-0.0015317	44	42	-0.0009083	-0.0007141
44	43	0.0006748	-0.0018544	44	44	0.0000649	0.0000643				
45	1	0.0001330	-0.0002666	45	2	0.0001873	-0.0001129	45	3	0.0000474	-0.0001683
45	4	0.0000055	-0.0002395	45	5	0.0000373	-0.0000072	45	6	0.0000391	0.0000213
45	7	0.0000133	-0.0001403	45	8	-0.0001722	0.0001808	45	9	-0.0001556	-0.0001381
45	10	0.0000786	-0.0002338	45	11	-0.0001268	-0.0000201	45	12	-0.0006201	-0.0008383
45	13	-0.0005235	-0.0013296	45	14	-0.0001716	-0.0004462	45	15	-0.0003399	0.0012049
45	16	0.0001184	-0.0000329	45	17	0.0000677	0.0000991	45	18	0.0000759	-0.0000263
45	19	-0.0000844	0.0000827	45	20	-0.0000532	-0.0002210	45	21	-0.0000622	0.0000632

TABLE 5.1 (continued)

Index		Value		Index		Value		Index		Value	
n	m	C	S	n	m	C	S	n	m	C	S
45	22	-0.0001196	-0.0001132	45	23	0.0000517	-0.0003245	45	24	-0.0011330	0.0001639
45	25	0.0006399	-0.0000022	45	26	0.0000600	0.0011835	45	27	-0.0028153	-0.0030360
45	28	0.0035059	0.0020001	45	29	-0.0007621	-0.0010657	45	30	0.0001551	0.0007760
45	31	0.0000563	-0.0000375	45	32	0.0000756	0.0000478	45	33	-0.0003659	0.0004937
45	34	-0.0000732	0.0001772	45	35	-0.0001250	0.0006483	45	36	-0.0011082	0.0015433
45	37	-0.0013207	-0.0000239	45	38	-0.0005849	-0.0001458	45	39	-0.0004025	-0.0009544
45	40	0.0003712	-0.0007213	45	41	0.0007662	-0.0021906	45	42	-0.0008726	-0.0013159
45	43	0.0001229	-0.0001389	45	44	0.0017498	0.0001443	45	45	0.0000520	-0.0000712
46	1	-0.0004168	0.0002594	46	2	-0.0003167	0.0002071	46	3	0.0002837	0.0000544
46	4	-0.0000273	0.0000966	46	5	-0.0000070	-0.0000357	46	6	-0.0001069	0.0001024
46	7	-0.0001932	0.0000355	46	8	0.0000741	0.0000022	46	9	0.0001083	0.0000936
46	10	0.0001846	-0.0001008	46	11	-0.0001684	0.0003888	46	12	-0.0006615	-0.0002657
46	13	-0.0005488	-0.0003230	46	14	-0.0002907	-0.0000760	46	15	-0.0007896	-0.0008140
46	16	0.0001162	-0.0000197	46	17	-0.0001335	-0.0002368	46	18	-0.0001090	0.0000056
46	19	-0.0000758	-0.0001933	46	20	0.0000061	0.0000338	46	21	-0.0000095	0.0001383
46	22	-0.0000409	0.0000078	46	23	0.0000498	0.0002734	46	24	-0.0003033	0.0002377
46	25	-0.0000758	-0.0019172	46	26	0.0009983	0.0020671	46	27	-0.0042107	0.0020997
46	28	0.0006129	-0.0040585	46	29	0.0003102	0.0004763	46	30	-0.0005024	-0.0001956
46	31	-0.0002056	0.0002854	46	32	0.0002710	-0.0003066	46	33	0.0003567	0.0005343
46	34	-0.0000940	0.0004022	46	35	-0.0001695	0.0013407	46	36	0.0001999	0.0001550
46	37	-0.0010972	-0.0000174	46	38	-0.0000368	-0.0000550	46	39	-0.0002748	0.0002421
46	40	0.0012088	-0.0020216	46	41	-0.0000058	0.0020528	46	42	0.0018486	0.0004507
46	43	-0.0025352	0.0040539	46	44	-0.0003271	-0.0002511	46	45	-0.0000658	0.0001563
46	46	0.0000070	-0.0000140								
47	1	0.0000284	-0.0001998	47	2	0.0000671	0.0000033	47	3	-0.0000160	-0.0002192
47	4	0.0000068	-0.0000334	47	5	-0.0000806	0.0000399	47	6	0.0000459	-0.0000232
47	7	0.0000934	-0.0000883	47	8	-0.0001030	-0.0000470	47	9	-0.0002000	0.0000126
47	10	0.0000476	0.0000124	47	11	-0.0000053	-0.0000828	47	12	-0.0001024	-0.0000621
47	13	-0.0005565	-0.0001592	47	14	0.0006071	-0.0003120	47	15	-0.0005710	-0.0001637
47	16	0.0000272	-0.0000262	47	17	-0.0000276	0.0000575	47	18	-0.0001351	-0.0000695
47	19	-0.0000180	0.0001307	47	20	0.0000545	0.0001154	47	21	-0.0001059	0.0000078
47	22	-0.0002701	-0.0000881	47	23	-0.0003609	0.0002366	47	24	-0.0003448	-0.0003816
47	25	-0.0002885	0.0000462	47	26	0.0026509	-0.0003834	47	27	0.0002445	-0.0008886
47	28	-0.0011169	-0.0049578	47	29	0.0029262	0.0003369	47	30	-0.0001443	0.0013175
47	31	0.0001204	0.0000858	47	32	-0.0001828	-0.0000499	47	33	-0.0002921	-0.0006239
47	34	0.0001592	-0.0001366	47	35	0.0001488	-0.0005105	47	36	0.0007626	-0.0008720
47	37	0.0011411	0.0004661	47	38	0.0002520	0.0000613	47	39	0.0002983	0.0006747
47	40	-0.0004613	0.0003563	47	41	-0.0017384	0.0054079	47	42	0.0010642	-0.0001644
47	43	-0.0021722	0.0019330	47	44	-0.0046778	-0.0004143	47	45	-0.0001894	0.0003461
47	46	-0.0001561	-0.0001918	47	47	0.0000203	-0.0000301				
48	1	-0.0001904	0.0002115	48	2	-0.0001549	-0.0000721	48	3	0.0001168	0.0000891
48	4	0.0001007	-0.0000659	48	5	0.0000299	-0.0000385	48	6	-0.0000637	-0.0000584
48	7	-0.0001115	0.0000332	48	8	-0.0000046	0.0000482	48	9	0.0000570	0.0000474
48	10	0.0000348	-0.0000196	48	11	-0.0001004	-0.0000590	48	12	0.0000520	0.0005122
48	13	-0.0001264	0.0000661	48	14	0.0005530	0.0002052	48	15	0.0012478	0.0004021
48	16	0.0000989	-0.0000279	48	17	0.0000959	0.0001635	48	18	-0.0000166	0.0000482
48	19	0.0000279	-0.0000927	48	20	0.0000303	-0.0002179	48	21	-0.0000182	0.0001792
48	22	0.0000187	0.0000396	48	23	0.0001863	-0.0006446	48	24	-0.0002831	0.0000305
48	25	0.0004551	-0.0003401	48	26	-0.0002312	-0.0009891	48	27	-0.0011871	0.0016478
48	28	0.0004768	-0.0007853	48	29	0.0008530	-0.0007754	48	30	-0.0000379	0.0000533
48	31	0.0002385	-0.0001742	48	32	0.0004152	0.0003072	48	33	0.0001466	0.0003248
48	34	-0.0000620	-0.0002566	48	35	0.0002108	-0.0004911	48	36	-0.0002955	-0.0002620
48	37	0.0006742	-0.0003197	48	38	0.0000483	0.0005084	48	39	0.0005774	-0.0004655
48	40	-0.0017643	0.0004353	48	41	-0.0011360	-0.0022011	48	42	-0.0014808	0.0007372
48	43	0.0044226	-0.0020206	48	44	0.0003692	0.0002494	48	45	0.0001556	-0.0003960
48	46	-0.0000317	0.0000493	48	47	0.0000058	-0.0000122	48	48	0.0000093	0.0000003

TABLE 5.1 (*continued*)

Index		Value		Index		Value		Index		Value	
n	m	C	S	n	m	C	S	n	m	C	S
49	1	-0.0001245	-0.0000624	49	2	-0.0001112	0.0001419	49	3	0.0000086	-0.0000316
49	4	-0.0000006	0.0000945	49	5	-0.0001072	0.0000473	49	6	0.0000260	-0.0000260
49	7	0.0000259	-0.0000156	49	8	0.0000135	-0.0000986	49	9	-0.0000102	0.0000617
49	10	0.0000174	0.0000919	49	11	0.0000367	-0.0000269	49	12	0.0000909	-0.0000905
49	13	-0.0001325	0.0008216	49	14	0.0007070	0.0002420	49	15	0.0004845	0.0002076
49	16	0.0000408	0.0000722	49	17	0.0000352	-0.0000287	49	18	-0.0000779	-0.0000277
49	19	0.0000345	-0.0000226	49	20	0.0000497	0.0001481	49	21	0.0000618	0.0000147
49	22	-0.0000588	-0.0000232	49	23	-0.0000809	-0.0000225	49	24	0.0004073	0.0001157
49	25	-0.0001435	-0.0003704	49	26	-0.0011948	0.0000848	49	27	0.0005678	0.0011395
49	28	-0.0009033	-0.0029050	49	29	0.0007355	0.0005088	49	30	-0.0002477	0.0004640
49	31	-0.0002616	-0.0002242	49	32	0.0000590	-0.0001352	49	33	0.0001630	-0.0001737
49	34	-0.0000772	0.0000699	49	35	0.0001306	0.0000943	49	36	-0.0004283	0.0005774
49	37	-0.0008257	-0.0003902	49	38	-0.0000293	0.0001603	49	39	0.0002395	-0.0002940
49	40	-0.0000077	-0.0002543	49	41	0.0034106	-0.0101665	49	42	-0.0014549	0.0020688
49	43	0.0050697	-0.0039608	49	44	0.0042554	0.0003230	49	45	0.0003285	-0.0005330
49	46	0.0004203	0.0005136	49	47	-0.0001563	0.0001688	49	48	-0.0000147	-0.0000093
49	49	-0.0000169	-0.0000030								
50	1	0.0001100	0.0000380	50	2	-0.0000548	-0.0000486	50	3	-0.0001166	0.0000003
50	4	0.0001187	-0.0000842	50	5	0.0000339	-0.0000112	50	6	-0.0000488	-0.0000636
50	7	0.0000212	0.0000366	50	8	-0.0000259	0.0000278	50	9	-0.0000121	-0.0000397
50	10	-0.0001071	0.0000140	50	11	0.0000242	0.0001143	50	12	0.0001140	0.0001535
50	13	0.0004406	0.0001640	50	14	-0.0000097	-0.0000178	50	15	-0.0006869	-0.0002899
50	16	0.0000339	-0.0000085	50	17	0.0000955	0.0001749	50	18	0.0000235	-0.0000178
50	19	0.0000428	0.0000128	50	20	0.0000216	-0.0000794	50	21	0.0000192	-0.0000495
50	22	-0.0000147	0.0000543	50	23	-0.0001378	-0.0000779	50	24	0.0002329	-0.0002118
50	25	-0.0001658	0.0009838	50	26	-0.0003467	-0.0000013	50	27	0.0025001	-0.0013269
50	28	-0.0006287	0.0017959	50	29	0.0003907	-0.0003540	50	30	0.0000512	-0.0000059
50	31	0.0000522	-0.0000771	50	32	-0.0000317	-0.0000971	50	33	-0.0002914	-0.0003761
50	34	0.0000980	-0.0001763	50	35	-0.0000984	-0.0000009	50	36	0.0003274	0.0002896
50	37	-0.0005064	0.0001804	50	38	0.0000915	-0.0004243	50	39	-0.0004816	0.0007204
50	40	0.0025019	0.0013518	50	41	0.0025674	0.0037702	50	42	0.0017986	0.0006239
50	43	-0.0045268	-0.0016842	50	44	-0.0000014	-0.0000062	50	45	-0.0001531	0.0004103
50	46	0.0000021	-0.0001335	50	47	0.0000104	-0.0000009	50	48	-0.0000570	-0.0000148
50	49	0.0000066	-0.0000041	50	50	-0.0000031	-0.0000042				

TABLE 5.2 GEM-T3 Normalized Coefficients for Zonals
Units of 10^{-6}

Index n	m	Value C	Index n	m	Value C	Index n	m	Value C	Index n	m	Value C	Index n	m	Value C
2	0	-484.1650994	3	0	0.9572011	4	0	0.5395212	5	0	0.0683433	6	0	-0.1495135
7	0	0.0913009	8	0	0.0488832	9	0	0.0268624	10	0	0.0540650	11	0	-0.0494638
12	0	0.0356285	13	0	0.0401122	14	0	-0.0215549	15	0	0.0032275	16	0	-0.0061891
17	0	0.0174266	18	0	0.0085246	19	0	-0.0021551	20	0	0.0199238	21	0	0.0060954
22	0	-0.0095105	23	0	-0.0216426	24	0	-0.0002292	25	0	0.0051981	26	0	0.0057590
27	0	0.0037752	28	0	-0.0099775	29	0	-0.0025026	30	0	0.0067263	31	0	0.0059286
32	0	-0.0040391	33	0	-0.0011500	34	0	-0.0045042	35	0	0.0068919	36	0	-0.0037241
37	0	-0.0066619	38	0	0.0006767	39	0	0.0004215	40	0	-0.0017227	41	0	-0.0023976
42	0	0.0018083	43	0	0.0045338	44	0	0.0024867	45	0	-0.0028338	46	0	-0.0015925
47	0	0.0000205	48	0	0.0031619	49	0	-0.0011610	50	0	-0.0032544			

TABLE 5.2 GEM-T3 Normalized Coefficients for Sectorials and Tesserals
Units of 10^{-6}

Index n	m	Value C	S	Index n	m	Value C	S	Index n	m	Value C	S
2	2	2.4390658	-1.4000946								
3	1	2.0277142	0.2492171	3	2	0.9044707	-0.6194477	3	3	0.7203425	1.4138845
4	1	-0.5361511	-0.4734360	4	2	0.3502181	0.6630152	4	3	0.9909337	-0.2009274
4	4	-0.1887706	0.3094237								
5	1	-0.0582802	-0.0960839	5	2	0.6527110	-0.3238637	5	3	-0.4523301	-0.2152958
5	4	-0.2955841	0.0496903	5	5	0.1737635	-0.6689070				
6	1	-0.0768942	0.0269984	6	2	0.0487345	-0.3740131	6	3	0.0572032	0.0093728
6	4	-0.0868265	-0.4713064	6	5	-0.2673304	-0.5367802	6	6	0.0096846	-0.2371348
7	1	0.2748687	0.0974659	7	2	0.3277950	0.0932467	7	3	0.2512201	-0.2152927
7	4	-0.2755610	-0.1237672	7	5	0.0013262	0.0186200	7	6	-0.3588314	0.1517387
7	7	0.0009703	0.0240836								
8	1	0.0236282	0.0588472	8	2	0.0775985	0.0660087	8	3	-0.0177852	-0.0863470
8	4	-0.2463398	0.0701796	8	5	-0.0250411	0.0894628	8	6	-0.0649237	0.3091226
8	7	0.0674622	0.0750948	8	8	-0.1241984	0.1201722				
9	1	0.1460968	0.0199707	9	2	0.0224514	-0.0335532	9	3	-0.1612938	-0.0759683
9	4	-0.0101377	0.0189722	9	5	-0.0171468	-0.0537733	9	6	0.0639143	0.2226482
9	7	-0.1190107	-0.0969910	9	8	0.1871323	-0.0023539	9	9	-0.0481324	0.0987392
10	1	0.0814935	-0.1302777	10	2	-0.0912766	-0.0511029	10	3	-0.0086059	-0.1550282
10	4	-0.0853424	-0.0787340	10	5	-0.0510215	-0.0511065	10	6	-0.0370547	-0.0783798
10	7	0.0075611	-0.0033501	10	8	0.0400547	-0.0916800	10	9	0.1243124	-0.0380328
10	10	0.0997532	-0.0224543								
11	1	0.0151438	-0.0266145	11	2	0.0167542	-0.0984958	11	3	-0.0284259	-0.1462895
11	4	-0.0406835	-0.0644826	11	5	0.0376146	0.0503126	11	6	-0.0003918	0.0349216
11	7	0.0038817	-0.0895537	11	8	-0.0069703	0.0253251	11	9	-0.0322248	0.0432902
11	10	-0.0520650	-0.0173310	11	11	0.0453181	-0.0690741				
12	1	-0.0545002	-0.0420954	12	2	0.0123808	0.0319206	12	3	0.0421598	0.0246728
12	4	-0.0695574	0.0028552	12	5	0.0319159	0.0096522	12	6	0.0041892	0.0401345
12	7	-0.0183894	0.0358166	12	8	-0.0255168	0.0161921	12	9	0.0409053	0.0243333
12	10	-0.0064899	0.0317633	12	11	0.0105182	-0.0068164	12	12	-0.0033602	-0.0108797

TABLE 5.2 (continued)

Index		Value		Index		Value		Index		Value	
n	m	C	S	n	m	C	S	n	m	C	S
13	1	-0.0559665	0.0395293	13	2	0.0543242	-0.0634283	13	3	-0.0211569	0.0963808
13	4	-0.0038557	-0.0133028	13	5	0.0607207	0.0646537	13	6	-0.0341536	-0.0042568
13	7	0.0035556	-0.0058836	13	8	-0.0116966	-0.0088473	13	9	0.0241467	0.0460357
13	10	0.0414659	-0.0361843	13	11	-0.0445391	-0.0043063	13	12	-0.0312803	0.0877964
13	13	-0.0614129	0.0678124								
14	1	-0.0206693	0.0304582	14	2	-0.0371952	-0.0033551	14	3	0.0329887	0.0210216
14	4	-0.0007851	-0.0192933	14	5	0.0259548	-0.0162511	14	6	-0.0188109	0.0054356
14	7	0.0376788	-0.0063813	14	8	-0.0348919	-0.0149848	14	9	0.0322984	0.0276200
14	10	0.0385106	-0.0010119	14	11	0.0147653	-0.0394554	14	12	0.0083128	-0.0313314
14	13	0.0319584	0.0452989	14	14	-0.0517851	-0.0050039				
15	1	0.0130794	0.0070987	15	2	-0.0235054	-0.0333181	15	3	0.0542768	0.0150957
15	4	-0.0434805	0.0070734	15	5	0.0113901	0.0088505	15	6	0.0342069	-0.0358331
15	7	0.0568236	0.0061453	15	8	-0.0327261	0.0235054	15	9	0.0117403	0.0374328
15	10	0.0114793	0.0155961	15	11	-0.0008754	0.0191309	15	12	-0.0324556	0.0147756
15	13	-0.0287572	-0.0042554	15	14	0.0054459	-0.0243198	15	15	-0.0195731	-0.0051538
16	1	0.0237694	0.0340855	16	2	-0.0212918	0.0268320	16	3	-0.0341109	-0.0271230
16	4	0.0391220	0.0454734	16	5	-0.0141227	0.0000332	16	6	0.0169119	-0.0328518
16	7	-0.0069833	-0.0070595	16	8	-0.0206218	0.0056652	16	9	-0.0240037	-0.0383121
16	10	-0.0109552	0.0128282	16	11	0.0184275	-0.0029384	16	12	0.0198974	0.0061632
16	13	0.0137124	0.0012041	16	14	-0.0196596	-0.0386771	16	15	-0.0134780	-0.0333624
16	16	-0.0361270	0.0037964								
17	1	-0.0273808	-0.0318449	17	2	-0.0191519	0.0077318	17	3	0.0127131	0.0085514
17	4	0.0068147	0.0210642	17	5	-0.0125322	0.0050564	17	6	-0.0109756	-0.0274779
17	7	0.0247642	-0.0035158	17	8	0.0378171	0.0039291	17	9	0.0022023	-0.0283061
17	10	-0.0025898	0.0186970	17	11	-0.0157889	0.0118557	17	12	0.0291379	0.0193775
17	13	0.0164865	0.0207531	17	14	-0.0140956	0.0116438	17	15	0.0053064	0.0053556
17	16	-0.0294099	0.0032961	17	17	-0.0329779	-0.0190370				
18	1	0.0012802	-0.0362621	18	2	0.0131239	0.0129394	18	3	-0.0033638	-0.0014744
18	4	0.0521647	0.0020212	18	5	0.0019873	0.0291036	18	6	0.0156997	-0.0115996
18	7	0.0058839	0.0033474	18	8	0.0301291	0.0024813	18	9	-0.0178758	0.0344506
18	10	0.0047002	-0.0051744	18	11	-0.0078403	0.0021961	18	12	-0.0287346	-0.0169012
18	13	-0.0061816	-0.0346579	18	14	-0.0088533	-0.0128693	18	15	-0.0393857	-0.0208743
18	16	0.0113318	0.0071843	18	17	0.0036682	0.0050833	18	18	0.0027594	-0.0105434
19	1	-0.0096289	-0.0029679	19	2	0.0275281	-0.0023289	19	3	-0.0033835	-0.0009951
19	4	0.0121511	-0.0042207	19	5	0.0154597	0.0273694	19	6	-0.0038121	0.0201077
19	7	0.0050712	-0.0063049	19	8	0.0294184	-0.0093126	19	9	0.0022164	0.0025673
19	10	-0.0337049	-0.0069966	19	11	0.0157465	0.0102937	19	12	-0.0021222	0.0081173
19	13	-0.0070964	-0.0280235	19	14	-0.0048124	-0.0129043	19	15	-0.0175393	-0.0137024
19	16	-0.0210506	-0.0075292	19	17	0.0306525	-0.0137472	19	18	0.0330342	-0.0087291
19	19	-0.0023480	0.0042819								
20	1	0.0052111	0.0058030	20	2	0.0174860	0.0137476	20	3	-0.0081594	0.0303065
20	4	0.0014180	-0.0229616	20	5	-0.0134176	-0.0035994	20	6	0.0113814	0.0008935
20	7	-0.0194055	-0.0015386	20	8	0.0049122	0.0034216	20	9	0.0190121	-0.0048859
20	10	-0.0301615	-0.0054108	20	11	0.0131223	-0.0184290	20	12	-0.0059513	0.0173580
20	13	0.0277741	0.0067269	20	14	0.0108561	-0.0139252	20	15	-0.0246481	-0.0014079
20	16	-0.0106927	-0.0002663	20	17	0.0044349	-0.0125965	20	18	0.0152411	-0.0005928
20	19	-0.0047068	0.0106734	20	20	0.0040221	-0.0112091				
21	1	-0.0171788	0.0205518	21	2	-0.0061390	0.0047932	21	3	0.0263792	0.0187134
21	4	-0.0094317	0.0139320	21	5	0.0043733	-0.0009704	21	6	-0.0116607	0.0018168
21	7	-0.0118226	0.0035729	21	8	-0.0152436	0.0040667	21	9	0.0150203	0.0068850
21	10	-0.0096824	-0.0005874	21	11	0.0084047	-0.0351392	21	12	-0.0019522	0.0140674

TABLE 5.2 (continued)

Index		Value		Index		Value		Index		Value	
n	m	C	S	n	m	C	S	n	m	C	S
21	13	-0.0185066	0.0136367	21	14	0.0203698	0.0079163	21	15	0.0178471	0.0109014
21	16	0.0084445	-0.0073172	21	17	-0.0056776	-0.0059467	21	18	0.0243699	-0.0094126
21	19	-0.0277508	0.0153133	21	20	-0.0263062	0.0158605	21	21	0.0075180	-0.0022236
22	1	0.0096642	-0.0009644	22	2	-0.0196408	-0.0020826	22	3	0.0092976	0.0082274
22	4	-0.0038186	0.0143386	22	5	-0.0082423	0.0035020	22	6	0.0138314	-0.0052023
22	7	0.0146058	0.0018228	22	8	-0.0234988	0.0021983	22	9	0.0102897	0.0083148
22	10	0.0051671	0.0241261	22	11	-0.0034556	-0.0164381	22	12	0.0038281	-0.0087932
22	13	-0.0169513	0.0197295	22	14	0.0101780	0.0077608	22	15	0.0263472	0.0042003
22	16	0.0012215	-0.0071400	22	17	0.0089480	-0.0134798	22	18	0.0087670	-0.0149852
22	19	0.0125137	-0.0037544	22	20	-0.0166678	0.0189291	22	21	-0.0246156	0.0223187
22	22	-0.0089299	0.0024228								
23	1	0.0063465	0.0130062	23	2	-0.0130827	-0.0040371	23	3	-0.0121940	-0.0173193
23	4	-0.0191162	0.0064667	23	5	0.0080082	-0.0023536	23	6	-0.0128872	0.0167174
23	7	-0.0061313	0.0028610	23	8	0.0055469	-0.0015897	23	9	-0.0005856	-0.0184242
23	10	0.0145345	-0.0031764	23	11	0.0080666	0.0153789	23	12	0.0170577	-0.0133824
23	13	-0.0111264	-0.0044652	23	14	0.0068014	-0.0020947	23	15	0.0184178	-0.0031340
23	16	0.0068979	0.0111168	23	17	-0.0040494	-0.0116880	23	18	0.0074796	-0.0120752
23	19	-0.0071169	0.0090105	23	20	0.0098040	-0.0068659	23	21	0.0157680	0.0132542
23	22	-0.0170923	0.0036873	23	23	0.0045640	-0.0108964				
24	1	-0.0050423	-0.0033127	24	2	-0.0021465	0.0134247	24	3	-0.0033462	-0.0082340
24	4	0.0071525	0.0037349	24	5	-0.0060088	-0.0126654	24	6	0.0042666	0.0009019
24	7	-0.0024921	0.0028966	24	8	0.0156587	-0.0048357	24	9	-0.0074084	-0.0162834
24	10	0.0113588	0.0172884	24	11	0.0118893	0.0185777	24	12	0.0116255	-0.0055536
24	13	-0.0025191	0.0027378	24	14	-0.0201557	-0.0006099	24	15	0.0066161	-0.0161023
24	16	0.0094515	0.0037852	24	17	-0.0119890	-0.0046886	24	18	-0.0007572	-0.0095976
24	19	-0.0049208	-0.0086425	24	20	-0.0049044	0.0076167	24	21	0.0081466	0.0126573
24	22	0.0033959	-0.0019883	24	23	-0.0071693	-0.0091901	24	24	0.0111403	-0.0032617
25	1	0.0065866	-0.0105297	25	2	0.0164017	0.0104728	25	3	-0.0068317	-0.0146739
25	4	0.0051081	0.0041833	25	5	-0.0037811	-0.0036623	25	6	0.0146476	0.0039237
25	7	0.0069129	-0.0074194	25	8	0.0051782	0.0016270	25	9	-0.0297856	0.0136280
25	10	0.0075753	-0.0047882	25	11	0.0044306	0.0079569	25	12	-0.0082098	0.0122275
25	13	0.0080624	-0.0116876	25	14	-0.0206731	0.0078295	25	15	-0.0036319	-0.0072531
25	16	0.0015538	-0.0128630	25	17	-0.0131607	-0.0014118	25	18	0.0006051	-0.0129151
25	19	0.0065226	0.0084412	25	20	-0.0062665	-0.0021786	25	21	0.0120874	0.0078646
25	22	-0.0127725	0.0041807	25	23	0.0084211	-0.0108240	25	24	0.0048718	-0.0077411
25	25	0.0089668	0.0052191								
26	1	-0.0026664	-0.0082430	26	2	-0.0015746	0.0092185	26	3	0.0090689	-0.0031308
26	4	0.0147221	-0.0165285	26	5	0.0038380	0.0106647	26	6	0.0114084	-0.0064852
26	7	-0.0002373	0.0011771	26	8	0.0035161	0.0014723	26	9	-0.0072798	0.0016990
26	10	-0.0130950	-0.0042049	26	11	-0.0017838	0.0018849	26	12	-0.0167307	0.0017457
26	13	0.0001750	0.0021769	26	14	0.0073958	0.0065215	26	15	-0.0136750	0.0076166
26	16	0.0025097	-0.0075036	26	17	-0.0108818	0.0080828	26	18	-0.0131056	0.0059036
26	19	-0.0011322	0.0029262	26	20	0.0066384	-0.0129144	26	21	-0.0065967	0.0016121
26	22	0.0121192	0.0084746	26	23	-0.0002176	0.0118854	26	24	0.0067431	0.0131699
26	25	0.0036502	0.0014493	26	26	-0.0008396	0.0053570				
27	1	0.0039251	-0.0001427	27	2	0.0036962	0.0031720	27	3	0.0056586	0.0021285
27	4	0.0005868	0.0092714	27	5	0.0157567	0.0079196	27	6	0.0000031	0.0062788
27	7	-0.0128755	-0.0023621	27	8	-0.0052481	-0.0098613	27	9	0.0001650	0.0076483
27	10	-0.0128522	0.0007021	27	11	0.0027288	-0.0076154	27	12	-0.0086416	0.0004264
27	13	-0.0045566	-0.0025631	27	14	0.0161760	0.0106701	27	15	-0.0023151	0.0010878
27	16	0.0043339	0.0016663	27	17	0.0045031	0.0009341	27	18	-0.0026533	0.0109539
27	19	-0.0008081	-0.0041454	27	20	0.0006343	0.0023214	27	21	0.0059841	-0.0055616
27	22	-0.0054096	0.0034241	27	23	-0.0050968	-0.0080894	27	24	0.0000222	-0.0006148

TABLE 5.2 (continued)

Index		Value		Index		Value		Index		Value	
n	m	C	S	n	m	C	S	n	m	C	S
27	25	0.0107286	0.0039942	27	26	-0.0058367	-0.0029276	27	27	0.0068460	0.0021541
28	1	-0.0073065	0.0062148	28	2	-0.0119628	-0.0116064	28	3	0.0024984	0.0090420
28	4	0.0042378	0.0033269	28	5	0.0055800	0.0003283	28	6	-0.0023067	0.0049177
28	7	-0.0008591	0.0052729	28	8	-0.0020045	-0.0053160	28	9	0.0082431	-0.0064753
28	10	-0.0075322	0.0079033	28	11	-0.0041603	0.0023566	28	12	0.0014296	0.0109002
28	13	0.0016576	0.0055353	28	14	-0.0062353	-0.0109321	28	15	-0.0108597	-0.0009772
28	16	-0.0031454	-0.0119188	28	17	0.0135711	-0.0034580	28	18	0.0038205	-0.0029946
28	19	0.0041720	0.0224177	28	20	-0.0018593	0.0046445	28	21	0.0077244	0.0053421
28	22	-0.0010523	-0.0058838	28	23	0.0045909	0.0029153	28	24	0.0096282	-0.0137817
28	25	0.0056097	-0.0172084	28	26	0.0086338	0.0029512	28	27	-0.0073755	0.0011044
28	28	0.0072606	0.0054995								
29	1	0.0019969	-0.0031928	29	2	-0.0025286	-0.0006536	29	3	0.0015286	-0.0082880
29	4	-0.0219913	-0.0001364	29	5	-0.0031615	0.0018419	29	6	0.0099066	0.0068548
29	7	-0.0044996	-0.0046636	29	8	-0.0121845	0.0074113	29	9	-0.0050682	-0.0038189
29	10	0.0084163	0.0018969	29	11	-0.0057378	0.0070722	29	12	-0.0026580	-0.0017172
29	13	-0.0007273	-0.0017458	29	14	-0.0061507	-0.0043946	29	15	-0.0077083	-0.0062682
29	16	-0.0001679	-0.0131772	29	17	0.0004103	-0.0028975	29	18	-0.0048796	-0.0036690
29	19	-0.0062727	0.0057826	29	20	-0.0060496	0.0030399	29	21	-0.0077158	-0.0040463
29	22	0.0124541	0.0007009	29	23	-0.0022660	0.0016815	29	24	0.0001001	-0.0009304
29	25	0.0056260	0.0063145	29	26	0.0090138	-0.0086781	29	27	-0.0067189	-0.0012353
29	28	0.0079715	-0.0053912	29	29	0.0104845	-0.0080465				
30	1	-0.0017521	0.0017543	30	2	-0.0092718	-0.0030842	30	3	0.0038608	-0.0094093
30	4	-0.0008453	-0.0030521	30	5	-0.0019984	-0.0033849	30	6	0.0000790	0.0014467
30	7	0.0070755	0.0014215	30	8	0.0016690	0.0025351	30	9	-0.0054353	-0.0075011
30	10	0.0016218	-0.0055395	30	11	-0.0110613	0.0099434	30	12	0.0123714	-0.0085305
30	13	0.0134213	0.0034719	30	14	0.0043796	0.0060830	30	15	-0.0016879	-0.0019559
30	16	-0.0088026	0.0033801	30	17	-0.0065044	-0.0043441	30	18	-0.0100442	-0.0078314
30	19	-0.0116142	0.0005241	30	20	-0.0039430	0.0107706	30	21	-0.0088595	-0.0065115
30	22	-0.0026737	-0.0055581	30	23	0.0033951	-0.0084043	30	24	-0.0026160	-0.0032619
30	25	0.0034385	-0.0150723	30	26	0.0003689	0.0100453	30	27	-0.0056395	0.0126688
30	28	-0.0037860	-0.0050892	30	29	0.0021892	0.0033030	30	30	-0.0000546	0.0041453
31	1	0.0046821	-0.0119952	31	2	0.0013617	0.0057275	31	3	-0.0063297	-0.0086681
31	4	0.0078644	-0.0008477	31	5	-0.0046503	-0.0020512	31	6	-0.0019375	0.0033188
31	7	0.0003401	-0.0024004	31	8	-0.0001190	0.0001917	31	9	-0.0014884	0.0017420
31	10	0.0001981	-0.0080774	31	11	0.0008508	0.0157155	31	12	0.0027783	0.0031965
31	13	0.0093805	0.0036678	31	14	-0.0060838	0.0031072	31	15	0.0017530	-0.0033483
31	16	-0.0046678	0.0052229	31	17	-0.0039763	0.0074653	31	18	-0.0011249	0.0019858
31	19	0.0025044	0.0022134	31	20	-0.0022369	0.0056220	31	21	-0.0061490	0.0052115
31	22	-0.0074700	-0.0090753	31	23	0.0086392	0.0061025	31	24	-0.0030547	-0.0029426
31	25	-0.0162449	-0.0017283	31	26	-0.0113406	-0.0009352	31	27	0.0006200	0.0101357
31	28	0.0089151	0.0028652	31	29	-0.0021781	-0.0041551	31	30	-0.0009474	-0.0056003
31	31	-0.0091732	-0.0018424								
32	1	-0.0019391	0.0003407	32	2	0.0083160	-0.0049377	32	3	-0.0015101	0.0013112
32	4	0.0020707	-0.0065448	32	5	0.0050124	0.0005448	32	6	-0.0059529	-0.0085579
32	7	0.0025425	0.0024856	32	8	0.0100396	0.0030255	32	9	0.0058074	0.0010645
32	10	0.0014409	-0.0056584	32	11	-0.0054062	0.0048110	32	12	-0.0125972	0.0139195
32	13	0.0041740	0.0023826	32	14	-0.0005282	0.0033685	32	15	0.0050419	-0.0077404
32	16	0.0025011	0.0031105	32	17	-0.0051155	0.0098834	32	18	0.0082254	0.0001041
32	19	-0.0001352	-0.0014221	32	20	0.0028538	0.0004540	32	21	-0.0015404	0.0090298
32	22	-0.0091125	-0.0020045	32	23	0.0067808	0.0000637	32	24	-0.0046501	0.0006893
32	25	-0.0180762	-0.0055121	32	26	0.0042350	-0.0037772	32	27	-0.0036280	-0.0070195
32	28	0.0029940	-0.0025111	32	29	0.0031745	0.0034310	32	30	-0.0042626	-0.0014378
32	31	-0.0032430	0.0005946	32	32	0.0050965	0.0024247				

TABLE 5.2 (continued)

Index		Value		Index		Value		Index		Value	
n	m	C	S	n	m	C	S	n	m	C	S
33	1	-0.0031761	0.0007467	33	2	-0.0068686	0.0015229	33	3	-0.0054440	0.0026048
33	4	-0.0032131	0.0031032	33	5	-0.0048493	0.0011091	33	6	0.0011795	-0.0048727
33	7	-0.0048291	-0.0001447	33	8	0.0011497	0.0110768	33	9	0.0030106	0.0036264
33	10	-0.0027285	0.0005344	33	11	0.0020113	-0.0077170	33	12	-0.0006898	0.0101392
33	13	0.0034057	0.0052654	33	14	0.0037931	0.0034850	33	15	-0.0050422	-0.0017867
33	16	0.0043555	0.0037108	33	17	-0.0043786	0.0094764	33	18	-0.0096200	-0.0049603
33	19	0.0084762	0.0024841	33	20	-0.0008262	-0.0080769	33	21	0.0017740	0.0030135
33	22	-0.0060013	-0.0132287	33	23	-0.0007092	-0.0071528	33	24	0.0090193	-0.0062329
33	25	0.0029450	-0.0104979	33	26	0.0105189	0.0027860	33	27	-0.0008576	0.0016316
33	28	0.0009262	0.0003210	33	29	-0.0159411	0.0040291	33	30	-0.0003193	-0.0173273
33	31	0.0036344	0.0022099	33	32	0.0065942	-0.0041506	33	33	0.0024732	0.0089333
34	1	-0.0001409	0.0024123	34	2	0.0096775	0.0063670	34	3	0.0101568	0.0074331
34	4	-0.0044927	-0.0037018	34	5	-0.0040991	0.0059137	34	6	-0.0003786	0.0035989
34	7	0.0044473	-0.0033291	34	8	-0.0135093	0.0037096	34	9	0.0000574	0.0040019
34	10	-0.0067002	0.0008173	34	11	-0.0042243	0.0024097	34	12	0.0103061	-0.0024785
34	13	-0.0052038	0.0031756	34	14	-0.0012806	0.0071895	34	15	-0.0009321	0.0071018
34	16	0.0005727	-0.0022595	34	17	-0.0055791	0.0004070	34	18	-0.0109181	-0.0058118
34	19	-0.0003830	0.0042619	34	20	0.0043770	-0.0057622	34	21	-0.0005696	-0.0057345
34	22	-0.0020442	0.0056377	34	23	-0.0014310	-0.0080674	34	24	0.0048197	0.0045287
34	25	0.0058310	-0.0095515	34	26	0.0024295	-0.0136956	34	27	0.0125297	-0.0041028
34	28	0.0010961	-0.0184406	34	29	0.0051354	-0.0047807	34	30	-0.0169733	-0.0019148
34	31	-0.0028722	0.0011197	34	32	0.0062400	0.0036500	34	33	0.0106401	0.0017421
34	34	-0.0057815	0.0009623								
35	1	-0.0110388	-0.0057405	35	2	-0.0132095	0.0024944	35	3	0.0021370	0.0035835
35	4	0.0001172	0.0018779	35	5	-0.0062657	-0.0089832	35	6	0.0015395	0.0060509
35	7	-0.0011804	0.0029285	35	8	0.0023739	0.0101232	35	9	-0.0041608	-0.0017540
35	10	-0.0063195	0.0068520	35	11	0.0032848	-0.0018095	35	12	0.0067832	-0.0054193
35	13	-0.0017808	0.0025409	35	14	-0.0068707	-0.0067366	35	15	-0.0143511	0.0087397
35	16	-0.0041017	-0.0012433	35	17	0.0007911	-0.0072514	35	18	-0.0044956	-0.0091086
35	19	0.0004439	-0.0043685	35	20	-0.0011466	0.0028395	35	21	0.0104901	-0.0001515
35	22	0.0022850	0.0041636	35	23	-0.0067572	-0.0019524	35	24	0.0021631	0.0048391
35	25	0.0053014	0.0017015	35	26	-0.0046326	0.0017638	35	27	0.0116954	-0.0131225
35	28	0.0068818	-0.0150441	35	29	0.0080871	0.0018070	35	30	-0.0026502	0.0036857
35	31	0.0064792	0.0066707	35	32	-0.0053443	-0.0060513	35	33	0.0060071	-0.0016236
35	34	-0.0020539	0.0025193	35	35	-0.0055092	-0.0049306				
36	1	0.0023560	0.0050525	36	2	-0.0048740	-0.0020946	36	3	-0.0006015	-0.0099549
36	4	0.0008456	-0.0030955	36	5	-0.0035798	0.0001649	36	6	0.0073452	-0.0046862
36	7	0.0007953	0.0041388	36	8	0.0003665	-0.0034356	36	9	0.0023524	-0.0012762
36	10	0.0013133	0.0053536	36	11	-0.0004069	0.0019427	36	12	-0.0007252	-0.0034005
36	13	-0.0065508	0.0056450	36	14	-0.0080168	-0.0041710	36	15	0.0007518	0.0021176
36	16	0.0003254	0.0020824	36	17	0.0054933	-0.0044269	36	18	0.0003531	0.0040581
36	19	-0.0042858	-0.0035370	36	20	-0.0057191	0.0016195	36	21	0.0062678	-0.0047130
36	22	0.0009862	-0.0006426	36	23	-0.0009853	0.0000774	36	24	0.0017057	-0.0045421
36	25	0.0034153	0.0137161	36	26	0.0030975	0.0073591	36	27	-0.0071208	0.0073981
36	28	0.0019694	-0.0034621	36	29	0.0027623	-0.0001453	36	30	-0.0089974	0.0043111
36	31	-0.0058913	-0.0007781	36	32	0.0074786	0.0047942	36	33	0.0013699	-0.0066836
36	34	-0.0057021	0.0048662	36	35	-0.0014267	-0.0090704	36	36	0.0013751	-0.0038035
37	1	-0.0049156	0.0000010	37	2	-0.0040717	-0.0121681	37	3	-0.0012606	0.0023331
37	4	0.0030456	0.0004847	37	5	-0.0067343	-0.0012726	37	6	-0.0025474	0.0067216
37	7	0.0032984	0.0016145	37	8	-0.0003339	-0.0016667	37	9	0.0014276	-0.0018175
37	10	-0.0002799	0.0016925	37	11	0.0023445	0.0001202	37	12	-0.0023757	-0.0007566
37	13	-0.0001109	-0.0071643	37	14	-0.0027542	-0.0027844	37	15	0.0081779	-0.0015877
37	16	0.0025799	0.0121828	37	17	0.0034629	-0.0018732	37	18	-0.0006381	0.0028466
37	19	-0.0056396	0.0002456	37	20	-0.0066777	-0.0041323	37	21	0.0015215	-0.0018213
37	22	0.0065414	0.0008810	37	23	-0.0011832	0.0008553	37	24	-0.0053148	-0.0060258

TABLE 5.2 (continued)

Index		Value		Index		Value		Index		Value	
n	m	C	S	n	m	C	S	n	m	C	S
37	25	0.0047611	-0.0027142	37	26	0.0034336	0.0087185	37	27	-0.0029964	0.0033606
37	28	0.0128425	0.0045323	37	29	0.0070112	0.0043474	37	30	-0.0064958	0.0123353
37	31	0.0025817	-0.0060123	37	32	-0.0030583	0.0053792	37	33	0.0001545	-0.0156965
37	34	0.0019726	-0.0008856	37	35	-0.0081669	-0.0085347	37	36	-0.0033317	-0.0040689
37	37	0.0035724	-0.0024595								
38	1	0.0051868	0.0005152	38	2	0.0053427	0.0012862	38	3	-0.0012612	-0.0011765
38	4	0.0006688	-0.0003666	38	5	-0.0046791	0.0051471	38	6	-0.0079824	0.0034923
38	7	-0.0020373	-0.0012743	38	8	0.0010329	0.0019980	38	9	0.0035695	0.0004752
38	10	-0.0031151	-0.0034466	38	11	-0.0011352	0.0056709	38	12	-0.0012791	-0.0028368
38	13	-0.0009556	-0.0083390	38	14	-0.0025002	0.0012922	38	15	0.0021553	-0.0027905
38	16	-0.0050750	0.0054249	38	17	0.0014166	0.0016680	38	18	0.0065761	-0.0012532
38	19	0.0010060	-0.0013716	38	20	0.0010583	-0.0021540	38	21	0.0016723	-0.0001027
38	22	0.0004339	0.0071497	38	23	-0.0002480	0.0043683	38	24	-0.0084124	0.0001756
38	25	-0.0014453	-0.0007891	38	26	-0.0039493	0.0045460	38	27	-0.0016060	0.0069831
38	28	-0.0043893	-0.0038518	38	29	0.0059171	0.0020835	38	30	0.0011511	0.0026892
38	31	0.0023266	-0.0043175	38	32	0.0025487	0.0030305	38	33	-0.0000432	0.0075551
38	34	-0.0044932	0.0019497	38	35	0.0041587	0.0040092	38	36	-0.0004538	-0.0020779
38	37	-0.0018945	0.0010750	38	38	0.0030752	-0.0011208				
39	1	-0.0029291	0.0049006	39	2	0.0039756	0.0045104	39	3	-0.0014023	0.0044364
39	4	-0.0025898	-0.0028432	39	5	0.0007810	0.0031819	39	6	0.0006507	0.0041436
39	7	0.0004544	-0.0029071	39	8	0.0009166	0.0091713	39	9	0.0051866	0.0038905
39	10	0.0001178	0.0000877	39	11	0.0099610	-0.0001755	39	12	-0.0029172	0.0067749
39	13	-0.0008276	-0.0035592	39	14	-0.0044839	0.0007530	39	15	-0.0024110	0.0017039
39	16	-0.0014517	-0.0027009	39	17	-0.0014440	-0.0020140	39	18	0.0010577	-0.0019332
39	19	0.0037789	0.0047925	39	20	-0.0003241	-0.0097518	39	21	-0.0027525	-0.0020255
39	22	-0.0033813	-0.0004058	39	23	-0.0026940	0.0043824	39	24	-0.0068925	0.0057119
39	25	-0.0020101	-0.0027154	39	26	-0.0023117	0.0071160	39	27	-0.0077364	-0.0021167
39	28	-0.0024204	-0.0101477	39	29	-0.0020169	-0.0033467	39	30	0.0055821	-0.0098472
39	31	0.0018862	-0.0073454	39	32	0.0001311	0.0052857	39	33	-0.0083180	0.0003784
39	34	-0.0009031	0.0001508	39	35	-0.0103099	0.0028057	39	36	0.0028572	-0.0017494
39	37	-0.0016599	-0.0048817	39	38	-0.0016177	0.0037600	39	39	-0.0000654	0.0001047
40	1	0.0032840	-0.0001586	40	2	-0.0021234	0.0011420	40	3	-0.0031044	-0.0025156
40	4	0.0017363	-0.0043984	40	5	0.0088006	0.0003928	40	6	-0.0001346	0.0009513
40	7	-0.0026367	0.0053655	40	8	0.0040907	0.0007677	40	9	-0.0010176	0.0008677
40	10	-0.0042810	0.0032747	40	11	0.0020340	-0.0001802	40	12	0.0044421	0.0000164
40	13	-0.0037796	-0.0018936	40	14	0.0006834	0.0015879	40	15	-0.0038797	0.0005316
40	16	-0.0031858	-0.0037195	40	17	0.0005927	-0.0008076	40	18	-0.0005346	-0.0013222
40	19	-0.0012587	-0.0000521	40	20	-0.0043835	0.0046265	40	21	-0.0014222	-0.0011424
40	22	-0.0063277	-0.0117123	40	23	-0.0012227	-0.0094841	40	24	0.0030406	0.0039924
40	25	0.0007345	-0.0028817	40	26	0.0060268	-0.0019383	40	27	-0.0005875	0.0011196
40	28	0.0029705	0.0049953	40	29	0.0017296	0.0011912	40	30	0.0008827	0.0011420
40	31	-0.0055260	0.0005049	40	32	-0.0033430	-0.0027049	40	33	-0.0031163	-0.0032749
40	34	0.0030161	-0.0004945	40	35	0.0052964	-0.0050303	40	36	0.0004912	0.0040246
40	37	-0.0023041	0.0009372	40	38	0.0000925	0.0051273	40	39	0.0057131	0.0021486
40	40	-0.0013794	-0.0021706								
41	1	-0.0032974	-0.0024119	41	2	0.0028399	0.0014783	41	3	0.0034184	0.0032957
41	4	-0.0015694	0.0019214	41	5	0.0012139	-0.0016050	41	6	-0.0001380	0.0005462
41	7	0.0009845	0.0007174	41	8	-0.0020735	-0.0031634	41	9	-0.0044253	0.0036733
41	10	0.0048671	-0.0006390	41	11	0.0020043	-0.0041575	41	12	0.0007892	0.0005245
41	13	-0.0014747	0.0009168	41	14	0.0012302	-0.0012876	41	15	-0.0005881	0.0013570
41	16	-0.0020793	-0.0004557	41	17	-0.0011739	0.0011708	41	18	0.0005731	0.0047586
41	19	0.0004196	-0.0008594	41	20	-0.0008079	-0.0009923	41	21	0.0001517	-0.0000071
41	22	-0.0056367	-0.0008416	41	23	0.0006823	-0.0092436	41	24	0.0039405	-0.0012279
41	25	-0.0009173	0.0025235	41	26	0.0042286	-0.0057720	41	27	0.0015488	-0.0000018
41	28	-0.0013986	-0.0042759	41	29	-0.0030313	0.0037440	41	30	0.0026878	-0.0015818

TABLE 5.2 (continued)

Index		Value		Index		Value		Index		Value	
n	m	C	S	n	m	C	S	n	m	C	S
41	31	0.0086719	0.0021279	41	32	-0.0052892	0.0042570	41	33	-0.0040296	0.0074972
41	34	-0.0022838	0.0005172	41	35	-0.0098255	0.0043609	41	36	0.0017542	-0.0012226
41	37	-0.0009056	-0.0100823	41	38	-0.0065801	-0.0000297	41	39	-0.0035437	-0.0002503
41	40	0.0020794	-0.0019584	41	41	0.0022039	0.0040887				
42	1	-0.0010549	0.0024804	42	2	-0.0020493	-0.0017886	42	3	-0.0000935	0.0054527
42	4	0.0019032	0.0017889	42	5	-0.0056812	-0.0044196	42	6	-0.0006180	-0.0007461
42	7	0.0035194	-0.0021540	42	8	0.0008779	0.0015092	42	9	-0.0003542	0.0011971
42	10	0.0030211	0.0044013	42	11	0.0008017	0.0014187	42	12	0.0043636	-0.0077228
42	13	0.0006714	0.0010780	42	14	-0.0036389	0.0031713	42	15	-0.0008635	0.0052410
42	16	0.0030972	-0.0029467	42	17	-0.0027801	-0.0024590	42	18	-0.0085518	0.0038762
42	19	-0.0012846	-0.0015350	42	20	0.0058399	0.0020848	42	21	0.0012403	-0.0011678
42	22	-0.0009454	-0.0015454	42	23	-0.0031263	-0.0008805	42	24	0.0009781	0.0017079
42	25	-0.0049920	0.0015279	42	26	-0.0014004	-0.0054051	42	27	0.0046599	-0.0009781
42	28	-0.0028763	0.0024781	42	29	-0.0048047	-0.0004893	42	30	0.0035784	0.0007136
42	31	0.0055411	0.0046499	42	32	0.0039092	0.0044224	42	33	0.0016808	0.0037711
42	34	0.0031443	0.0069991	42	35	-0.0029544	-0.0002303	42	36	0.0045869	-0.0055909
42	37	-0.0026086	0.0037980	42	38	0.0018011	-0.0067936	42	39	0.0024849	0.0089295
42	40	0.0019980	-0.0027079	42	41	-0.0001768	0.0009606	42	42	-0.0063007	0.0022353
43	1	-0.0008316	0.0020286	43	2	-0.0056119	-0.0006628	43	3	0.0031178	0.0007431
43	4	0.0019077	-0.0006349	43	5	-0.0070054	0.0026595	43	6	0.0050181	0.0041881
43	7	-0.0016264	-0.0010956	43	8	-0.0008173	0.0041930	43	9	-0.0025299	-0.0053650
43	10	0.0000195	-0.0005122	43	11	-0.0027799	0.0039610	43	12	-0.0013027	0.0001380
43	13	0.0024777	-0.0028463	43	14	-0.0022186	0.0014669	43	15	0.0025039	0.0060175
43	16	0.0012199	0.0007061	43	17	0.0003756	-0.0009282	43	18	-0.0002852	-0.0039074
43	19	-0.0060716	-0.0032356	43	20	-0.0003431	0.0016274	43	21	0.0009576	0.0061367
43	22	0.0019677	-0.0000828	43	23	0.0001647	-0.0064914	43	24	0.0020583	0.0023257
43	25	-0.0014060	0.0002575	43	26	-0.0021524	0.0016623	43	27	0.0040223	0.0010344
43	28	-0.0016798	0.0071065	43	29	-0.0010411	0.0008117	43	30	-0.0079572	-0.0061139
43	31	-0.0033059	-0.0019594	43	32	-0.0026257	0.0050419	43	33	0.0033950	-0.0020095
43	34	0.0028516	-0.0021425	43	35	-0.0016056	0.0051703	43	36	-0.0012074	-0.0011083
43	37	0.0029798	0.0030621	43	38	-0.0031235	0.0005426	43	39	0.0027912	0.0005902
43	40	0.0073136	-0.0003218	43	41	-0.0024349	0.0013503	43	42	-0.0045843	0.0035128
43	43	-0.0011373	-0.0064975								
44	1	0.0029297	0.0011940	44	2	0.0010687	0.0032316	44	3	-0.0002384	-0.0036957
44	4	0.0018471	-0.0012678	44	5	0.0034121	0.0017682	44	6	-0.0038622	0.0025786
44	7	0.0013370	0.0075225	44	8	-0.0018939	0.0016363	44	9	0.0002772	-0.0035145
44	10	-0.0024947	-0.0021794	44	11	0.0012324	-0.0000826	44	12	-0.0003520	-0.0006908
44	13	0.0016425	-0.0016159	44	14	-0.0009325	-0.0043967	44	15	0.0001944	-0.0044618
44	16	0.0039739	0.0025995	44	17	0.0018932	0.0029772	44	18	0.0026380	-0.0025727
44	19	-0.0009661	-0.0023623	44	20	-0.0033284	-0.0017765	44	21	-0.0077975	-0.0000412
44	22	0.0038111	0.0014278	44	23	-0.0000186	0.0044105	44	24	0.0006760	-0.0032237
44	25	-0.0006909	-0.0005947	44	26	-0.0026699	-0.0003930	44	27	0.0038838	-0.0032201
44	28	-0.0016089	0.0027245	44	29	-0.0051754	0.0032688	44	30	0.0042510	0.0020496
44	31	-0.0009448	0.0033906	44	32	-0.0031967	0.0009834	44	33	-0.0029287	-0.0003965
44	34	-0.0028548	0.0028183	44	35	-0.0040191	-0.0027811	44	36	0.0003855	-0.0061805
44	37	0.0078193	0.0055376	44	38	0.0030486	-0.0050440	44	39	0.0053568	0.0019902
44	40	-0.0022656	0.0049728	44	41	0.0004467	0.0001770	44	42	-0.0026354	-0.0019834
44	43	0.0035684	-0.0032760	44	44	0.0037782	-0.0006886				
45	1	0.0026951	-0.0027440	45	2	0.0000148	-0.0017983	45	3	-0.0007616	-0.0023328
45	4	0.0002985	-0.0012819	45	5	0.0035373	-0.0005212	45	6	-0.0014242	0.0009479
45	7	-0.0008588	0.0015494	45	8	-0.0031837	0.0012239	45	9	0.0015806	-0.0015151
45	10	0.0002887	0.0015372	45	11	0.0001222	-0.0004875	45	12	-0.0021671	-0.0010538
45	13	-0.0034052	-0.0008497	45	14	0.0007696	-0.0037004	45	15	-0.0026414	0.0016431
45	16	0.0032011	-0.0003423	45	17	0.0020754	-0.0006589	45	18	0.0004705	-0.0043553
45	19	-0.0043586	-0.0023125	45	20	0.0021153	0.0009336	45	21	-0.0034361	-0.0013003

TABLE 5.2 (continued)

Index		Value		Index		Value		Index		Value	
n	m	C	S	n	m	C	S	n	m	C	S
45	22	0.0024224	0.0019235	45	23	0.0002953	0.0000911	45	24	-0.0057726	0.0034637
45	25	0.0041370	-0.0030598	45	26	-0.0007239	0.0031661	45	27	-0.0042952	-0.0002781
45	28	0.0062681	-0.0008717	45	29	-0.0059262	-0.0033256	45	30	-0.0000580	-0.0003571
45	31	-0.0017040	-0.0018854	45	32	-0.0020496	-0.0030384	45	33	-0.0030386	-0.0017780
45	34	-0.0003018	0.0033467	45	35	-0.0036964	0.0054399	45	36	-0.0056363	0.0065188
45	37	-0.0066606	0.0032181	45	38	-0.0032027	0.0037589	45	39	-0.0038397	-0.0046705
45	40	0.0007054	-0.0033151	45	41	0.0016370	-0.0013952	45	42	-0.0027772	-0.0081510
45	43	0.0006000	0.0030227	45	44	0.0084758	0.0004522	45	45	-0.0005275	0.0001983
46	1	0.0003902	0.0019348	46	2	0.0039107	0.0003363	46	3	-0.0015697	0.0003988
46	4	0.0016600	-0.0049421	46	5	-0.0027228	-0.0029434	46	6	-0.0031675	-0.0015616
46	7	0.0020442	-0.0053048	46	8	-0.0002472	0.0023184	46	9	0.0048027	0.0043677
46	10	-0.0005557	0.0010901	46	11	-0.0025667	-0.0015273	46	12	-0.0002748	0.0009639
46	13	-0.0015386	-0.0006741	46	14	0.0003575	0.0006596	46	15	-0.0028107	-0.0010545
46	16	0.0006898	0.0023582	46	17	-0.0034898	-0.0005418	46	18	0.0022656	-0.0029780
46	19	-0.0002686	-0.0023467	46	20	-0.0021061	-0.0041320	46	21	-0.0052484	0.0014604
46	22	0.0063494	0.0008493	46	23	0.0012049	0.0010192	46	24	-0.0001629	-0.0017623
46	25	0.0028610	-0.0050933	46	26	0.0029405	0.0080656	46	27	-0.0011910	0.0001431
46	28	-0.0001483	-0.0055951	46	29	-0.0016279	-0.0022368	46	30	-0.0028077	-0.0057572
46	31	-0.0020010	0.0002963	46	32	-0.0021572	-0.0005208	46	33	0.0109984	0.0002125
46	34	-0.0017368	0.0025661	46	35	-0.0043511	0.0001382	46	36	0.0002680	-0.0011718
46	37	-0.0028315	0.0028776	46	38	-0.0053348	-0.0027991	46	39	0.0055427	-0.0007327
46	40	0.0006478	0.0002631	46	41	-0.0011737	-0.0022143	46	42	-0.0009337	0.0050951
46	43	-0.0022300	0.0103393	46	44	0.0001587	-0.0016435	46	45	-0.0027172	0.0031762
46	46	0.0005050	-0.0020583								
47	1	-0.0053435	-0.0007635	47	2	0.0016198	0.0000823	47	3	0.0009059	0.0023499
47	4	-0.0017473	0.0002132	47	5	-0.0012637	-0.0022936	47	6	0.0013596	-0.0012630
47	7	0.0001166	-0.0040506	47	8	0.0008843	-0.0008776	47	9	-0.0011285	0.0017593
47	10	0.0019215	0.0015586	47	11	0.0008545	-0.0027904	47	12	0.0058705	0.0016457
47	13	-0.0027401	-0.0010902	47	14	0.0002416	0.0010597	47	15	-0.0014275	-0.0001426
47	16	-0.0017942	-0.0005419	47	17	-0.0017814	0.0024817	47	18	-0.0006259	0.0068878
47	19	0.0025376	0.0012821	47	20	-0.0065500	0.0006051	47	21	-0.0039365	-0.0010039
47	22	-0.0040330	0.0007903	47	23	0.0026870	0.0008748	47	24	-0.0007888	-0.0013627
47	25	-0.0016422	-0.0064498	47	26	0.0050061	-0.0007265	47	27	-0.0037071	-0.0028474
47	28	0.0019022	-0.0060338	47	29	0.0053198	0.0005651	47	30	-0.0014446	0.0029410
47	31	0.0007062	0.0024173	47	32	-0.0026391	0.0011748	47	33	-0.0042830	0.0021022
47	34	-0.0008726	0.0006783	47	35	-0.0039723	0.0003526	47	36	0.0058505	-0.0021634
47	37	0.0074399	0.0019451	47	38	0.0007072	-0.0011637	47	39	-0.0005401	0.0065295
47	40	-0.0080805	0.0041903	47	41	-0.0018862	0.0077747	47	42	-0.0022845	-0.0014633
47	43	-0.0014626	0.0011128	47	44	-0.0020330	0.0057069	47	45	0.0054800	0.0027301
47	46	-0.0019032	-0.0015629	47	47	0.0024330	-0.0034586				
48	1	0.0005538	0.0012148	48	2	0.0035724	0.0015917	48	3	-0.0006864	-0.0003342
48	4	-0.0007062	-0.0007040	48	5	0.0044193	0.0004521	48	6	0.0030947	0.0036867
48	7	-0.0014992	0.0018387	48	8	0.0004006	0.0012714	48	9	0.0006931	0.0021397
48	10	-0.0015349	0.0015451	48	11	0.0026793	0.0005879	48	12	0.0001334	-0.0019480
48	13	0.0018516	0.0001842	48	14	-0.0004517	0.0002950	48	15	0.0031099	0.0004613
48	16	0.0009952	0.0013374	48	17	0.0008646	0.0005053	48	18	-0.0007917	0.0022628
48	19	-0.0009128	0.0023804	48	20	-0.0013079	0.0041606	48	21	0.0021234	-0.0008577
48	22	-0.0037062	0.0036039	48	23	-0.0030785	-0.0005105	48	24	-0.0044177	-0.0010251
48	25	-0.0004567	0.0001535	48	26	-0.0011981	-0.0039966	48	27	-0.0053468	0.0042815
48	28	0.0013954	-0.0050730	48	29	0.0022356	-0.0043115	48	30	-0.0016900	-0.0007810
48	31	0.0001248	-0.0017717	48	32	0.0010593	-0.0007825	48	33	0.0004008	0.0009590
48	34	-0.0009807	0.0040984	48	35	-0.0027110	-0.0007886	48	36	-0.0017322	0.0013982
48	37	-0.0031590	0.0001357	48	38	-0.0079164	-0.0003110	48	39	0.0021019	-0.0070046
48	40	0.0019652	0.0016491	48	41	-0.0026586	-0.0096586	48	42	0.0012291	0.0026088
48	43	0.0034306	0.0042050	48	44	-0.0000205	-0.0015323	48	45	0.0049022	0.0011523
48	46	-0.0020915	0.0067677	48	47	0.0030068	0.0051068	48	48	0.0041556	-0.0019210

TABLE 5.2 (*continued*)

Index		Value		Index		Value		Index		Value	
n	m	C	S	n	m	C	S	n	m	C	S
49	1	0.0043368	0.0000709	49	2	0.0010682	0.0042526	49	3	-0.0001052	-0.0001249
49	4	0.0009678	0.0066156	49	5	0.0007732	-0.0003730	49	6	-0.0006717	0.0001671
49	7	0.0015788	0.0023319	49	8	-0.0021954	0.0026171	49	9	-0.0017627	0.0032456
49	10	-0.0034344	-0.0006411	49	11	0.0044174	-0.0000399	49	12	-0.0033296	-0.0015868
49	13	0.0013113	0.0018309	49	14	0.0003211	-0.0007456	49	15	-0.0005472	-0.0009267
49	16	0.0002820	-0.0036641	49	17	-0.0018398	-0.0003205	49	18	-0.0003905	-0.0005100
49	19	-0.0017828	-0.0007865	49	20	0.0038187	0.0000889	49	21	-0.0010906	-0.0030666
49	22	-0.0009327	0.0038366	49	23	0.0017917	0.0007186	49	24	0.0025186	0.0003714
49	25	-0.0018632	0.0023003	49	26	-0.0061364	0.0010063	49	27	-0.0023229	0.0031887
49	28	-0.0027142	-0.0090119	49	29	-0.0002811	0.0011873	49	30	0.0016574	0.0016788
49	31	0.0005052	-0.0058855	49	32	0.0011389	-0.0050365	49	33	0.0010842	-0.0009892
49	34	0.0036489	0.0000702	49	35	0.0022276	0.0022634	49	36	-0.0019451	0.0022716
49	37	-0.0019750	0.0020364	49	38	0.0011548	-0.0001104	49	39	0.0017274	0.0000864
49	40	-0.0019194	0.0010767	49	41	0.0017339	-0.0057150	49	42	-0.0034542	0.0018620
49	43	0.0032430	-0.0077262	49	44	0.0057092	0.0051676	49	45	0.0037451	-0.0008910
49	46	0.0019567	0.0005388	49	47	0.0023910	-0.0013929	49	48	0.0000523	0.0009792
49	49	0.0022866	0.0011051								
50	1	0.0017666	-0.0022281	50	2	-0.0058765	-0.0036022	50	3	0.0004426	-0.0008402
50	4	-0.0047777	0.0001146	50	5	-0.0019977	0.0002767	50	6	0.0000882	0.0003448
50	7	0.0025973	0.0024513	50	8	-0.0032385	-0.0013418	50	9	-0.0010077	0.0018888
50	10	-0.0033841	-0.0007892	50	11	-0.0010069	0.0016175	50	12	-0.0029256	0.0039480
50	13	0.0009021	-0.0004416	50	14	-0.0026214	0.0027302	50	15	-0.0014314	-0.0022591
50	16	-0.0007214	-0.0052738	50	17	-0.0000520	-0.0018828	50	18	0.0011816	-0.0023998
50	19	0.0011347	0.0018687	50	20	0.0015556	-0.0011293	50	21	0.0000305	-0.0001589
50	22	-0.0004390	0.0004109	50	23	-0.0028784	-0.0042220	50	24	0.0058694	-0.0003756
50	25	0.0048968	0.0001811	50	26	-0.0054587	-0.0016869	50	27	0.0043118	-0.0016602
50	28	-0.0006827	0.0052310	50	29	0.0047011	0.0029798	50	30	0.0034870	0.0054217
50	31	-0.0028706	0.0041099	50	32	-0.0010662	0.0014943	50	33	-0.0025429	-0.0017283
50	34	-0.0014786	-0.0012403	50	35	0.0003762	0.0005054	50	36	-0.0002935	0.0006947
50	37	-0.0010860	-0.0002919	50	38	-0.0026838	-0.0055295	50	39	-0.0045147	0.0060185
50	40	0.0044884	0.0040792	50	41	-0.0007966	-0.0009059	50	42	0.0044166	-0.0017972
50	43	-0.0022517	-0.0008207	50	44	-0.0015030	-0.0013688	50	45	-0.0022066	0.0033629
50	46	-0.0019619	0.0021132	50	47	-0.0056726	-0.0081046	50	48	-0.0010699	-0.0019044
50	49	0.0025218	-0.0049950	50	50	0.0023135	0.0019352				

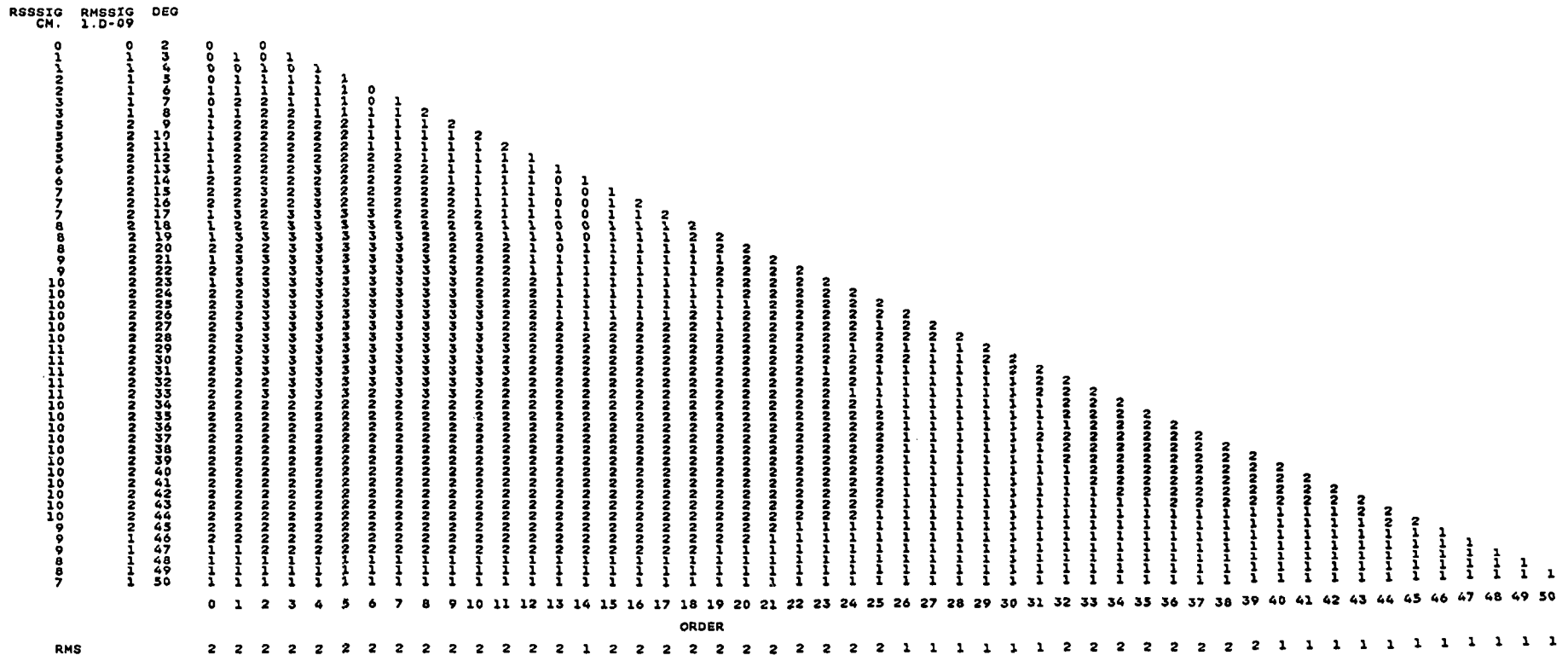

Fig 5.1 Estimated Error for GEM-T3 coefficients. Error x 10^9

Fig 5.2 Estimated Error for GEM-T3S coefficients. Error x 10^9

Figure 5.3

Geoid Surface Computed from GEM–T3 Gravity Model

Height in meters above the reference ellipsoid, f=1/298.257

Contour interval=5m.

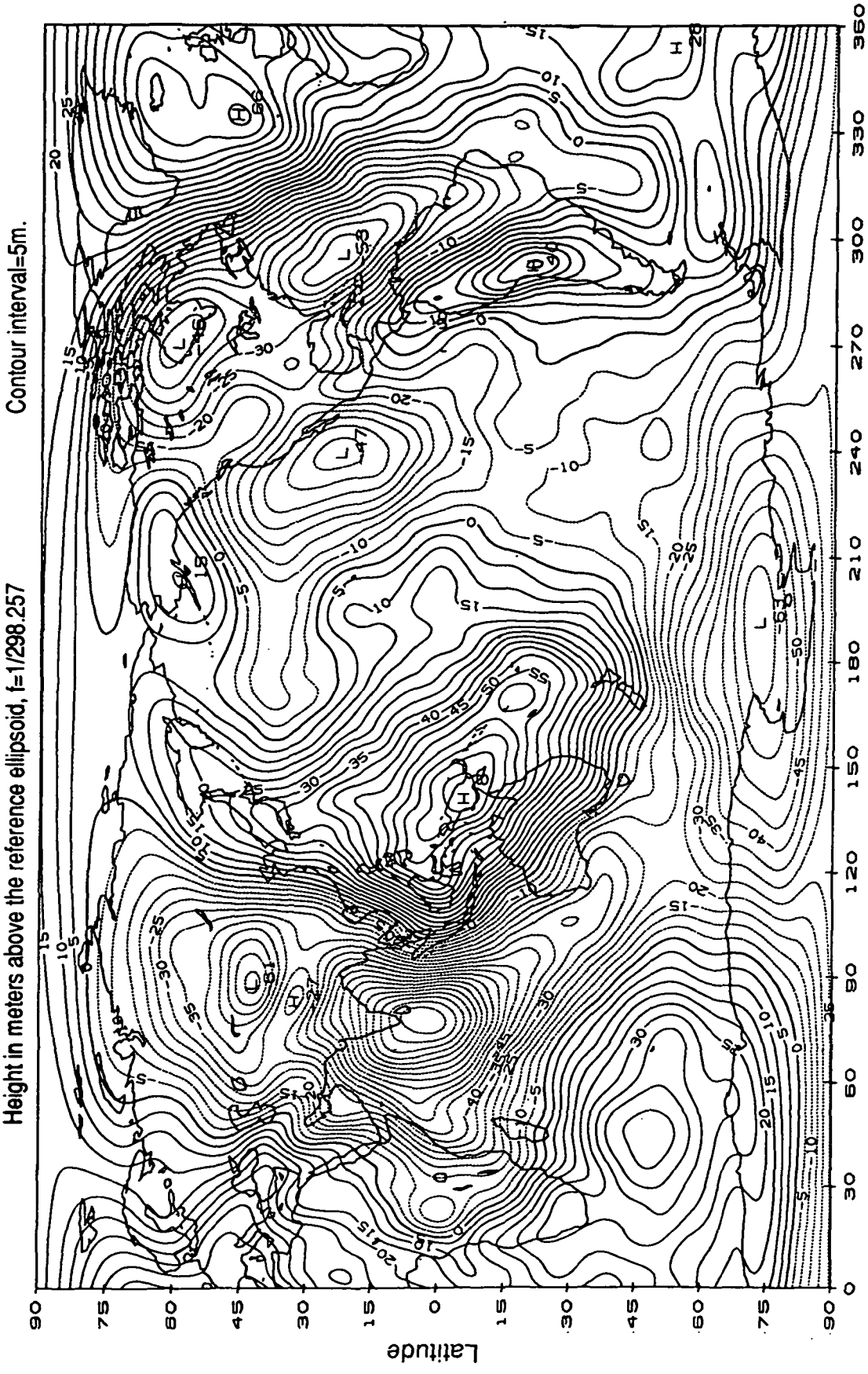

Figure 5.3.a

Free Air Gravity Anomalies from GEM–T3

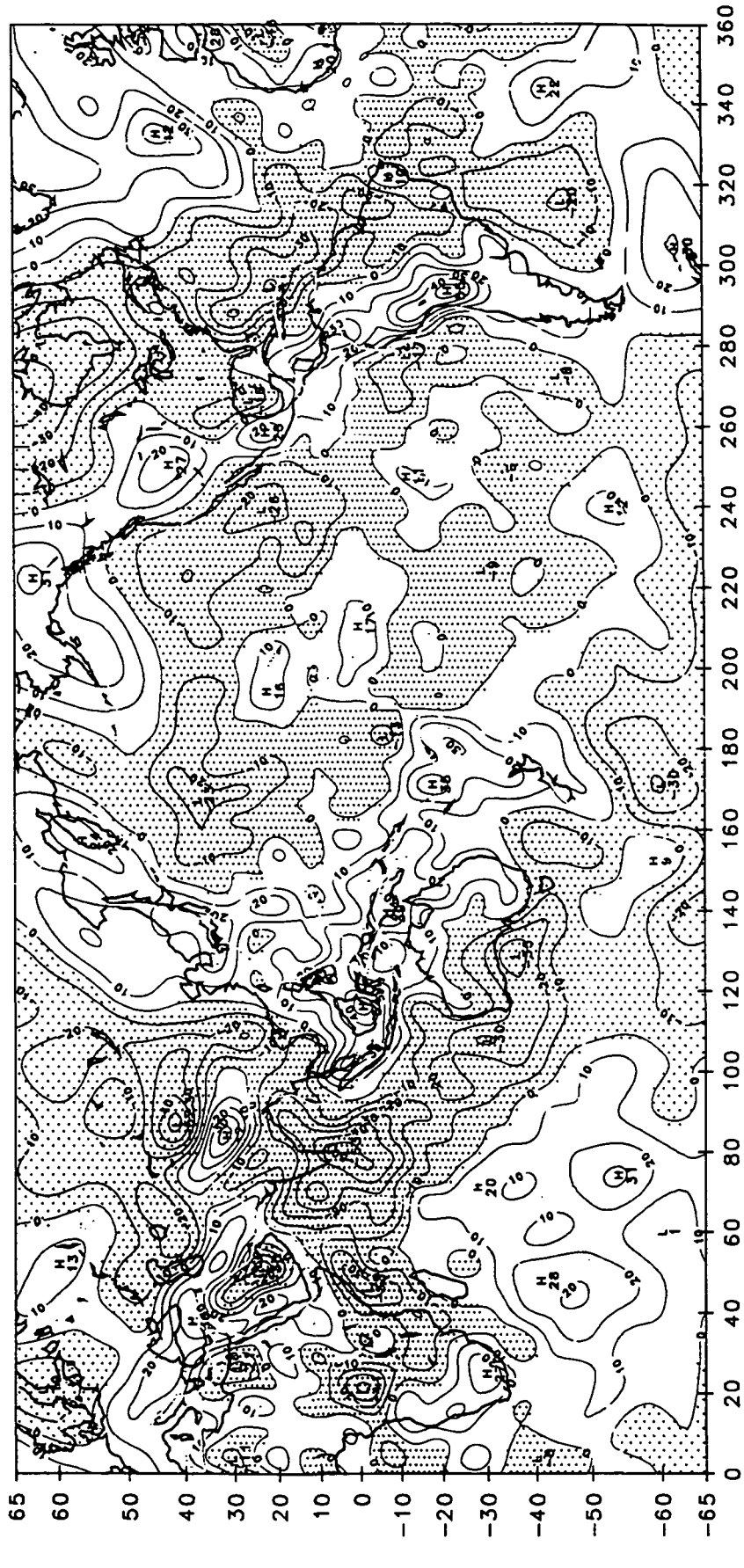

Figure 5.4a

Geoid Height Errors from GEM–T3 to 10 x 10

Contour Interval = 1cm

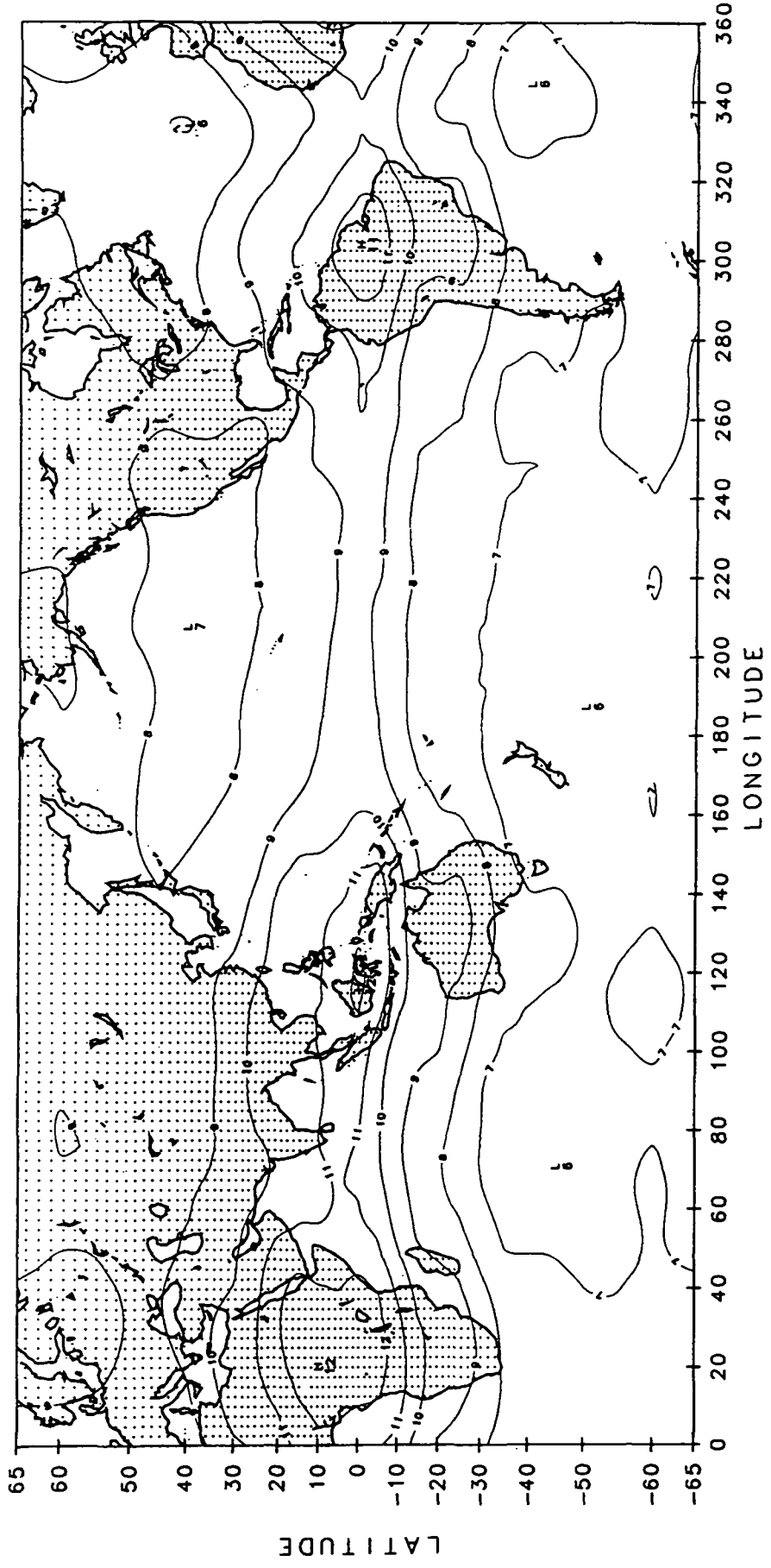

Figure 5.4b

Geoid Height Errors from GEM–T3 to 50 x 50

Contour Interval = 5 cm

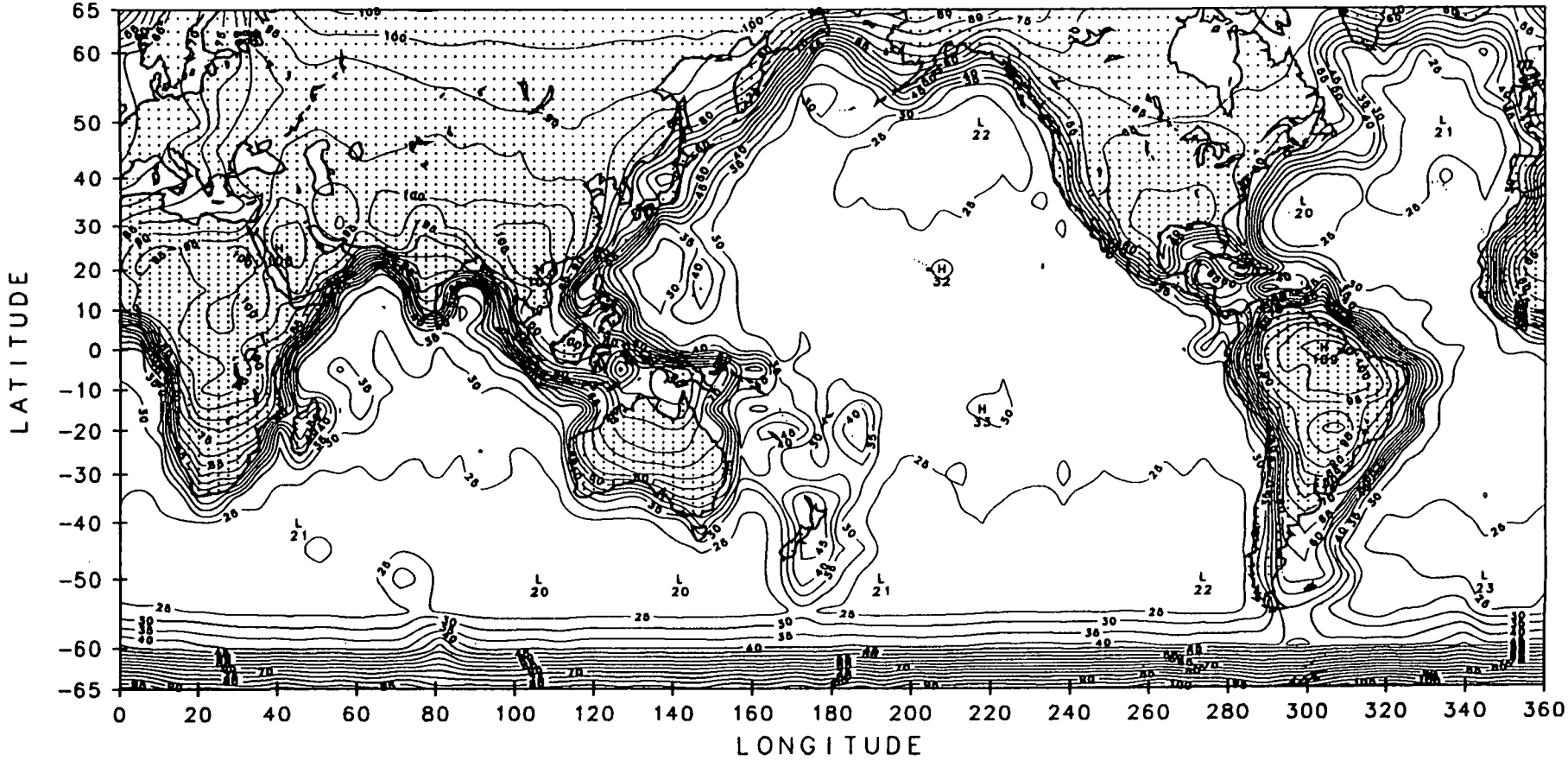

Figure 5.5

Geoid Uncertainty as a Function of Model Truncation

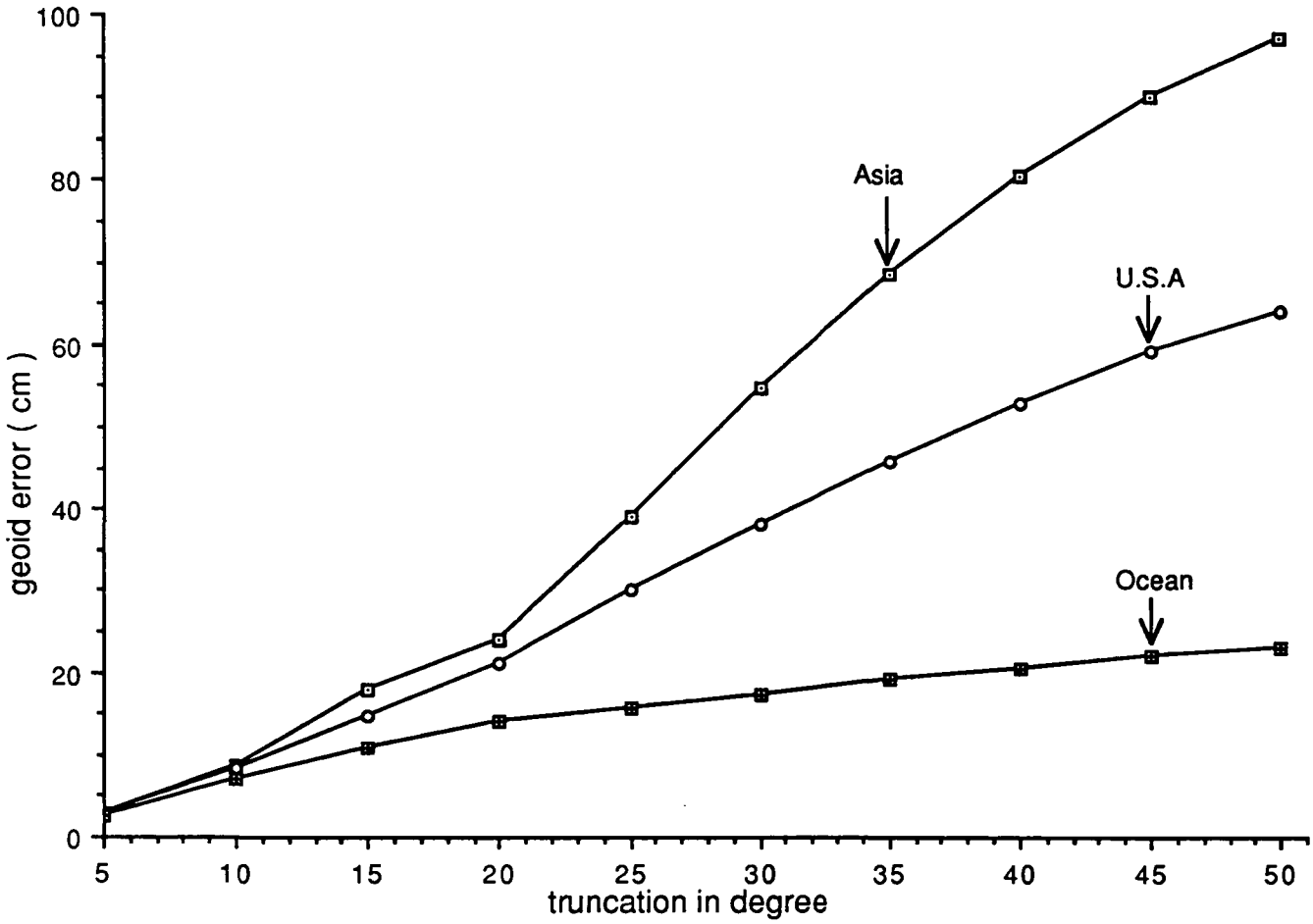

Figure 5.6

RMS OF COEFFICIENT ERRORS PER DEGREE

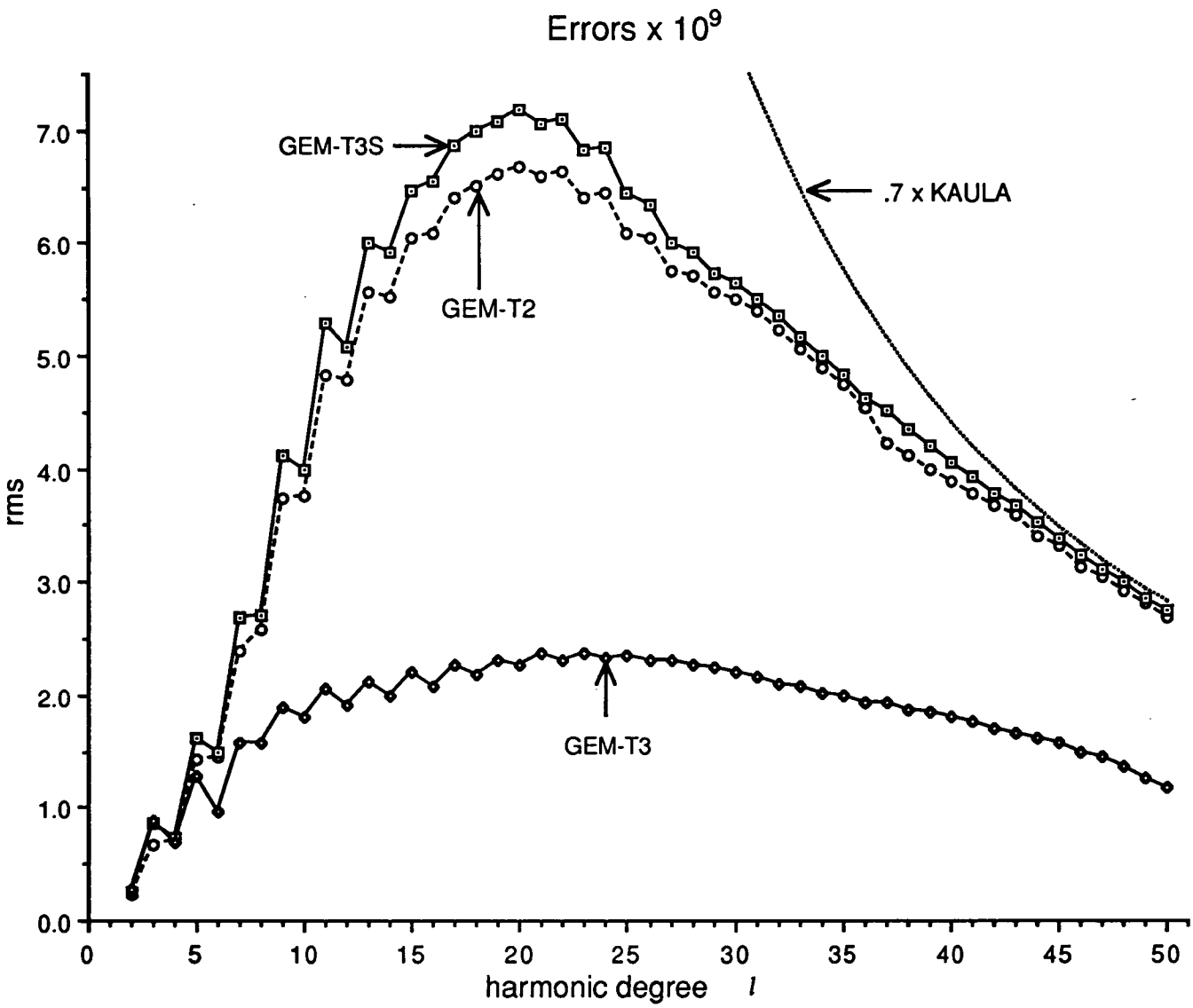

GEM-T2 Total geoid error = 141.2 cm

GEM-T3S Total geoid error = 158.7 cm

GEM-T3 Total geoid error = 58.9 cm

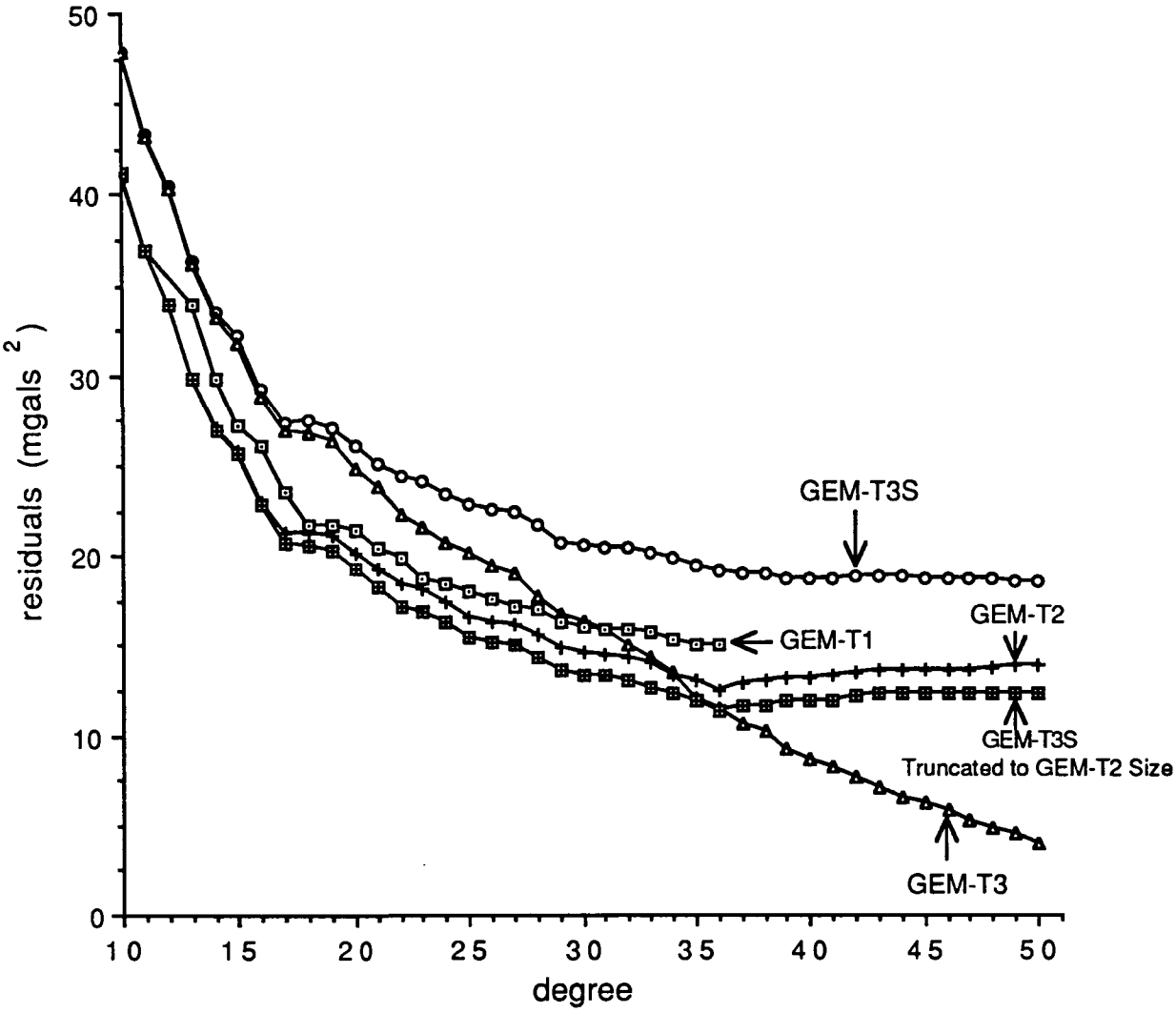

Fig. 5.7 Gravity model comparision with 1071 5° x 5° Seasat Altimeter gravity anomalies. Anomalies are corrected for truncation error

5.2 THE GEM-T3 AND T3S OCEAN TIDAL SOLUTION

The GEM-T3 and T3s solutions solve for temporal changes in the external gravitational attraction of the Earth sensed by near-Earth orbiting objects at the major astronomical frequencies. These tidal terms represent the attenuated signal from the solid Earth/oceans/atmosphere systems as a combined effect. We solve for terms in the space of ocean tides using a classical spherical harmonic representation as described in Christodoulidis et al., (1988). This approach is chosen because contemporary models of the frequency-dependent solid Earth tidal response (Wahr, 1981) are better known at the wavenumbers of interest for orbital computations than are the ocean tidal terms at the same wavenumbers. Because of the combined origin of the satellite sensed tidal signal, caution must be exercised when comparing dynamic satellite solutions for ocean tidal terms with those obtained oceanographically. Within the semi-diurnal and diurnal bands, ocean tidal effects are dominant and a comparison between ocean models and satellite solutions is reasonably straightforward under the assumption that the solid Earth tides have been well modeled. However, at monthly, semi-annual, annual and longer periods, there are important climatological effects (e.g., Gutierrez and Wilson, 1987), changes in the hydrosphere pertaining to ground water retention cycles and the volume of water stored in continental aquifers (e.g., Chao, 1988), in snow cover (e.g., Chao and O'Connor, 1988) and other sources of mass redistribution which are not "tidal" in origin, and certainly not separated from changes in the ocean surface at these periods.

Table 5.3 presents the GEM-T3 and GEM-T3S tidal solutions. These models agree well with those previously reported for the GEM-T2 solution as well as with those obtained by the German/French collaboration which produced the GRIM4 series of gravitational and tidal models (Reigber et al., 1991) and those obtained by the University of Texas (Cheng et al., 1990) from a "long-arc" study of Starlette's orbit evolution also shown in Table 5.3. These models are all satellite derived and this avoids the inherent difficulties of modeling the unattenuated shorter wavelength effects seen on the sea surface. The difference between the individual ocean tidal coefficients is typically much smaller than the inherent uncertainty of the recovered coefficients. However, it is not surprising to see substantial disagreement for the hard-to-recover zonal tides.

Table 5.3a presents a comparison of the secular changes in the lunar orbit based on these tide models. Again, good agreement is seen and these results compare favorably with those obtained using lunar laser ranging [cf. Christodoulidis et al., (1988) for the computational method].

The ocean tide signal sensed in the motion of near-Earth satellites results in recovery of a low degree and order set of coefficients for the spherical harmonics at each major ocean tide frequency. Much like the static geopotential recovery, significant correlations are anticipated between coefficients within the same order associated with each particular tide as well as between tides whose effects on-orbit manifest themselves at similar frequencies. Effects of truncation and acts of commission are similar in character to those in the static geopotential solution in that the tidal field rapidly attenuates at altitude. The comparison with the lunar orbit evolution tests the correlated set of coefficients in modeling the exterior temporal geopotential against a totally independent measure. Table 5.3a shows significantly larger differences for individual terms than in the aggregate sum: this is one indication of some problematic correlation effects in the various satellite-derived tidal solutions.

5.3 STATION COORDINATE SOLUTIONS

Mis-positioning of Earth-fixed tracking stations can contribute to the residual misclosure between the calculated and observed satellite position. An aliased gravity model can be produced if an error similar in character to that of the gravitational perturbations occurs in the orbital residuals. Given the Earth's rotation under the orbital plane, a station views the satellite during opposite ascending and descending satellite groundtracks, which alternate approximately every 12 hours.

Table 5.3 Comparison of Satellite Derived Ocean Tide Models

CONSTITUENTS TIDE	deg	ord	AMP. (cm)	PHASE (deg)	σ_{AMP} (cm)	σ_{PHASE} (deg)	GRAVITY MODEL
				-- Second Degree --			
MM^2	2	0	0.84	262.3	0.27	18.6	GEMT3S[a]
			0.84	260.1	0.27	18.6	GEMT3[a]
			0.74	256.3	0.32	24.0	GEMT2[b]
			1.42	245.5	0.67	7.5	STARLETTE[c]
			1.76	271.3	-	-	GRIM4C2[d]
SA^2	2	0	2.70	26.3	0.29	6.7	GEMT3S
			2.65	26.3	0.29	6.8	GEMT3
			3.03	28.8	0.40	8.0	GEMT2
			2.83	39.0			STARLETTE
			1.10	2.3	-	-	GRIM4C2
MF^2	2	0	2.07	239.8	0.28	7.8	GEMT3S
			2.05	240.4	0.28	7.8	GEMT3
			2.07	237.1	0.31	8.7	GEMT2
			2.84	242.1	0.41	25.3	STARLETTE
			1.16	234.8	-	-	GRIM4C2
SSA^2	2	0	1.58	253.4	0.30	11.0	GEMT3S
			1.61	255.9	0.30	10.8	GEMT3
			1.28	249.5	0.42	17.9	GEMT2
			1.59	253.3	0.68	5.2	STARLETTE
			1.70	246.4	-	-	GRIM4C2
K1	2	1	2.78	325.0	0.12	2.5	GEMT3S
			2.78	325.1	0.12	2.6	GEMT3
			2.85	325.5	0.17	3.3	GEMT2
			2.68	324.9	0.09	6.9	STARLETTE
			2.66	320.1	-	-	GRIM4C2
O1	2	1	2.71	314.8	0.11	2.4	GEMT3S
			2.70	314.5	0.11	2.4	GEMT3
			2.72	315.4	0.13	2.7	GEMT2
			2.66	326.7	0.23	10.3	STARLETTE
			2.69	321.4	-	-	GRIM4C2
P1	2	1	0.94	314.7	0.13	7.8	GEMT3S
			0.97	313.9	0.13	7.5	GEMT3
			1.11	313.2	0.17	8.7	GEMT2
			0.99	331.0	0.07	2.8	STARLETTE
			1.04	320.0	-	-	GRIM4C2

Table 5.3 Continued

CONSTITUENTS TIDE	deg	ord	AMP. (cm)	PHASE (deg)	σ_{AMP} (cm)	σ_{PHASE} (deg)	GRAVITY MODEL
K2	2	2	0.34	316.2	0.04	6.6	GEMT3S
			0.34	315.9	0.04	6.6	GEMT3
			0.32	313.5	0.04	7.8	GEMT2
			0.29	315.9	0.06	2.5	STARLETTE
			0.25	297.3	-	-	GRIM4C2
M2	2	2	3.31	321.1	0.04	0.7	GEMT3S
			3.31	321.1	0.04	0.7	GEMT3
			3.32	321.3	0.05	0.8	GEMT2
			3.22	319.3	0.06	2.4	STARLETTE
			3.10	318.4	-	-	GRIM4C2
S2	2	2	0.78[1]	300.7	0.04	2.9	GEMT3S
			0.78[1]	301.0	0.02	2.9	GEMT3
			0.83[1]	300.4	0.04	3.0	GEMT2
			1.20	315.7	0.11	11.3	STARLETTE
			0.73[1]	307.5	-	-	GRIM4C2
N2	2	2	0.70	334.1	0.06	4.7	GEMT3S
			0.69	334.3	0.06	4.7	GEMT3
			0.68	334.4	0.06	5.2	GEMT2
			0.92	329.3	0.05	5.5	STARLETTE
			0.76	325.2	-	-	GRIM4C2
T2	2	2	0.04	324.6	0.04	57.6	GEMT3S
			0.05	321.1	0.04	49.1	GEMT3
			0.05	273.2	0.04	55.9	GEMT2
			0.03	13.1	0.06	2.4	STARLETTE
				-- third degree--			
MM[2]	3	0	0.98	35.4	0.59	34.2	GEMT3S
			0.97	37.7	0.59	34.6	GEMT3
			0.81	16.7	0.67	46.2	GEMT2
			1.42	245.5	-	-	STARLETTE
			1.12	88.8	-	-	GRIM4C2
SA[2]	3	0	5.19	313.8	0.53	5.8	GEMT3S
			5.17	314.0	0.52	5.8	GEMT3
			6.47	320.1	0.57	5.2	GEMT2
			1.98	245.2	0.36	11.2	STARLETTE
			10.7	293.4	-	-	GRIM4C2

Table 5.3 Continued

CONSTITUENTS TIDE	deg	ord	AMP. (cm)	PHASE (deg)	σ_{AMP} (cm)	σ_{PHASE} (deg)	GRAVITY MODEL
MF^2	3	0	0.37	334.0	0.71	104.2	GEMT3S
			0.44	337.1	0.69	84.8	GEMT3
			1.03	354.6	0.83	42.7	GEMT2
			2.84	242.1	-	-	STARLETTE
			0.70	303.3	-	-	GRIM4C2
SSA^2	3	0	0.56	50.3	0.51	52.7	GEMT3S
			0.53	54.1	0.51	55.3	GEMT3
			0.87	89.4	0.56	36.5	GEMT2
			0.78	69.2	0.62	6.5	STARLETTE
			2.22	60.5	-	-	GRIM4C2
K1	3	1	0.78	12.8	0.09	7.0	GEMT3S
			0.79	13.6	0.09	6.9	GEMT3
			0.90	14.5	0.11	7.1	GEMT2
			1.41	346.5	0.10	7.1	STARLETTE
			1.04	12.6	-	-	GRIM4C2
O1	3	1	1.33	80.7	0.14	5.9	GEMT3S
			1.37	79.5	0.13	5.6	GEMT3
			1.39	83.0	0.15	6.3	GEMT2
			1.05	63.3	0.20	10.6	STARLETTE
			1.46	71.2	-	-	GRIM4C2
P1	3	1	0.41	8.7	0.09	13.7	GEMT3S
			0.38	6.5	0.09	14.5	GEMT3
			0.34	359.5	0.11	19.0	GEMT2
			0.86	0.9	0.03	2.8	STARLETTE
			0.28	276.3	-	-	GRIM4C2
K2	3	2	0.19	187.3	0.04	8.4	GEMT3S
			0.19	188.5	0.04	8.0	GEMT3
			0.23	190.0	0.04	7.5	GEMT2
			0.08	242.8	0.06	2.9	STARLETTE
			0.15	4.5	-	-	GRIM4C2
M2	3	2	0.26	154.9	0.05	10.8	GEMT3S
			0.25	155.8	0.05	11.2	GEMT3
			0.30	156.5	0.06	10.6	GEMT2
			0.12	160.6	0.04	2.2	STARLETTE
			0.31	188.4	-	-	GRIM4C2

Table 5.3 Continued

CONSTITUENTS TIDE	deg	ord	AMP. (cm)	PHASE (deg)	σ_{AMP} (cm)	σ_{PHASE} (deg)	GRAVITY MODEL
S2	3	2	0.28	223.7	0.03	6.4	GEMT3S
			0.29	223.1	0.03	6.3	GEMT3
			0.33	221.5	0.03	6.1	GEMT2
			0.23	191.6	0.04	1.8	STARLETTE
			0.37	205.8	-	-	GRIM4C2
N2	3	2	0.09	151.3	0.05	33.1	GEMT3S
			0.10	152.2	0.05	30.0	GEMT3
			0.09	155.8	0.06	39.5	GEMT2
			0.14	187.8	-	-	GRIM4C2
T2	3	2	0.02	18.6	0.03	89.1	GEMT3S
			0.02	19.1	0.03	79.7	GEMT3
			0.01	119.7	0.03	360.0	GEMT2
				-- fourth degree --			
K1	4	1	2.39	256.6	0.17	4.2	GEMT3S
			2.39	257.2	0.17	4.2	GEMT3
			2.49	258.2	0.21	4.9	GEMT2
			2.59	253.8	0.08	12.8	STARLETTE
			1.87	245.7	-	-	GRIM4C2
O1	4	1	1.89	281.2	0.18	5.3	GEMT3S
			1.84	282.5	0.18	5.4	GEMT3
			1.90	279.7	0.21	6.2	GEMT2
			2.25	295.5	0.31	20.4	STARLETTE
			2.10	274.9	-	-	GRIM4C2
P1	4	1	0.88	255.6	0.18	11.5	GEMT3S
			0.84	256.1	0.18	12.1	GEMT3
			0.84	262.9	0.21	14.4	GEMT2
			0.78	267.1	0.03	8.4	STARLETTE
			1.06	261.6	-	-	GRIM4C2
K2	4	2	0.15	105.9	0.04	13.8	GEMT3S
			0.15	105.5	0.04	14.1	GEMT3
			0.17	112.7	0.04	14.5	GEMT2
			0.10	97.0	0.05	4.1	STARLETTE
			0.20	123.5	-	-	GRIM4C2

Table 5.3 Continued

CONSTITUENTS TIDE	deg	ord	AMP. (cm)	PHASE (deg)	σ_{AMP} (cm)	σ_{PHASE} (deg)	GRAVITY MODEL
M2	4	2	0.99	125.9	0.04	2.4	GEMT3S
			0.98	125.8	0.04	2.3	GEMT3
			0.99	127.2	0.05	2.7	GEMT2
			1.15	120.6	0.06	4.3	STARLETTE
			1.03	136.2	-	-	GRIM4C2
S2	4	2	0.36	93.8	0.04	6.0	GEMT3S
			0.36	94.0	0.04	5.9	GEMT3
			0.33	87.2	0.04	7.6	GEMT2
			0.32	89.1	0.06	6.2	STARLETTE
			0.41	105.9	-	-	GRIM4C2
N2	4	2	0.24	140.7	0.04	10.3	GEMT3S
			0.23	140.2	0.04	10.2	GEMT3
			0.25	139.0	0.05	11.2	GEMT2
			0.13	148.2	0.05	2.9	STARLETTE
			0.22	126.6	-	-	GRIM4C2
T2	4	2	0.05	134.8	0.04	43.5	GEMT3S
			0.05	149.9	0.04	45.5	GEMT3
			0.04	242.6	0.05	72.2	GEMT2
				-- fifth degree --			
K1	5	1	2.24	107.7	0.20	4.9	GEMT3S
			2.23	107.8	0.20	4.9	GEMT3
			2.18	106.5	0.22	5.7	GEMT2
			2.35	91.4	-	-	GRIM4C2
O1	5	1	1.51	124.5	0.20	7.7	GEMT3S
			1.59	121.6	0.18	6.6	GEMT3
			1.52	118.6	0.21	7.8	GEMT2
			0.86	132.8	-	-	GRIM4C2
P1	5	1	0.77	126.0	0.20	14.5	GEMT3S
			0.76	122.9	0.20	14.3	GEMT3
			0.44	148.9	0.22	27.8	GEMT2
			1.37	92.0	-	-	GRIM4C2
K2	5	2	0.06	94.6	0.03	26.2	GEMT3S
			0.06	90.3	0.03	27.1	GEMT3
			0.08	96.3	0.03	23.5	GEMT2
			0.11	94.7	-	-	GRIM4C2

Table 5.3 Continued

CONSTITUENTS TIDE	deg	ord	AMP. (cm)	PHASE (deg)	σ_{AMP} (cm)	σ_{PHASE} (deg)	GRAVITY MODEL
M2	5	2	0.31	13.6	0.03	5.6	GEMT3S
			0.31	15.2	0.03	5.3	GEMT3
			0.29	8.1	0.04	6.9	GEMT2
			0.27	6.0	-	-	GRIM4C2
S2	5	2	0.16	21.5	0.03	11.5	GEMT3S
			0.16	17.0	0.03	11.3	GEMT3
			0.14	9.6	0.03	16.0	GEMT2
			0.09	77.4	-	-	GRIM4C2
N2	5	2	0.08	358.0	0.03	23.2	GEMT3S
			0.08	354.5	0.03	23.0	GEMT3
			0.09	341.6	0.04	22.9	GEMT2
			0.11	12.0	-	-	GRIM4C2
T2	5	2	0.06	53.5	0.03	25.4	GEMT3S
			0.06	57.0	0.03	25.5	GEMT3
			0.09	70.7	0.03	21.1	GEMT2
				-- sixth degree --			
K2	6	2	0.05	352.1	0.04	42.6	GEMT3S
			0.04	358.3	0.04	50.0	GEMT3
			0.04	203.5	0.05	59.9	GEMT2
			0.10	272.2	-	-	GRIM4C2
M2	6	2	0.39	317.0	0.04	6.4	GEMT3S
			0.39	317.2	0.04	6.4	GEMT3
			0.40	320.8	0.05	6.9	GEMT2
			0.48	342.6	-	-	GRIM4C2
S2	6	2	0.16	273.6	0.04	13.8	GEMT3S
			0.17	276.8	0.04	13.3	GEMT3
			0.22	284.4	0.04	12.0	GEMT2
			0.17	261.4	-	-	GRIM4C2
N2	6	2	0.08	354.9	0.05	33.3	GEMT3S
			0.07	358.0	0.05	36.7	GEMT3
			0.06	3.2	0.05	52.7	GEMT2
			0.08	323.5	-	-	GRIM4C2

Table 5.3 Continued

CONSTITUENTS TIDE	deg	ord	AMP. (cm)	PHASE (deg)	σ_{AMP} (cm)	σ_{PHASE} (deg)	GRAVITY MODEL
T2	6	2	0.04	183.3	0.04	64.5	GEMT3S
			0.03	183.0	0.04	64.8	GEMT3
			0.04	221.1	0.05	63.8	GEMT2

1 uncorrected for atmospheric thermal tide

2 values shown are scaled to accommodate symmetries in potential formulation (see Christodoulidis et al., 1988)

a this paper

b Marsh et el., 1990a

c Cheng et al., 1990

d Reigber et al., 1991

Table 5.3a
Comparison of Dynamic Tide Models
for Secular Change in the Mean Motion of the Moon (ṅ)

Significant Tide	GEM-T2	GEM-T3S	GEM-T3	GRM4C2	STARLETTE
065.455 Mm	0.01	0.01	0.01	-0.00	0.03
075.555 Mf	0.19	0.18	0.17	0.11	0.22
135.655 Q1	-0.17	-0.17	-0.17	-0.23	-0.14
145.555 O1	-3.15	-3.10	-3.08	-3.42	-3.62
155.655 M1	-0.01	-0.01	-0.01	-0.01	-0.01
175.455 J1	-0.01	-0.01	-0.01	-0.01	-0.01
245.655 N2	-1.38	-1.42	-1.41	-1.41	-1.79
255.555 M2	-20.30	-20.23	-20.21	-18.17	-19.14
265.455 L2	0.01	0.01	0.01	0.01	0.01
TOTAL	-24.94	-24.91	-24.86	-23.25	-24.57

Lunar Laser Ranging

Newhall et al., 1986	-24.9
Dickey et al., 1990	-25.5

ṅ are in arc sec century^{-2}.

A station with a latitude position error (for example, with a position that is too far north) when tracking a high inclination satellite will encounter the computed satellite position early for descending passes and, twelve hours later, late for ascending passes. This is the same signal as an error in along track perturbations arising from the m=1 m-daily gravity terms. Hence, station errors can induce systematic orbit residuals which can alias the gravitational field.

In the GEM-T3 and GEM-T3S solutions, the tracking stations were permitted to adjust. Minimal constraints were used to resolve the Earth-fixed longitude of the networks and for defining the Conventional Terrestrial Reference System required for simultaneous polar motion adjustment. For the modern laser stations, the Lageos data dominated the solution. However, Lageos positioning at the state-of-the-art requires detailed modeling of current tectonic motions (cf. Smith et al., 1990) at a few mm/y. The laser station recovery however, did not provide for this level of modeling, and aggregate positions representing multi-year averages were obtained in these solutions. Since better time-resolved laser positions are available elsewhere, a detailed description of the laser results will not be attempted herein.

The TRANET Doppler systems which tracked Oscar, Nova-1, Seasat and Geosat comprise a worldwide network of approximately 45 stations which operates two kinds of receivers. TRANET II is used at the permanent sites and consists of an Electrac 547B Doppler Tracking Receiver which employs either rubidium or cesium frequency standards. The portable TRANET stations use a Magnavox 1502-DS receiver with rubidium oscillators. Within our analysis we see little receiver dependent change in performance. The TRANET sites have also undergone upgrades which can change the location of their electronic center as well as improving the quality of the data. We have little information available to relate the tracking point of these sites to local survey markers as they are moved over time. As a result, we are forced to solve for separate sets of stations representing the then current network configuration tracking a given satellite. The time periods for each are summarized below:

Seasat	July through October, 1978
Oscar-14	August through October, 1980
Nova-1	March through July, 1984
Geosat	November, 1986 through January, 1987

Seasat carried both a TRANET beacon and a laser retroreflector array and was tracked by both the TRANET and laser networks. Some of these same laser stations tracked Lageos, with excellent knowledge of their geocentric positions being available as a result. This has permitted us to determine the Seasat TRANET sites within the reference system defined by Satellite Laser Ranging (SLR). We were fortunate that survey ties between the TRANET sites which tracked SEASAT and GEOSAT were made available to us at three locations: Ottawa (station nos. 21 and 547), Brussels (128 and 564), and Calgary (563 and 30414). We independently were able to recover TRANET sites which agreed with these survey ties at the 10-60 cm level. We used these ties as constraints on the GEOSAT/SEASAT site recovery which consequently enabled us to obtain a common TRANET network adjustment in a reference frame consistent with SLR. Table 5.4 presents the Doppler station positions obtained in the GEM-T3S solution.

Table 5.5 presents the corresponding location of the S-Band Radar sites which tracked Landsat.

TABLE 5.4 Doppler Station Coordinates of GEM-T3S

Name	Satellite	Number	X meters	Y meters	Z meters
UCLDOP	Oscar-14	21	4027831.4203	307026.2473	4919547.0763
MSADOP	"	27	-3857199.1022	3108662.5069	4004055.2801
CALGRY	"	125	-1659602.7240	-3676752.7281	4925488.2002
OTTDOP	"	128	1091455.7541	-4351280.9564	4518714.9036
HERNDN	"	407	1090146.4080	-4842517.6596	3991991.4591
SMTH412	"	412	-3942245.7869	3468852.7352	-3608191.7230
ANCHOR	"	414	-2656162.9198	-1544368.9122	5570663.6803
SAMOA	"	424	-6100053.3304	-997198.4968	-1568301.4914
WETZEL	"	643	4075531.9185	931833.5252	4801617.7390
UKIAH	"	5170	-2713391.3874	-4144624.5444	4004325.6553
SANJOS	"	7116	4084894.9641	-4209295.8219	-2498396.2142
PAPEET	"	7118	-5245200.8716	-3080485.3881	-1912810.3005
DJIBOU	"	7120	4583115.0670	4250960.5564	1266249.3998
PRETOR	"	7122	5067177.2171	2736603.7872	-2735030.7188
ORRORL	"	7143	-4446451.9016	2678221.7137	-3696186.9844
PURPLE	"	7185	-2608502.8627	4740114.1911	3366875.8008
SANTAG	"	7190	1776344.3494	-5026530.7737	-3491203.8051
SANFER	"	8804	5105461.7608	-555111.1095	3769900.4927
SJEDOP	Seasat	8	4083912.6286	-4209801.8938	-2499112.1623
MCMDOP	"	19	-1310714.4769	310460.0907	-6213365.1876
MAHDOP	"	20	3602879.9974	5238220.4320	-515939.6291
UCCLE	"	21	4027833.2221	307022.0884	4919537.5372
SMGDOP	"	22	-3088046.8942	5333056.6389	1638812.6492
GWMDOP	"	23	-5059775.3342	3591210.9130	1472783.1084
TAFDOP	"	24	-6100052.5547	-997193.3179	-1568313.2277
MISAWA	"	27	-3857198.4513	3108659.6611	4004040.9387
PRTDOP	"	105	5051977.7996	2725636.3943	-2774470.4734
VIRDOP	"	107	1090139.5812	-4842519.9208	3991981.3448
STFDOP	"	112	-3942239.2423	3468855.5871	-3608203.6057
NMXDOP	"	113	-1556216.4356	-5169444.2862	3387248.8918
ANCDOP	"	114	-2656164.6273	-1544367.3596	5570655.0694
BSEDOP	"	116	4004964.6338	-96560.5528	4946540.8719
TULDOP	"	118	539846.0896	-1388555.1428	6180981.7531
ALTDOP	"	127	-3850349.6603	397641.9041	5052349.2989
OTTAWA	"	128	1091451.0705	-4351283.3864	4518704.9989
TEXDOP	"	192	-740293.2435	-5457072.2721	3207244.0759
FLODOP	"	641	4522402.8341	898009.7615	4392485.8333
ACSDOP	"	10068	6119383.2701	-1571426.3703	-871689.7779
KWJDOP	"	10214	-6160996.5325	1339620.0842	960418.7480
QUIDOP	"	30121	1280855.9377	-6250960.1974	-10805.2377
SHIDOP	"	30123	6104421.7024	-611089.3337	-1740832.2743
HONDOP	"	30188	-5511607.7645	-2226970.6334	2303885.9309
STODOP	"	30280	1743939.4601	-5022700.2647	-3512032.5234
CALDOP	"	30414	-1659603.1496	-3676719.6854	4925498.6255
NAPDOP	"	30448	-4923685.7435	270897.1997	-4031781.3889
EASDOP	"	30730	-1888660.9369	-5355676.6429	-2893868.6900
TVEDOP	"	30793	-5037685.3429	3301867.3001	-2090789.0125
BGKDOP	"	30800	-1139091.1983	6089773.4035	1510693.3724
DGCDOP	"	30939	1915630.6892	6030275.2825	-801054.9556
LAJDOP	"	30966	4432068.8540	-2268085.3935	3973469.6199
BDADOP	"	30967	2293703.6058	-4883220.5673	3390597.1572
PERDOP	"	30968	-2353566.3527	4877202.4215	-3358333.0110

TABLE 5.4 (continued)

Name	Satellite	Number	X meters	Y meters	Z meters
CNIDOP	Seasat	30970	5384987.6970	-1576476.1171	3023843.0621
UKIDOP	"	51960	-2713392.0941	-4144609.5580	4004304.8508
SMTH545	Geosat	545	-3942243.6110	3468862.4595	-3608192.7764
BRUSSE	"	547	4027867.2521	307035.7484	4919514.3172
MIZUSA	"	548	-3857197.2879	3108669.3208	4004045.8581
WETZ549	"	549	4075574.5828	931803.3171	4801583.2258
HERN550	"	550	1090141.2854	-4842516.6081	3991986.0169
LASC552	"	552	-1556212.4648	-5169444.5277	3387247.4723
GUAM	"	553	-5059777.2809	3591208.7617	1472781.1299
PRET554	"	554	5051978.1289	2725638.2968	-2774470.0505
SANJ555	"	555	4083914.9582	-4209799.1646	-2499111.9538
ANCH556	"	556	-2656166.5298	-1544367.1268	5570654.9540
THULE	"	557	539848.1355	-1388554.0793	6180981.7632
MAHES	"	558	3602879.2239	5238219.7963	-515940.0993
SANMI	"	559	-3088049.1845	5333057.5849	1638811.2299
TAFU560	"	560	-6100052.1682	-997198.9791	-1568313.3224
AUST561	"	561	-740302.5480	-5457070.5749	3207245.5966
MCMURD	"	562	-1310717.7327	310464.5672	-6213364.4895
CALGAR	"	563	-1659603.1596	-3676719.7054	4925498.6555
OTTAWA	"	564	1091451.8805	-4351284.6364	4518704.0989
KERGUE	"	567	1406289.0232	3918134.2904	-4816212.5272
TAHITI	"	568	-5245203.0002	-3080480.7634	-1912826.9203
HERM570	"	570	3981775.7400	-89246.2651	4965289.5695
SANFR	"	590	5105460.9471	-555117.8122	3769895.2833
FRENCH	"	591	3850658.6111	-5052185.6493	571073.8365
HERN690	"	30690	1090120.0455	-4842520.0861	3991982.4996
ASCENS	"	35000	6119380.9552	-1571428.4450	-871689.8138
STHEL	"	35004	6104421.3836	-611088.9867	-1740832.5309
CYPRUS	"	35006	4349913.0512	2904404.1888	3638097.3836
HAWAI07	"	35007	-5511592.3389	-2226878.0069	2304027.8383
DIEGO	"	35010	1915630.1862	6030274.2927	-801055.7949
CAMBRI	"	35011	-594793.4207	-2201192.7264	5936679.2929
BAHRAI	"	35012	3633912.3241	4425272.6235	2799863.0566
ASUNCI	"	35013	3090627.3180	-4872489.1002	-2709322.6696
WICHIT	"	35015	-783476.6222	-5236529.9928	3544680.5051
SIOUX	"	35017	-523527.1482	-4687699.2715	4279317.4250
SHEMYA	"	35018	-3850347.5958	397640.4079	5052351.5166
LASC021	"	35021	-1556214.4784	-5169444.0977	3387247.4170
QUITO	"	35022	1272867.2335	-6252770.4973	-23789.7269
SIGONE	"	35024	4901702.2860	1306302.9468	3853345.8885
SANTIA	"	35025	1769924.6120	-5044557.7565	-3468244.6025
KINS026	"	35026	6136058.4058	1673471.8544	-482835.0357
DENVER	"	35027	-1252440.1217	-4752035.9675	4054736.8291
BANGK28	"	35028	-1133938.9841	6092553.8607	1503378.2917
RAPID	"	35029	-1038826.5831	-4464423.6118	4421688.3933
IDHAO	"	35036	-1738444.7831	-4295171.4575	4370322.7768
ARIZON	"	35037	-1939536.0579	-4843748.4689	3659828.5226
NEVADA	"	35038	-2369578.2484	-4327790.8622	4030082.1104
NASMS	"	35039	130023.0231	-5379940.2756	3412098.3402
PERU	"	35040	327215.1309	-4835515.2246	4132677.2698

TABLE 5.4 (continued)

Name	Satellite	Number	X meters	Y meters	Z meters
DIONYSD	Nova	3041	4595218.6725	2039466.9890	3912621.8195
MADRIDD	"	3061	4849193.2184	-360295.1392	4114933.8490
SIMSATOD	"	3091	-3822377.1045	3699393.2101	3507569.2487
CANBERAD	"	3101	-4446484.3977	2678126.2748	-3696275.0491
HUAHINED	"	3111	-5345895.0155	-2958234.1706	-1824585.6567
POTSDAMD	"	3121	3800591.5452	881922.2790	5028912.2689
HERSTMCD	"	3131	4033588.5389	24246.9924	4924220.5363
EFFELSBD	"	3141	4029170.7261	490757.3703	4904016.6311
HAYSTACD	"	3161	1492397.8231	-4457288.2226	4296834.8167
FTDAVISD	"	3171	-1324205.9321	-5332052.2992	3232060.3383
PLATTEVD	"	3181	-1240643.2742	-4720479.7021	4094479.0098
PARISD	"	3711	4201864.7891	177906.7906	4779214.0113
GRASSED	"	3721	4588034.5714	556441.2394	4381674.0942
BAIRESD	"	3791	2745491.5732	-4483597.7095	-3599082.7115
RIGRNDD	"	3811	1429893.0817	-3495352.9013	-5122699.9038
PENCHUND	"	3831	4052450.5274	1417636.6117	4701419.4581

TABLE 5.5 LANDSAT Station Coordinates of GEM-T3S

Name	Number	X meters	Y meters	Z meters
BDA3	2	2308455.5364	-4874293.5621	3393397.0171
CYI3	4	5439153.5525	-1522099.6112	2953511.6422
HAW3	12	-5543852.5244	-2054559.7456	2387810.8980
GDSA	14	-2354713.6931	-4646803.9081	3669383.5426
MAD8	23	4847825.5406	-353313.1737	4117137.2740
GWM3	24	-5068920.7150	3584109.3448	1458900.7273
GDS8	28	-2354765.6400	-4646782.9405	3669386.9513
ACN3	75	6121231.9294	-1563360.8095	-876915.6451
ETC3	77	1129797.1874	-4833151.4293	3992205.8591
ETCA	91	1129871.4279	-4833149.8424	3992190.2355

6.0 DYNAMIC HEIGHT MODELS

The method by which the dynamic height of the ocean has been measured has undergone considerable evolution in the past decade. Traditional oceanographic techniques which are based on classical hydrodynamic principles have been carried out for many years with variable success. These models are primarily based upon measurements of temperature and salinity along ship tracks. This approach suffers from difficulties in establishing an absolute reference surface and in the lack of global data distribution and infrequent time sampling. Time-averaged models of dynamic height have been produced from in situ observations (e.g., Levitus, 1982), but these models are not likely to reproduce the true long term mean surface over poorly sampled regions. While a description of the long term mean surface is enlightening, fundamentally, oceanographers require a much more detailed understanding of the evolution of the dynamic height field over time. Space-based radar altimeter systems have shown the capacity to regularly monitor the ocean surface topography and have effectively overcome data distribution shortcomings. However, by introducing a complex and highly dynamical measurement origin, the use of altimetry presents many new complications to the accurate solution of the dynamic height field.

Marsh et al., (1990b), Nerem et al., (1990) and Tapley et al., (1988) have shown that altimeter data can effectively be used directly in the orbit and geodetic model determination processes. Simultaneous solutions for the orbits, gravitational field, and dynamic topography surfaces have many advantages. The altimeter data provides valuable information on the shape of the ocean surface which at shorter wavelengths over many time samples predominately reflects the geoid. This improves the geoid determination over the oceans and complements the surface gravimetry. Direct use of altimeter observations for defining the satellite ephemerides provides a significant improvement in orbit accuracies. These data map the satellite's radial position over the ocean surface uniformly, and provide information which would otherwise be lacking given the large gaps in conventional land-based tracking coverage over many of the ocean basins. The data also complement the information provided by normal tracking data. Laser ranging and TRANET Doppler observations are much more sensitive to the satellite's along track position (where the velocity with respect to the station is dramatically changing over a pass) whereas altimetry directly senses the satellite's radial position.

The above solutions showed that by solving for the geoid and dynamic heights simultaneously: (a) the cm level laser ranging is able to define the geoid at long wavelengths; (b) the altimeter improves the gravitational coefficient deconvolution within the sensed orbital perturbations at intermediate and short wavelengths; (c) the dynamic sea surface topography field represents the departure of the ocean surface from the geoid over the most critical long-wavelength bandwidth; and (d) the orbital definition is dramatically improved in its radial direction as a result of using ordinary tracking and altimeter data in common within the orbit adjustment process.

The design of the GEM-T3 solution accounted for temporal changes in the dynamic height field. Large scale fluctuations in sea surface topography are important indications of global change. Such variations include secular trends in the total mass or volume of the ocean (e.g., Barnett, 1983; Peltier, 1988), interrannual variations on a basin scale such as the anomalous undulations of the tropical thermocline caused by the El Nino Southern Oscillation (e.g., Wyrtki, 1975; Miller et al., 1988) and hemispheric fluctuations on an annual basis that are caused by the seasonal heating and cooling of the upper ocean (Pattullo et al., 1955; Wyrtki and Leslie, 1980; Levitus and Koblinsky, 1991). Satellite altimetry has provided a measurement system capable of the global synoptic monitoring of large scale sea level changes through the solution of time-specific dynamic height models. Possible temporal evolution of the sea surface topography was factored into the design of the GEM-T3 solution. The altimeter data employed in the GEM-T3 model span more than a decade (April 1975 to January 1987). While the GEOSAT and SEASAT observations were each acquired during concentrated tracking intervals of limited duration, the GEOS-3 data was inhomogeneously acquired over a 14 month time period. There was a strong El Nino event during

the fall of 1986 which is coincident with the time period of the GEOSAT altimeter data utilized in GEM-T3. Given the sparsity and lower accuracy of the GEOS-3 data, no global sensitivity to temporal variations within its data span are recoverable. Hence, it was decided to simultaneously estimate separate dynamic topography models for each of the altimeter missions.

Each dynamic topography model is referenced to the same geoid, it is best understood as a temporally averaged snapshot of the surface, and can be compared across missions to assess temporal changes in the long wavelength dynamic height field. The strength of the El Nino signal detected by the difference between GEM-T3's SEASAT and GEOSAT dynamic height surfaces is discussed in Nerem et al., (1991a, submitted). A sequence of near-monthly dynamic height fields determined from GEOSAT altimetry are described in Koblinsky et al., (1991, submitted) where the evolution of the surface topography is extensively compared to tide gauge and hydrographic observations. A secular, annual and semi-annual time-varying model of the dynamic height field also determined using GEOSAT is given in Nerem et al., (1991b, submitted).

6.1 MATHEMATICAL MODEL OF DYNAMIC TOPOGRAPHY

The altimetric model of the dynamic topography, η, is that of a spherical harmonic series which is truncated at a specific degree and is restricted by the presence of geoid errors. This representation is:

$$\eta = \bar{\eta} = \sum_{n=0}^{n_1} \sum_{m=0}^{n} \sum_{\alpha=1}^{2} \eta_{\alpha mn} S_{\alpha mn} \qquad \text{(eq 15)}$$

and:

$$S_{\alpha nm} = P_{nm}(\sin\phi)\cos m\lambda \quad \text{for } \alpha = 1$$
$$= P_{nm}(\sin\phi)\sin m\lambda \quad \text{for } \alpha = 2$$

where the overbar is used to indicate averaging over the solution interval, and n_1 corresponds to the truncation limits of the model which was degree 15 for the GEM-T3 models. Mathematical stabilization of the dynamic height recovery is required since altimeter data does not provide uniform coverage over the sphere. A form of least squares collocation (Moritz, 1980) was used to control the power in the recovered coefficients paralleling the application of Kaula's rule for gravity field stabilization described in (3.0). This approach reduces the modeling instability over areas lacking data. A constraint is introduced into the solution which is based on the power observed in the dynamic height field obtained from climatology from a 2250db reference surface (Levitus, 1982). This climatological model is the best in situ information available. The need for the application of this constraint, its form and its effect on the behavior of the SEASAT solution is more completely described in Marsh et al., (1990b).

6.2 DISCUSSION OF GEM-T3 DYNAMIC HEIGHT FIELDS

Figure 6.1 presents a map of the dynamic height field developed from a spectral harmonic decomposition of the Levitus (op. cit) climatology complete to degree and order 15. The dominant signal in the dynamic height field is well represented by this 15x15 harmonic model. Clearly, the largest part of the dynamic height field is due to the basin-wide oceanic gyre systems. Also, the strongest surface expression is seen in the western boundaries of these current systems. Figure 6.2 presents the three dynamic height fields recovered in the GEM-T3 solution. These models are shown for GEOS-3, SEASAT and GEOSAT and each are complete to degree and order 15. There is good consistency across the GEM-T3 models and good overall agreement with climatology.

Figure 6.1

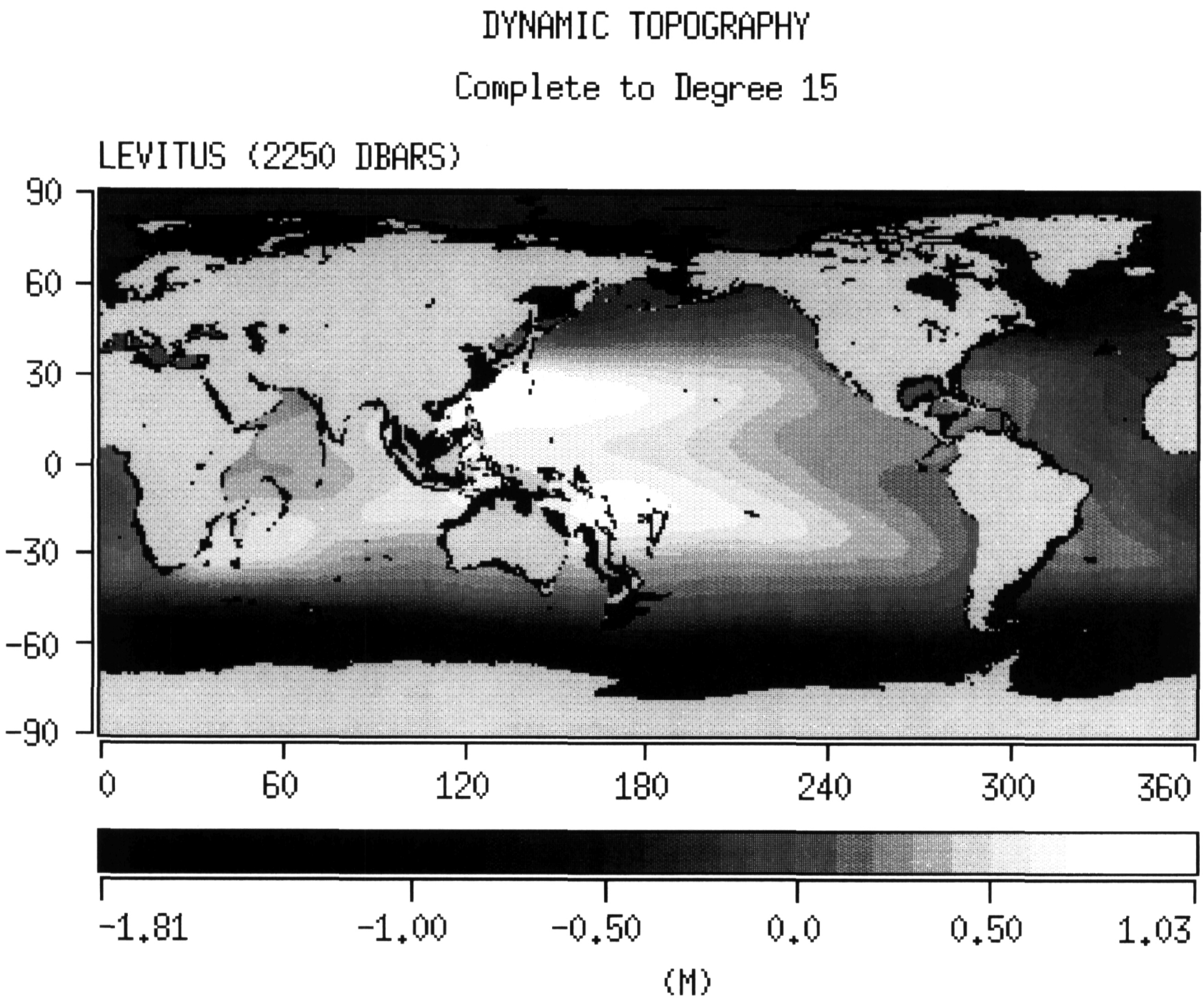
DYNAMIC TOPOGRAPHY
Complete to Degree 15
LEVITUS (2250 DBARS)
90
60
30
0
-30
-60
-90
0
60
120
180
240
300
360
-1.81
-1.00
-0.50
0.0
0.50
1.03
(M)

Figure 6.2

GEM-T3 DYNAMIC TOPOGRAPHY

Complete to Degree 15

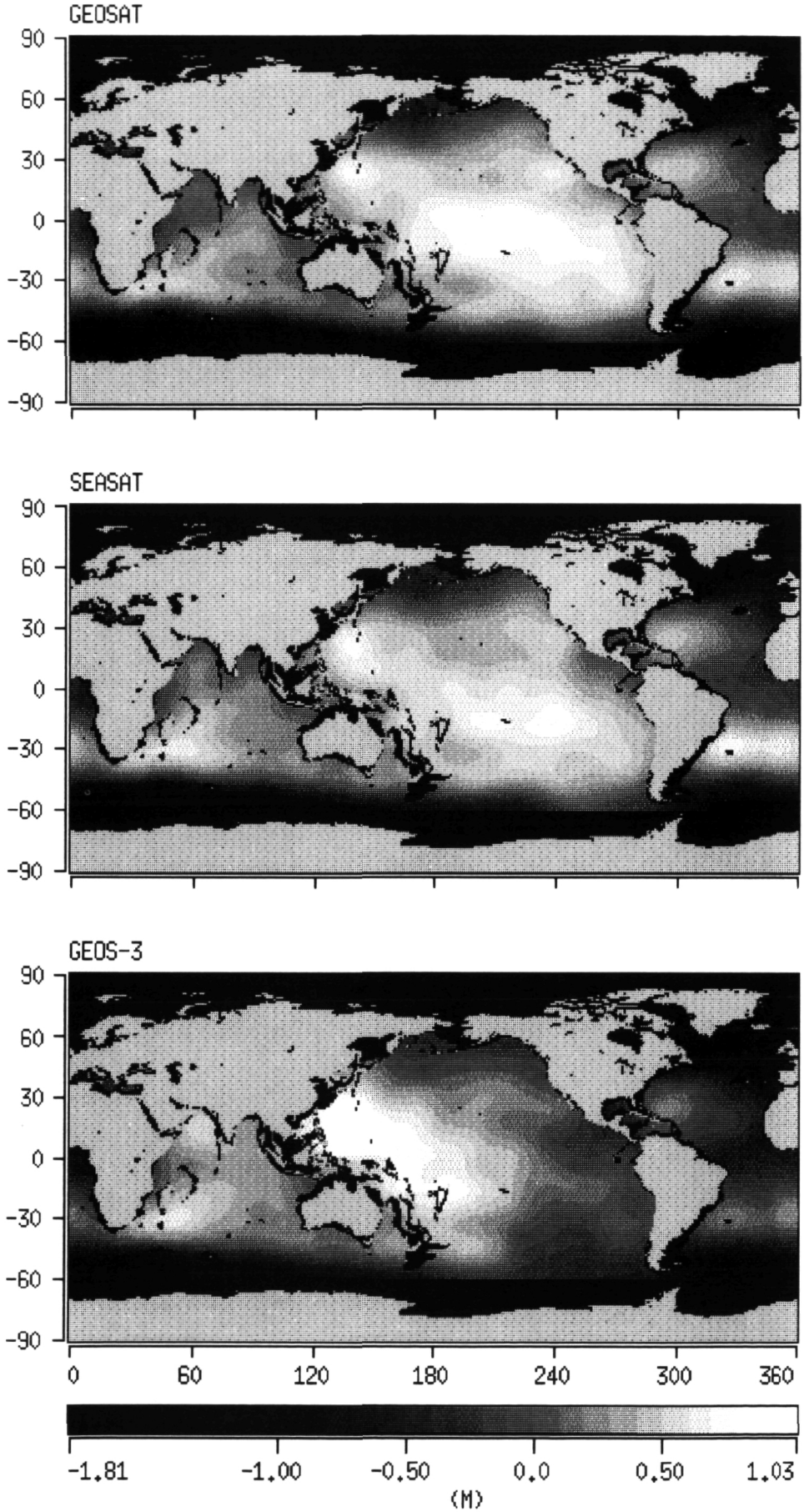

Table 6.1 presents the recovered harmonics for these dynamic height solution and the values obtained from climatology.

The separation of oceanographic and gravitational signals within the altimeter observations is the critical problem in dynamic height solutions using our methodology. Since the geoid signal exceeds that of the dynamic height field by an order of magnitude, small geoid errors can severely alias the recovery of dynamic height models. Figure 6.3 compares the spectrum of the global geoid height error within GEM-T3 with the expected global power of the QSST field deduced from climatology. While this figure indicates that the power of the estimated geoid error exceeds the expected QSST signal at about degree 8, there are several mitigating factors which were considered in solving for 15x15 dynamic height models in GEM-T3.

(a) The values shown in Figure 6.3 represent global RMS statistics. As demonstrated in Figure 5.5, the geoid definition over the oceans areas tracked by altimetry is superior to the global average.

(b) Least squares collocation insures that the altimeter signal which is not resolvable as belonging to either the gravity or QSST fields, will be absorbed into the gravitational model. This is due to the tighter constraint on zero as the coefficient values for unresolvable terms within the QSST model (see Marsh et al., 1990b; Section 5.6 for a discussion of this solution characteristic).

(c) The correlation between the QSST fields and GEM-T3 geoid model, shown in Figure 6.4 indicates that the models are well resolved apart from the geoid; spatial correlation between the GEM-T3 gravity and any of the QSST models in the open oceans is rarely stronger than -.25.

Figure 6.5 presents the uncertainty of the three dynamic height models. The lower weight given to the GEOS-3 data and gaps in this data set are evident. The higher density of geographic data distribution for the three day repeating groundtrack segment of the SEASAT Mission is also reflected in the correlation of the SEASAT QSST and geoid models. In all cases, the geoid uncertainty is the dominating error source in the definition of the QSST model.

Table 6.1 GEM-T3 Dynamic Sea Surface Topography Coefficients

		GEOSAT		SEASAT		GEOS-3	
n	m	C	S	C	S	C	S
0	0	.0000	.0000	.0000	.0000	.0000	.0000
1	0	.0707	.0000	.0319	.0000	.0927	.0000
1	1	-.1813	-.0983	-.1739	-.0602	-.2070	.1428
2	0	-.4237*	.0000	-.3909*	.0000	-.3225*	.0000
2	1	-.0241	.0765	-.0309	.0674	-.0140	.0990
2	2	-.0228	.0292	-.0239	.0227	-.0058	.0106
3	0	.1771	.0000	.1677	.0000	.1004	.0000
3	1	.0156	.0009	.0001	-.0121	.0081	.0004
3	2	-.0119	-.0270	-.0120	-.0263	-.0492	-.0236
3	3	-.0188	-.0297	-.0291	-.0255	-.0663	-.0141
4	0	-.0534	.0000	-.0542	.0000	-.0127	.0000
4	1	.0544	.0795	.0476	.0699	.0528	.0583
4	2	-.0305	.0192	-.0257	.0179	-.0178	.0276
4	3	-.0020	.0022	-.0052	.0090	.0082	.0070
4	4	-.0116	-.0454	-.0327	-.0454	-.0285	-.0247
5	0	.0201	.0000	.0133	.0000	.0139	.0000
5	1	-.0435	-.0148	-.0434	-.0033	-.0420	-.0110
5	2	-.0209	.0541	-.0159	.0573	-.0043	.0450
5	3	.0144	.0175	.0150	.0142	-.0020	.0028
5	4	-.0433	.0165	-.0399	.0173	-.0503	.0083
5	5	.0055	-.0139	.0054	-.0110	.0052	-.0171
6	0	.1172	.0000	.1261	.0000	.0954	.0000
6	1	-.0155	.0411	-.0208	.0491	.0071	.0410
6	2	-.0300	.0262	-.0365	.0221	-.0132	.0202
6	3	.0127	-.0133	.0053	-.0200	.0124	-.0085
6	4	-.0218	.0074	-.0145	.0028	-.0141	.0194
6	5	.0092	.0145	.0158	.0159	.0145	.0107
6	6	.0029	-.0050	.0135	-.0089	.0054	-.0039
7	0	-.0407	.0000	-.0429	.0000	-.0402	.0000
7	1	.0398	-.0061	.0363	-.0119	.0409	-.0109
7	2	.0087	.0072	.0091	.0055	.0001	-.0104
7	3	.0075	-.0107	.0094	.0051	.0145	.0075
7	4	.0058	.0055	.0052	-.0012	.0113	-.0072
7	5	-.0048	-.0009	-.0041	-.0017	-.0043	-.0052
7	6	.0171	.0089	.0125	.0083	.0125	.0076
7	7	-.0021	-.0030	.0010	-.0020	.0009	-.0021
8	0	.0408	.0000	.0344	.0000	.0171	.0000
8	1	-.0433	-.0240	-.0393	-.0249	-.0234	-.0257
8	2	0.0000	-.0111	-.0024	-.0104	-.0045	.0037
8	3	.0180	.0015	.0118	.0018	.0049	.0077
8	4	.0190	.0003	.0205	-.0050	.0112	.0071
8	5	-.0006	-.0038	-.0040	.0010	-.0045	.0052
8	6	-.0005	-.0018	-.0033	-.0051	.0046	-.0004
8	7	.0027	-.0114	-.0060	-.0129	-.0096	-.0096
8	8	.0077	.0023	-.0004	.0048	.0050	.0011
9	0	-.0131	.0000	-.0090	.0000	-.0033	.0000
9	1	.0022	.0034	.0024	.0051	.0031	.0052

* 11.52 cm needs to be added to C_{20} values to remove the contribution of direct and indirect permanent tidal deformations.

Table 6.1 (Continued) GEM-T3 Dynamic SST Coefficients

		GEOSAT		SEASAT		GEOS-3	
n	m	C	S	C	S	C	S
9	3	-.0048	.0084	-.0016	.0085	.0016	.0043
9	4	.0015	.0034	-.0006	.0007	-.0009	-.0009
9	5	-.0001	-.0105	.0007	-.0053	.0007	-.0071
9	6	-.0035	-.0002	-.0041	-.0010	-.0042	.0018
9	7	-.0036	-.0011	-.0025	.0018	.0007	-.0025
9	8	-.0022	.0015	-.0019	.0030	-.0056	.0001
9	9	-.0005	.0035	0.0000	.0027	-.0019	.0029
10	0	-.0068	.0000	-.0077	.0000	-.0039	.0000
10	1	.0151	-.0034	.0138	-.0029	.0067	-.0012
10	2	-.0029	.0046	.0006	.0036	-.0026	.0025
10	3	-.0023	.0057	-.0001	-.0003	.0023	.0019
10	4	.0028	-.0068	.0005	-.0049	.0012	-.0034
10	5	-.0041	-.0045	-.0034	-.0040	-.0074	-.0034
10	6	-.0055	.0056	-.0057	.0034	-.0063	.0036
10	7	-.0004	-.0024	.0010	-.0017	-.0002	-.0032
10	8	-.0042	.0033	-.0033	.0028	-.0053	.0042
10	9	-.0066	.0038	-.0060	.0054	-.0025	.0055
10	10	-.0010	-.0045	-.0014	-.0061	-.0008	-.0033
11	0	.0148	.0000	.0113	.0000	.0091	.0000
11	1	-.0109	.0022	-.0093	-.0004	-.0135	-.0004
11	2	.0063	-.0018	.0054	-.0037	.0021	-.0002
11	3	-.0021	-.0045	-.0060	-.0042	-.0007	-.0003
11	4	.0035	.0037	.0030	.0063	.0064	-.0010
11	5	.0023	-.0041	.0025	-.0038	.0060	-.0027
11	6	-.0065	-.0031	-.0038	-.0057	-.0013	.0012
11	7	-.0001	.0048	-.0001	.0019	.0009	.0045
11	8	-.0028	.0002	-.0035	.0007	-.0028	0.0000
11	9	.0040	0.0000	.0056	-.0030	.0027	.0042
11	10	-.0008	.0042	.0004	.0052	-.0008	-.0005
11	11	.0057	-.0047	.0054	-.0020	.0050	.0008
12	0	-.0122	.0000	-.0113	.0000	-.0093	.0000
12	1	.0124	.0028	.0154	.0030	.0076	.0020
12	2	.0029	-.0018	.0019	.0013	.0043	-.0049
12	3	.0004	.0002	-.0006	.0035	-.0009	-.0035
12	4	-.0019	-.0032	.0007	-.0046	-.0050	.0046
12	5	.0008	.0078	.0009	.0025	-.0010	.0058
12	6	.0090	-.0018	.0076	-.0008	.0025	.0033
12	7	-.0009	.0043	.0013	.0050	-.0005	.0026
12	8	.0044	-.0014	.0023	.0004	.0026	.0001
12	9	-.0018	.0073	-.0011	.0051	-.0028	.0022
12	10	.0072	-.0060	.0077	-.0056	.0083	-.0026
12	11	-.0053	.0036	-.0009	.0041	-.0026	.0043
12	12	.0068	-.0017	.0060	-.0021	0.0000	.0010
13	0	.0108	.0000	.0111	.0000	.0026	.0000
13	1	-.0022	-.0096	.0014	-.0058	.0004	-.0057
13	2	-.0074	.0052	-.0082	.0030	-.0023	.0049
13	3	-.0012	-.0060	-.0004	-.0019	0.0000	-.0002
13	4	.0011	.0042	-.0013	.0009	.0012	.0039
13	5	-.0023	-.0027	-.0055	-.0018	.0041	-.0003
13	6	.0017	-.0004	.0005	.0005	-.0026	-.0038
13	7	-.0033	-.0070	-.0023	-.0048	.0005	-.0022
13	8	.0031	.0014	.0029	.0008	.0036	.0014
13	9	.0006	-.0069	-.0009	-.0062	0.0000	-.0039

Table 6.1 (Continued) GEM-T3 Dynamic SST Coefficients

		GEOSAT		SEASAT		GEOS-3	
n	m	C	S	C	S	C	S
13	10	-.0043	.0012	-.0037	.0044	-.0001	.0010
13	11	.0044	.0002	.0026	.0012	.0017	.0016
13	12	-.0010	.0017	-.0004	.0028	-.0009	-.0006
13	13	.0015	-.0008	.0029	-.0016	.0040	-.0044
14	0	-.0131	.0000	-.0072	.0000	-.0024	.0000
14	1	-.0064	.0060	-.0080	.0053	-.0106	.0056
14	2	.0097	-.0089	.0065	-.0095	.0042	-.0058
14	3	-.0032	0.0000	-.0062	-.0041	-.0001	.0013
14	4	.0030	.0008	.0010	.0008	-.0003	.0014
14	5	.0045	.0013	.0035	.0026	.0067	0.0000
14	6	.0055	-.0064	.0045	-.0042	.0063	-.0047
14	7	-.0078	-.0036	-.0115	-.0019	-.0051	-.0054
14	8	-.0089	-.0006	-.0076	.0021	-.0078	.0030
14	9	-.0047	-.0015	-.0016	.0004	-.0043	-.0010
14	10	-.0008	.0008	-.0003	.0029	-.0046	.0031
14	11	.0008	-.0008	0.0000	.0001	-.0020	.0007
14	12	-.0018	.0001	-.0025	-.0032	.0001	-.0055
14	13	.0014	.0026	-.0005	.0004	-.0001	.0057
14	14	-.0002	-.0015	-.0029	.0003	-.0003	-.0016
15	0	-.0080	.0000	-.0065	.0000	-.0059	.0000
15	1	.0141	.0047	.0063	.0020	.0097	-.0015
15	2	-.0048	.0007	-.0031	.0024	-.0004	.0030
15	3	.0092	-.0023	.0092	-.0044	.0038	-.0050
15	4	-.0084	-.0054	-.0030	-.0057	-.0050	-.0011
15	5	-.0068	.0023	-.0042	.0024	-.0035	.0015
15	6	.0036	.0052	.0003	.0022	.0015	.0038
15	7	-.0001	-.0098	-.0013	-.0086	-.0011	-.0055
15	8	.0046	.0012	.0020	-.0029	.0007	.0014
15	9	-.0006	-.0021	-.0003	-.0029	.0014	-.0031
15	10	.0017	.0078	.0009	.0084	.0033	.0048
15	11	-.0064	-.0015	-.0037	-.0023	-.0050	.0042
15	12	-.0052	.0033	-.0038	.0028	-.0020	.0014
15	13	-.0002	.0005	.0029	.0011	.0025	.0007
15	14	-.0002	-.0012	-.0017	-.0005	-.0013	-.0015
15	15	.0064	.0012	.0046	-.0009	.0022	0.0000

Figure 6.3

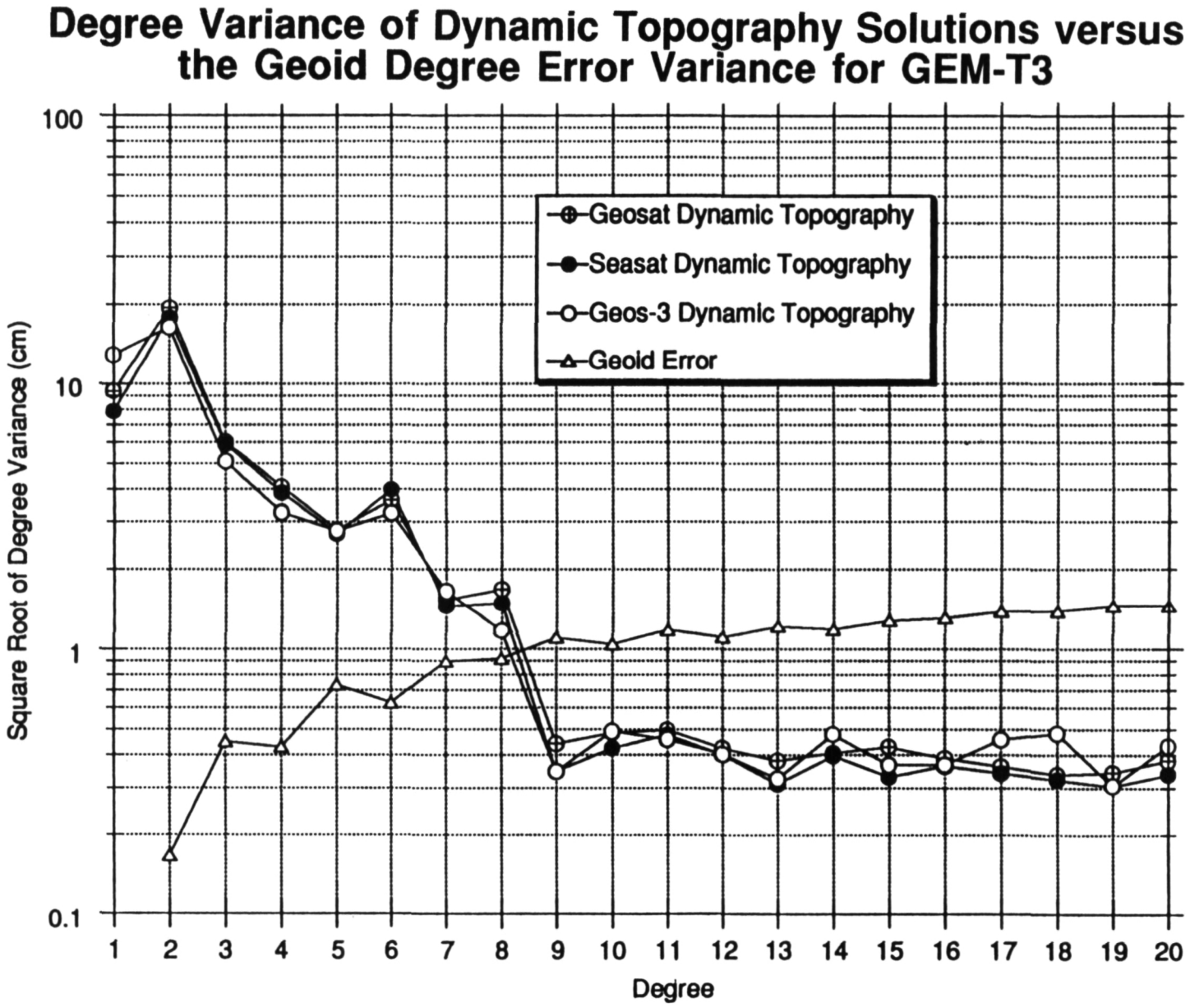
Degree Variance of Dynamic Topography Solutions versus the Geoid Degree Error Variance for GEM-T3
Geosat Dynamic Topography
Seasat Dynamic Topography
Geos-3 Dynamic Topography
Geoid Error
Square Root of Degree Variance (cm)
100
10
1
0.1
1 2 3 4 5 6 7 8 9 10 11 12 13 14 15 16 17 18 19 20
Degree

Figure 6.4

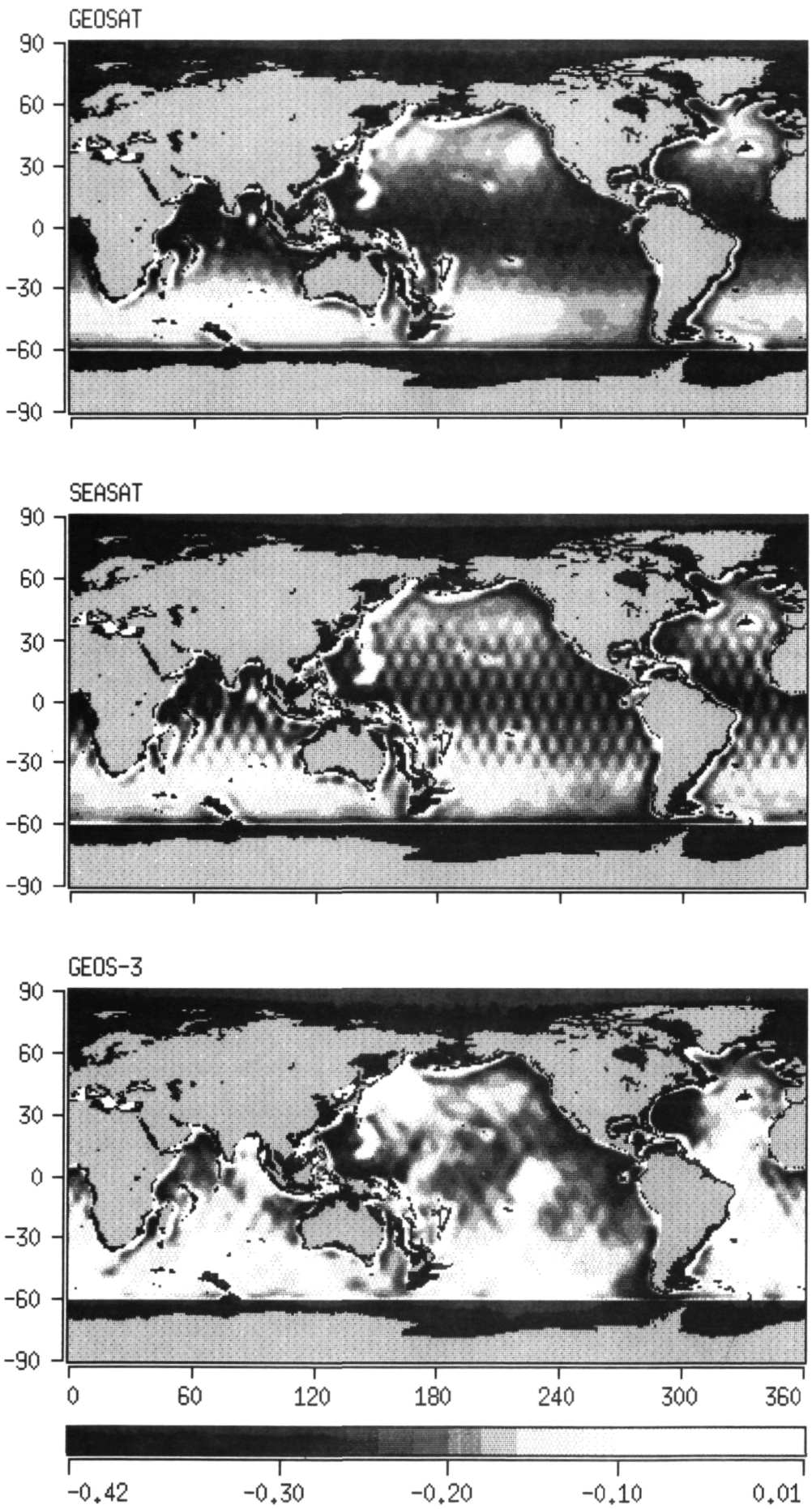
GEM-T3 DYNAMIC TOPOGRAPHY/GEOID CORRELATION COEFFICIENTS
GEOSAT
SEASAT
GEOS-3
90
60
30
0
-30
-60
-90
0
60
120
180
240
300
360
-0.42
-0.30
-0.20
-0.10
0.01

Figure 6.5

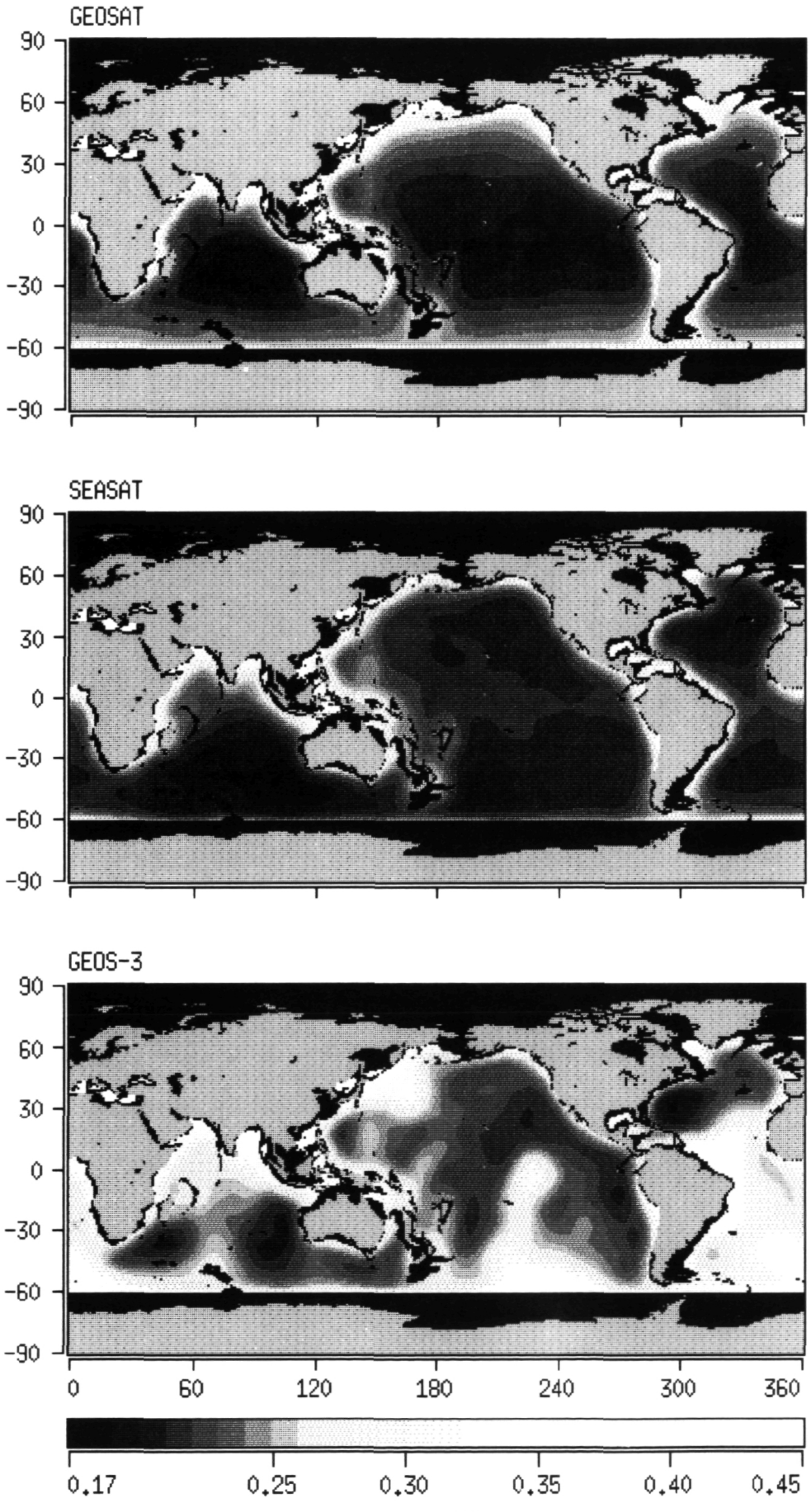
GEM-T3 DYNAMIC TOPOGRAPHY ERRORS
Complete to Degree 15
GEOSAT
SEASAT
GEOS-3
90
60
30
0
-30
-60
-90
0
60
120
180
240
300
360
0.17
0.25
0.30
0.35
0.40
0.45
(M)

7.0 ORBIT ACCURACIES

Satellite geodesy, space-based remote sensing, and satellite altimeter mapping missions flown to support physical oceanography all have a critical dependence on orbit determination. In many circumstances, it is the existence of systematic error of the orbit in time, and/or over certain critical spatial scales, which fundamentally limits the science yield of the missions themselves. The orbital motion of a satellite exhibits an integrated response to the forces generated by the inhomogeneous mass distribution on and within the Earth, the density of the atmospheric medium it traverses, and by the size, material characteristics and orientation of the satellite surfaces exposed to the Sun and Earth. There are many additional, although less significant forces acting on the spacecraft which require consideration. The observer monitoring the satellite's motion must be positioned over time with respect to the geocenter and within the inertial frame used to integrate the satellite orbit. The observer undergoes complex motion due to its position on an irregularly rotating and wobbling Earth, the motion and deformation of the tectonic plate it resides on, and experiences local motion due to various loading and tidal effects.

While improvements in orbit determination technologies have been forthcoming over the last twenty years, it has been the release of new and improved gravity models which has made the largest impact on the current accuracy of geodetic satellite positioning. The requirements for precise orbit modeling are an important element in the success of many missions. This includes satellites designed to monitor the Earth's tectonic motions like LAGEOS and those requiring accurate radial positioning of an altimeter to locate the ocean surface in a geocentric reference frame like GEOSAT and TOPEX/Poseidon. GEM-T3S and GEM-T3 have been tested using independent tracking data from a number of missions. Their performance is compared with recent GEM solutions and those developed elsewhere.

7.1 GRAVITY MODEL TESTS USING TRACKING OBSERVATIONS

Highly precise observations obtained by the laser tracking network have been used to compare the gravitational models. All of these observations, while taken on satellites which are included in each of the gravity models, represent observation subsets which have not been utilized in the development of any of the models tested. There is a question of reference frame in producing a fair comparison across different gravity models, especially for those not developed at GSFC. We have therefore used a multi-arc approach where the laser data themselves are able to define the polar motion parameters in each of the test solutions. Furthermore, we have incorporated a complete model for dynamic polar motion to account for the Earth's rotational deformation at the annual and Chandler periods (see Reigber, 1981; Marsh et al., 1988; Section 3). The use of this model causes the pole coordinates to have dynamic contributions. In these tests, the C,S(2,1) coefficients were also permitted to adjust enabling each of the tested models to define a mean figure axis based on the gravitational models and the laser observations. Laser tracking station coordinates obtained by Smith et al., (1990) from Lageos quarterly solutions were adopted coincident with the observations used for testing. In the case of the Lageos test solution, station positions were also freely adjusted. An expanded dynamic tide model (containing more than 90 ocean tidal lines and nearly 6000 terms) which is based on the GEM-T3 was utilized to minimize errors arising from omitted ocean tidal effects. As shown in Table 5.3, contemporary tide models agree quite well.

The test arcs are summarized below:

- Starlette: 8 5-day arcs of laser normal points obtained during 8/3/88 to 9/19/88

- Ajisai: 8 6-day arcs of laser normal points obtained during 4/4/89 to 5/14/89
- Lageos: 3 monthly arcs of laser normal points obtained during 4/88 to 6/88

The results of these test solutions are presented in Table 7.1. It is clear from this table that all of the contemporary gravitational solutions show good overall agreement. They all are capable of fitting these diverse laser observation subsets at the decimeter or better level. For the GEM model results contained therein, GEM-T3S is an improved model over GEM-T2 when "satellite-only" models are compared. The combination GEM-T3 model is a further improvement over GEM-T3S.

DORIS is a tracking system developed by the French which will be used to support their orbit determination on TOPEX/Poseidon. A prototype of the DORIS system is presently being flown on SPOT-2. The main component of the DORIS system is the DORIS onboard package which is essentially a radio receiver designed to accurately measure the carrier frequency of incoming ground signals. Whenever the satellite is within the visibility of a ground station, the DORIS onboard package measures the Doppler shift in the two transmit frequencies of the ground beacon. These signals are at 2036 and 401 MHz; the dual frequency measurement permits a cancellation of the ionospheric propagation effects to first order; this choice of frequencies effectively eliminates the ionospheric refraction effects as a problem.

The fundamental DORIS measurement is a one-way average range-rate signal from the ground based beacon to the satellite. The satellite clock is monitored by a master control station where the drift in the satellite clock is determined. The satellite clock is very stable, and the frequency drift over the ten-minute duration of a single station pass is not believed to be significant. Therefore only a solution of a frequency offset per pass is normally required when processing the DORIS data. The range-rate data provided by DORIS is very precise; noise levels of .3 to .7 mm/s are typical for the SPOT data set. Like all radiometric data, the tropospheric refraction path delay is the most serious measurement problem, and we have permitted a zenith delay tropospheric refraction scaling parameter to adjust for each pass of data.

The DORIS Network, with more than 35 globally deployed stations, provides a strong independent test for gravity solutions. Table 7.2 compares the RMS of fit obtained for three typical SPOT test arcs, of 3 to 5 days length. Again, GEM-T3, the combination model, outperforms the satellite GEM-T3S using this highly precise independent data.

7.2 Projected Orbit Errors Due to Static Gravitational Modeling Uncertainties

The error covariance matrix can be used to project the gravitational modeling error onto any orbital configuration. This projection uses the first-order analytical perturbation theory developed by Kaula (1966) and gives a harmonic estimate of modeling error. This estimate does not take into account the distribution of tracking data nor does it consider the additional error arising from the erroneous estimation of the orbital state (epoch) position which propagates with the well-known "once-per-revolution" orbit errors commonly seen in data analyses. It also neglects errors arising from long period gravitational effects like those due to the odd zonals. However, with the distribution of modern tracking networks and the typical performance of these tracking systems in their support of numerous missions, we have found through comparisons with numerical tests and data simulations, that these first-order projections are quite reliable in mapping a given gravity error into orbit error overall.

Table 7.3 presents the projected orbit uncertainties in the radial component for many existing and to-be-launched satellites. It compares the projected performance of GEM-T2, GEM-T3S and GEM-T3. For the TOPEX/Poseidon orbit in specific, these estimates indicate that we are approaching

Table 7.1
Orbit Tests Using Independent Laser Data

Model	LAGEOS	Ajisai	Starlette
GEM-T1	3.12 cm	16.42 cm	17.11 cm
GEM-T2	3.02 cm	8.83 cm	12.27 cm
GEM-T3S	2.89 cm	8.39 cm	10.77 cm
GEM-T3	2.89 cm	8.42 cm	10.76 cm
TEG-2B†	2.92 cm	8.71 cm	10.24 cm
OSU91A	2.98 cm	8.81 cm	11.84 cm
GRIM4-S2	2.92 cm	8.59 cm	12.19 cm
GRIM4-C2	2.93 cm	9.52 cm	11.56 cm

Fits computed using an expanded GEM-T3 tide model and GSFC SL7.1 station coordinates. Dynamic polar motion employed and $C_{2,1}$, $S_{2,1}$ are estimated in each multi-arc so that the mean figure axis is defined by the data in each test.

Lageos: 3 - 30 day arcs, 4/88 - 6/88
Ajisai: 8 - 5 day arcs, 4/4/89 - 5/14/89
Starlette: 8 - 6 day arcs, 8/3/88 - 9/19/88

† preliminary model

Table 7.2
Orbit Tests Using SPOT-2 DORIS Data

Model	900503 (5 days)	900620 (3 days)	900702 (3 days)
GEM-T3S	5.33	5.32	4.82
GEM-T3	2.67	2.72	2.04

Fits computed using an expanded GEM-T3 tide model estimating solar pressure, 6 hour drag, and troposphere & measurement biases for each Doppler pass.

Units are mm/sec

Table 7.3
Projected Radial Orbit Error due to Gravity

Model	Topex	Lageos	Starlette	Ajisai	Spot-2	Geosat
GEM-T2	9.4	0.8	12.3	5.9	119.7	19.8
GEM-T3S	11.6	1.1	10.9	5.4	144.7	29.6
GEM-T3	6.1	0.9	6.9	3.8	83.2	11.9

Long period errors omitted. units are in cm

Figure 7.1

Predicted Radial Error From Gravity Covariances
at 1341 km. Altitude (TOPEX)

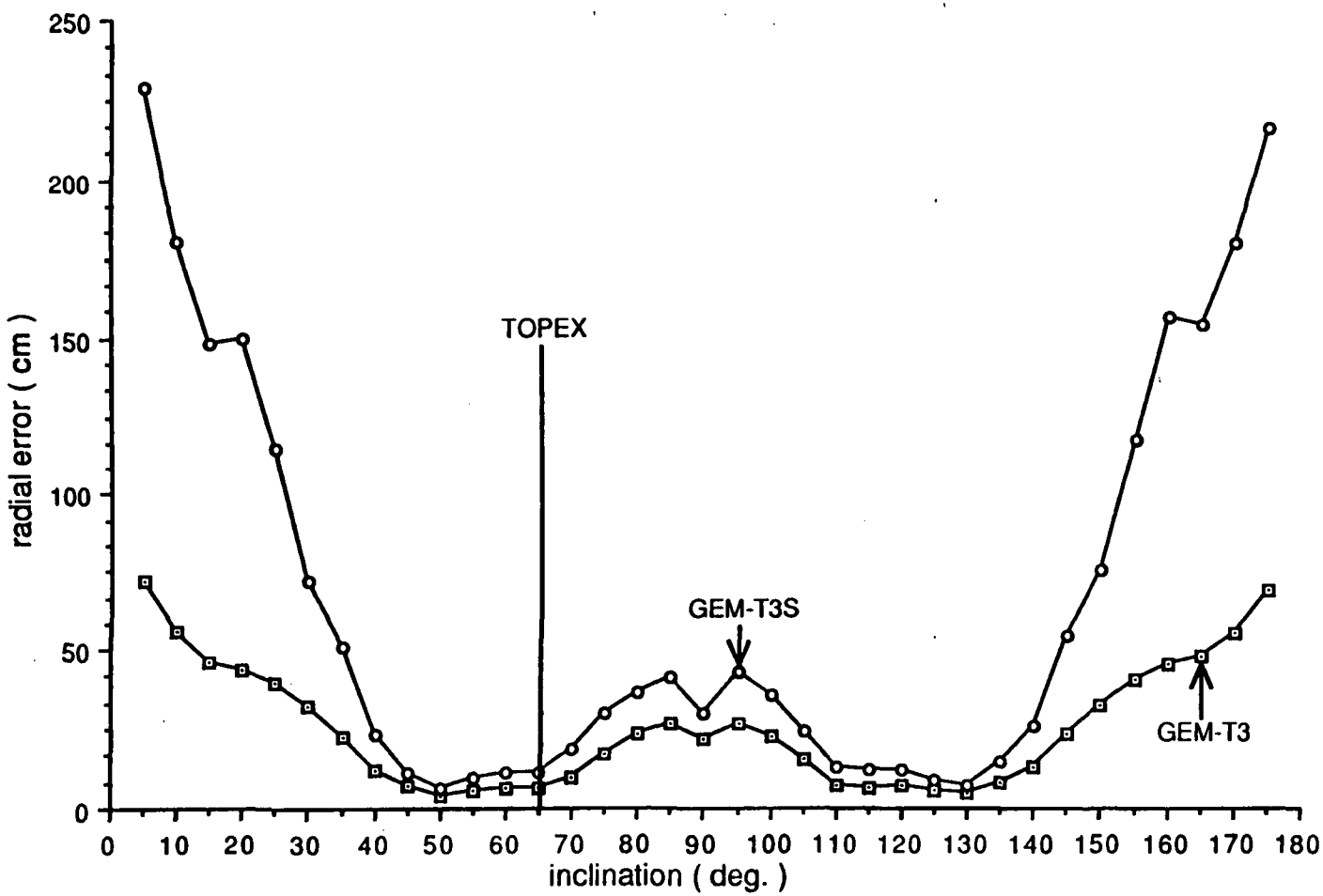

the level of modeling required to support this mission's radial error budget. Figure 7.1 presents a radial orbit uncertainty projection for a satellite at the nominal altitude of TOPEX/Poseidon (1341 km) using the GEM-T3 covariances for different orbital inclinations. For comparison purposes, also shown are the projections for GEM-T3S.

8.0 CONCLUSIONS

Improved models of the Earth's gravitational field have been developed from conventional tracking data (GEM-T3S) and from a combination of satellite tracking, satellite altimeter and surface gravimetric data (GEM-T3). This combination model represents a significant improvement in the modeling of the gravity field at half-wavelengths of 350 km and longer. Both models are complete to degree and order 50. The GEM-T3 model provides for more accurate computation of satellite orbital effects as well as giving a superior geoidal representation from that achieved in any previous Goddard Earth Model, estimated at 59 cm rms. The GEM-T3 model used altimeter data directly to define the orbits, geoid and dynamic height fields. Altimeter data acquired during the GEOS-3 (1975-76), SEASAT (1978) and GEOSAT (1986-87) Missions were used to form GEM-T3. In order to accommodate the non-gravitational signal mapped by these altimeters, spherical harmonic models of the dynamic height of the ocean surface were recovered for each mission simultaneously with the gravitational field. Herein, all of the dynamic height fields are referenced to a common geoidal model and are tied into the Conventional Terrestrial Reference System established by Satellite Laser Ranging (SLR).

The tracking data utilized in the solution includes more than 1300 arcs of data encompassing 31 different satellites. The observational data base is highly dependent on SLR, but also includes TRANET Doppler, optical, S-Band average range-rate and satellite-to-satellite tracking acquired between ATS-6 and GEOS-3. The tracking data are largely the same as used to develop GEM-T2 with certain important improvements in data treatment and expanded laser coverage. The GEM-T3 model utilized a total of almost 2,650,000 observations.

The 6330 recovered parameters in the GEM-T3 solution include:

- a 50x50 model of the time-invariant geopotential field
- long wavelength coefficients in the dynamic tide model for 12 main tide lines
- spherical harmonic models complete to degree and order 15 of the dynamic height field independently mapped by GEOS-3, SEASAT and GEOSAT
- tracking station coordinates for all sites contributing data to the solution; and
- continuous 5-day average polar motion and A1-UT1 values from 1980 to the end of 1987

These models have undergone extensive error calibration and employ an optimal data weighting technique which insures reliable estimates of the models' uncertainties. This method relies on statistical testing using a subset solution technique. The subset solution testing is based on the premise that the expected mean squares deviation of a subset gravity solution from the overall solution is predicted by the solution covariances. Data weights are iteratively adjusted until this condition is satisfied. It was shown that given the robustness of the data included in the combination solution, calibration of data "groups" was required for accurate results to be obtained.

Further gravity field tests were performed where strong satellite data sets were withheld from the solution (thusly insuring their independence) and the performance of the subset models were compared to error projections based on their calibrated covariances. This testing was made in the space of the observation residuals themselves. These results demonstrate that orbit accuracy projections based on the solution covariances yield reliable estimates for new satellites which are not in the solution.

9.0 REFERENCES

Anderle, R.J., "Doppler Satellite Data Characteristics," Naval Surface Weapons Center Document TR 83-353, October 1983.

Barlier, F., Berger, C., Falin, J., Kockarts, G., and Thuillier, G., "A Thermospheric Model Based on Satellite Drag Data," AERONOMICA ACTA, A-No. 185, 1977.

Barnett, T.P., "Possible Changes in Global Sea Level and Their Causes," *Climate Change*, Vol. 5, 15-38, 1983.

Chao, B.F., "Excitation of the Earth's Polar Motion due to Mass Variations in Major Hydrological Reservoirs," *J. Geophys. Res.*, 93, B11, pp. 13811-13819, 1988.

Chao, B.F., W.P. O'Connor, A.T. Chang, D.K. Hall, and J.L. Foster, "Snow Load Effect on the Earth's Rotation and Gravitational Field, 1979-1985," *J. Geophys. Res.*, 92, B9, pp. 9415-9422, 1987.

Chao, B.F. and W.P. O'Connor, "Global Surface-Water-Induced Seasonal Variations in the Earth's Rotation and Gravitational Field," *Geophys. J.*, 94, pp. 263-270, 1988.

Cheng, M.K., C.K. Shum, R.J. Eanes, B.E. Schutz, and B.D. Tapley, "Long-period Perturbations in Starlette Orbit and Tide Solution," *J. Geophys. Res.*, 95, B6, pp. 8723-8736, 1990.

Christodoulidis, D.C., D.E. Smith, S.M. Klosko, P.J. Dunn, J.W. Robbins, and M.H. Torrence, "Contemporary Plate Motions from LAGEOS: A Decade Later," *Adv. Space Res.*, Vol. 6, No. 9, pp. 41-51, 1986a.

Christodoulidis, D.C., R.G. Williamson, D. Chinn, and R. Estes, " On the Prediction of Ocean Tides for Minor Constituents," Proceedings of the 10th International Symposium on Earth Tides, edited by R. Vieira, pp. 659-678, Conseja Superior de Investigaciones, Madrid, Spain, 1986b.

Christodoulidis, D.C., D.E. Smith, R.G. Williamson, and S.M. Klosko, "Observed Tidal Braking in the Earth/Moon/Sun System," *J. Geophys. Res.*, 93, B6, pp. 6216-6236, 1988.

Eddy, W.F., D.E. Pavlis, J.J. McCarthy, J.A. Marshall, S.B. Luthcke, G. Leung, T.V. Martin, and D.D. Rowlands, "GEODYN II System Description: Vol 1-5," prepared for Space Geodesy Branch, GSFC, September, 1989.

Emery, W.J., G.H. Born, D.G. Baldwin, and C.L. Norris, "Satellite-Derived Water Vapor Correction for Geosat Altimetry," *J. Geophys. Res.*, 95, C3, 2953-2964, 1990.

Figgatte, C. and A. Polesco, "Laser Preprocessor Program User's Guide," Contract Report 5-24300, Task 769, Computer Science Corporation, June, 1982.

Fu, L.L., J. Vasquez and M.E. Parke, "Seasonal Variability of the Gulf Stream from Satellite Altimetry," *J. Geophys. Res.*, 92, pp. 749-754, 1987.

Goad, C., "A Modified Hopfield Tropospheric Refraction Correction Model," paper presented at the Fall Meeting of the American Geophysical Union, December 1974.

Gross, J.E., "Preprocessing Electronic Satellite Observations," Ohio State Contractor's Report, NASA CR 1183, November 1968.

Gutierrez, R. and C.R. Wilson, "Seasonal Air and Water Mass Redistribution Effects on LAGEOS and Starlette," *Geophys. Res. Letters*, 14, 929-932, 1987.

Hotter, F., "Preprocessing Optical Satellite Observations," Ohio State Report 82, Columbus, OH, May 1968.

Jacchia, L.G., "Revised Static Model of the Thermosphere and Exosphere with Empirical Temperature Profiles," Special Report 332, Smithsonian Astrophysical Observ., Cambridge, MA, 1971.

Jekeli, C. and R.H. Rapp, "Accuracy of the Determination of Mean Anomalies and Mean Geoid Undulations from a Satellite Gravity Field Mapping Mission," Report No. 307, Department of Geodetic Science, Ohio State University, Columbus, Ohio, August, 1980.

Kahn, W.D., S.M. Klosko, W.T. Wells, "Mean Gravity Anomalies from a Combination of Apollo/ATS 6 and GEOS-3/ATS 6 SST Tracking Campaigns," *J. Geophys. Res.*, 87, B4, pp. 2904-2918, 1982.

Kaula, W.M., Theory of Satellite Geodesy, Blaisdell, Waltham, MA, 1966.

Koblinsky, C.J., R.S. Nerem, S.M. Klosko, R.G. Williamson, "Observing Large Scale Sea Surface Topography from Space: Part II-Evaluation," Submitted to *J. Geophys. Res.*, 1991

Lerch, F.J., "Error Spectrum of Goddard Satellite Models for the Gravity Field," Geodynamics Branch Annual Report-1984, NASA Tech. Memo. 86223, Greenbelt, MD, August 1985.

Lerch, F.J., "Optimum Data Weighting and Error Calibration for Estimation of Gravitational Parameters," *Bullet. Geodesique*, 65, 44-52, 1991.

Lerch, F.J., S.M. Klosko, R.E. Laubscher, C.A. Wagner, "Gravity Model Improvement Using GEOS-3 (GEM-9 and 10)," *J. Geophys. Res.*, 84, 138, pp. 3897-3915, 1979.

Lerch, F.J., J.G. Marsh, S.M. Klosko, E.C. Pavlis, G.B. Patel, D.S. Chinn, and C.A. Wagner, "An Improved Error Assessment for the GEM-T1 Gravitational Model," NASA Tech. Memo 100713, Greenbelt, MD, November 1988.

Lerch, F.J., Patel, G.B., and Klosko, S.M., "Direct Calibration of GEM-T1 with 1071 5x5 Degree Mean Gravity Anomalies from Altimetry," *Manuscripta Geodaetica*, 16, 141-147, 1991a.

Lerch, F.J., Marsh, J.G., Klosko, S.M., Patel, G.B., Chinn, D.S., Pavlis, E.C., and Wagner, C.A., "An Improved Error Assessment for the GEM-T1 Gravitational Model," *J. Geophys. Res.*, 96, B12, pp. 20023-20040, 1991b.

Levitus, S., "Climatological Atlas of the World Ocean," NOAA Prof. Pap. 13, 173pp, US Govt. Print. Off., Washington, D.C., 1982.

Levitus, S., C.J. Koblinsky, "Fourier Analysis of the Climatological Annual Cycle of Steric Sea Level (0-1000m) of the World Ocean," *J. Mar. Res.*, submitted, 1990.

Lieske, J.H., "Precessional Matrix Based on IAU(1976) System of Astronomical Constants," *Astron. Astrophys.*, 73, 282, 1976.

Marini, J.W. and C.W. Murray, "Correction of Laser Range Tracking Data for Atmospheric Refraction at Elevations Above 10 Degrees," GSFC Report X-591-73-351, Greenbelt, MD, November 1973.

Marsh, J.G. and F.J. Lerch, "Earth Gravity Model Computation at Goddard Space Flight Center," paper presented at the Spring Meeting of the AGU, Baltimore, MD, May, 1989, *EOS*, Vol. 70, p. 301, (abstract), 1989.

Marsh, J.G., F.J. Lerch, B.H. Putney, D.C. Christodoulidis, D.E. Smith, T.L. Felsentreger, B.V. Sanchez, D.E. Smith, S.M. Klosko, E.C. Pavlis, T.V. Martin, J.W. Robbins, R.G. Williamson, O.L. Colombo, N.L. Chandler, K.E. Rachlin, G.B. Patel, S. Bhati, and D.S. Chinn, "An Improved Model of the Earth's Gravitational Field: GEM-T1," NASA Tech. Memo. 4019, pgs. 334, July, 1987.

Marsh, J.G., F.J. Lerch, B.H. Putney, D.C. Christodoulidis, D.E. Smith, T.L. Felsentreger, B.V. Sanchez, S. M. Klosko, E.C. Pavlis, T.V. Martin, J.W. Robbins, R.G. Williamson, O.L. Colombo, D.D. Rowlands, W.F. Eddy, N.L. Chandler, K.E. Rachlin, G.B. Patel, S. Bhati, and D.S. Chinn, "A New Gravitational Model for the Earth from Satellite Tracking Data: GEM-T1," *J. Geophys. Res.*, 93, B6, pp. 6169-6215, 1988.

Marsh, J.G., F.J. Lerch, B.H. Putney, T.L. Felsentreger, B.V. Sanchez, S.M. Klosko, E.C. Pavlis, G.B. Patel, J.W. Robbins, R.G. Williamson, T.L. Engelis, W.F. Eddy, N.L. Chandler, K.E. Rachlin, S. Kapoor, L.E. Braatz, and D.S. Chinn, "The GEM-T2 Gravitational Model," *J. Geophys. Res.*, 95, B13, 22,043-22,071, 1990a.

Marsh, J.G., F.J. Lerch, C.J. Koblinsky, S.M. Klosko, J.W. Robbins, R.G. Williamson, G.B. Patel, "Dynamic Sea Surface Topography, Gravity, and Improved Orbit Accuracies from the Direct Evaluation of SEASAT Altimeter Data," *J. Geophys. Res.*, 95, C8, 13,129-13,150, 1990b.

Melbourne, W. et al., "Project MERIT Standards," Circ. 167, U.S. Naval Observatory, Washington, D.C., 1983.

Miller, L., R.E. Cheney and B.C. Douglas, "GEOSAT Altimeter Observations of Kelvin Waves and the 1986-87 El Nino," *Science*, 239, pp. 52-4, 1988.

Moritz, H., Advanced Physical Geodesy, Abacus, Tunbridge Wells Kent, Kent, England, 1980.

Nerem, R.S., B.D. Tapley, and C.K. Shum, "Determination of the Ocean Circulation Using GEOSAT Altimetry," *J. Geophys. Res.*, 95, C3, 3163-3179, 1990.

Nerem, R.S., C.J. Koblinsky, S.M. Klosko, and R.G. Williamson, "Determining Large-scale Variations in Dynamic Topography Using GEOSAT Altimetry," paper presented at the IUGG, U13, Vienna, Austria, 1991a.

Nerem, R.S., C.J. Koblinsky, S.M. Klosko, and R.G. Williamson, "Observing Large Scale Sea Surface Topography from Space: Part I- Techniques and Initial Results," *J. Geophys. Res.*, submitted 1991b.

Newhall, X.X., J.G. Williams, and J.O. Dickey, "Earth Rotation From Lunar Laser Ranging," JPL Geod. Geophys. Preprint 153, Jet. Prolpul. Lab., Dec. 1986.

O'Toole, J., "CELEST Computer Program for Computing Satellite Orbits," Naval Surface Weapons Center/DL TR-3565, October 1976.

Pattulo, J., W. Munk, R. Revelle, and E. Strong, "The Seasonal Oscillation in Sea Level," *J. Mar. Res.*, 14, pp. 88-155, 1955.

Pavlis, N.K., "Modeling and Estimation of a Low Degree Geopotential Model from Terrestrial Gravity Data," Rep. 386, Dep. of Geod. Sci and Surv., Ohio State University, Columbus, 1988.

Peltier, W.R., "Global Sea Level and Earth Rotation," *Science*, Vol. 240, 895-901, 1988.

Rapp, R.H., "Gravity Anomalies and Sea Surface Heights Derived from a Combined GEOS-3/SEASAT Altimeter Data Set," *J. Geophys. Res.*, 91, E5, pp. 4867-4876, 1986.

Rapp, R.H. and J.Y. Cruz, "Spherical Harmonic Expansion of the Earth's Gravitational Potential to Degree 360 Using 30' Mean Anomalies," The Ohio State University Department of Geodetic Science Report No. 376, Columbus, OH, 1986.

Rapp, R.H. and N.K. Pavlis, "The Development and Analysis of Geopotential Coefficient Models to Spherical Harmonic Degree 360," *J. Geophys. Res.*, 95, B13, pp 21,885-21,912, 1990.

Rapp, R.H., R.S. Nerem, C.K. Shum, S.M. Klosko, R.G. Williamson, "Consideration of Permanent Tidal Deformation in the Orbit Determination and Data Analysis for the TOPEX/Poseidon Mission," NASA Tech. Memo. 100775, January, 1991.

Ray, R.D. and B.V. Sanchez, "Radial Deformation of the Earth by Oceanic Tidal Loading," NASA Tech. Memo. 100743, July, 1989.

Reigber, C., "Representation of Orbital Element Variations and Force Function with Respect to Various Reference Systems," *Bull. Geod.*, 55, pp. 111-131, 1981.

Reigber, Ch., P. Schwintzer, W. Barth, F.H. Massman, J.C. Raimondo, A. Bode, H. Li, G. Balmino, R. Biancale, B. Moynot, J.M. Lemoine, J.C. Marty, F. Barlier, Y. Boudon, "GRIM-4C1,-C2 Combination Solutions of the Global Earth Gravity Field," paper presented at the XVI General Assembly of the European Geophysical Society, Weisbaden, Germany, April, 1991.

Rosborough, G.W., "Satellite Orbit Perturbations Due to the Geopotential," University of Texas, Center for Space Research Report CSR-86-1, January, 1986.

Smith, D.E., R. Kolenkiewicz, P.J. Dunn, M.H. Torrence, J.W. Robbins, S.M. Klosko, R.G. Williamson, E.C. Pavlis, N.B. Douglas, and S.K. Fricke, "Tectonic Motion and Deformation from Satellite Laser Ranging to LAGEOS," *J. Geophys. Res.*, 95, B13, 22,013-22,041, 1990.

Stephenson, F.R. and L.V. Morrison, "Long-Term Changes in the Rotation of the Earth: 700 B.C. to A.D. 1980," *Philos. Trans. R. Soc. London*, Ser. A., 313, 47, 1984.

Tapley, B.D., R.S. Nerem, C.K. Shum, J.C. Ries and D.N. Yuan, "Determination of the General Ocean Circulation from a Joint Gravity Solution," *Geophys. Res. Lett.*, 15, 1109-1112, 1988.

Wahr, J.M., "The Tidal Motions of a Rotating, Elliptical, Elastic and Oceanless Earth," Ph.D. Thesis, Univ. Of Colorado, Boulder, 1979.

Wahr, J.M., "Body Tides on an Elliptical Rotating, Elastic and Oceanless Earth," *Geophys. J. R. Astron. Soc.*, 64,677, 1981.

Wyrtki, K., "Fluctuations of the Dynamic Topography in the Pacific Ocean," *J. Phys. Oceanogr.*, 5, pp. 450-459, 1975.

Wyrtki, K. and W.G. Leslie, "The Mean Annual Variation of Sea Level in the Pacific Ocean," Tech. Rept. HIG-80-5-, 159 pp., Inst. for Geophys., Univ. of Hawaii, Honolulu, 1980.

Yoder, C.F., J.G. Williams, M.E. Parke, "Tidal Variations of Earth Rotation," *J. Geophys. Res.*, 86, B2, pp. 881-891, 1981.

Yoder, C.F. et al., "Secular Variation of the Earth's Gravitational Harmonic J2 Coefficient from LAGEOS and Nontidal Acceleration of the Earth Rotation," *Nature*, 303, p. 757, 1983.

VonBun, F.O., W.D. Kahn, W.T. Wells, and T.D. Conrad, "Determination of 5 x 5 Degree Gravity Anomalies Using Satellite-to-Satellite Tracking Between ATS-6 and Apollo," *Geophys. J. R. Astron. Soc.*, 61, pp. 645-658, 1980.

10. ACKNOWLEDGEMENTS

The authors wish to dedicate this paper to the memory of James G. Marsh, who for many years was one of the leaders of the gravity modeling group at Goddard Space Flight Center. His contribution to these efforts over the last twenty-five years through his management style, science instincts, and kind and generous ways, makes him very much missed.

The authors wish to thank the Centre National D'Etudes Spatiales in France for making the DORIS tracking data taken on SPOT-2 available to us. We wish to thank Professor Richard Rapp at The Ohio State University for his efforts in processing the surface gravimetry, and the capable group at the Center for Space Research at the University of Texas for providing their preliminary gravity fields to us. The assistance of Dr. Chet Koblinsky in his help with the interpretation of the dynamic height fields is also acknowledged.

We would also like to acknowledge the important support we have received from the TOPEX Project enabling us to develop advanced gravity models for TOPEX/Poseidon. Likewise, the authors are indebted to the Geodynamics, the Geophysics and the Biogeochemistry Branches at NASA Headquarters for their support of this work.

We wish to thank Susan Poulose (RMS) for her programming and analysis support for special functions, Susie Blackwell (RMS) for benchmarking the GEODYN computer systems, and Shelly Rowton (STX) for GEODYN program support. Masahiro Nishihama and Richard Ullman (both of STX) are to be thanked for their support on the ERODYN and SOLVE programs respectively. Nikita Zelensky (STX) helped test the clone gravity model errors through simulations on the TOPEX orbit and we are indebted to him for these efforts.

APPENDIX A

ANALYSIS OF TERRESTRIAL GRAVITY DATA

by Nikolaos K. Pavlis

Surface gravity information was incorporated in the GEM-T3 gravitational model in the form of normal equations for the complete set of harmonic coefficients up to degree and order 50, developed on the basis of terrestrial gravity data. The modeling and estimation techniques employed in the formation of the surface gravity normals closely followed the procedures discussed in detail by Pavlis [1988]. The following paragraphs provide a brief description of the gravity anomaly data used in this analysis and emphasize on certain aspects of the modeling which were modified, as well as on the presentation of the results obtained. Additional details can be found in [Rapp, Wang and Pavlis, 1991].

The 1° x 1° Mean Anomaly Data Used in the Surface Gravity Normals

The fundamental terrestrial 1° x 1° mean gravity anomaly dataset used in this analysis is designated " OSU October 1990 " [Yi and Rapp, 1991] and represents the latest update of the global anomaly database maintained at The Ohio State University. With respect to its predecessor (OSU July 1989 - [Kim and Rapp, 1990]), it is improved by the incorporation of 944 1° x 1° mean anomalies covering areas in Asia. The OSU July 1989 dataset, on the other hand, is substantially better than the June 1986 file [Despotakis, 1986] which was originally used for the normal equations formed by Pavlis [1988] and used in PGS-3337 and PGS-3520. For example, improved gravity data for Africa, included in the July 1989 dataset, have replaced corresponding values in the June 1986 file, which were identified to be contaminated by significant systematic errors [Pavlis, 1988, section 5.3.2]. Statistics related to the mean anomalies of the October 1990 dataset are given in Table A.1, while the geographic distribution of the available data is shown in Figure A.1.

Table A.1. Statistics of the 1° x 1° Mean Free-air Anomalies in the OSU October 1990 Database[1]

	Gravity Measurements	Geophysical Prediction	Combined
Number of values	45932	4870	50802
Percentage of area	79.2	6.6	85.7
Minimum value	-270	-123	-270
Maximum value	303	127	303
Mean value	-0.5	-1.0	-0.5
RMS value	27.6	25.3	27.4
RMS standard deviation	12.0	17.3	12.5

[1] Gravity anomaly units are mgals; mean and RMS values are weighted by the area of each 1° x 1° block.

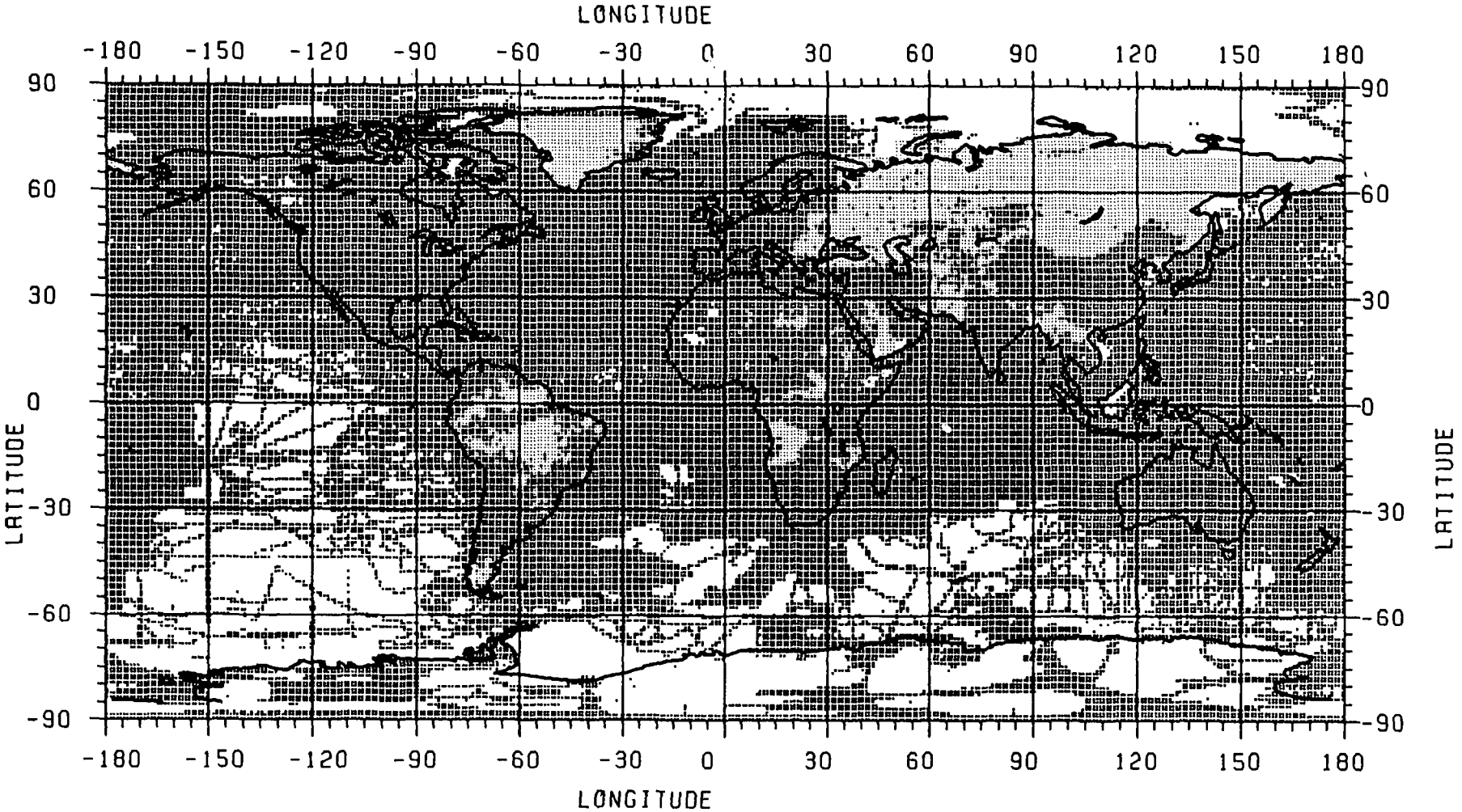

Figure A.1. Geographic Distribution of the 50802 1 x 1 Mean Free-air Anomalies in the OSU October 1990 Database. "x" Identifies Values Originating From Gravity Measurements (45932) and "." Geophysically Predicted Values (4870).

The 45932 1° x 1° mean anomalies of the October 1990 database originating from actual measurements (denoted $\bar{\Delta}g^{OCT\,90}$) require a number of systematic corrections before they can be used as input to the formation of normal equations. These corrections are [Pavlis, 1988]:

(i) Atmospheric correction (δg_A)
(ii) Ellipsoidal corrections (ϵ_h, ϵ_γ, ϵ_p)
(iii) Second-order vertical gradient of normal gravity correction (δg_h^2)
(iv) Gravity formula transformation (δg_γ).

The specific formulation used to evaluate 1° x 1° area-mean values of the above correction terms is given in detail in [ibid, section 2.3]. The OSU89B geopotential model [Rapp and Pavlis, 1990], complete to degree 180, was used to evaluate 1° x 1° area-mean values of the ellipsoidal corrections (denoted IE_h, IE_γ, IE_p). The transformation of the October 1990 anomalies from the GRS 1967 gravity formula to which they refer, to the gravity formula implied by the "GEM-T3" constants (see [Pavlis, 1988, p.60]) was performed as explained in [ibid, pp. 60-61]. Denoting by $\bar{\Delta}g_{ij}^c$ the corrected anomaly one has:

$$\bar{\Delta}g_{ij}^c = \bar{\Delta}g_{ij}^{OCT\,90} + (\delta gs)_{ij} \tag{A1}$$

where the total correction $(\delta gs)_{ij}$ is:

$$(\delta gs)_{ij} = [\delta g_A - (IE_h + IE_\gamma + IE_p) + \delta g_h^2 + \delta gr]_{ij} \tag{A2}$$

As for the 4870 geophysically predicted anomalies of the October 1990 database, the analysis made by Pavlis [ibid] has demonstrated that such values are in many cases systematically biased with respect to anomalies implied by satellite-only global geopotential models [ibid, section 5.3.2]. Pavlis and Rapp [1990] have shown that a preferable alternative to their use, is the use of synthetic anomalies obtained from the lower-degree harmonics of a satellite-only model augmented by higher harmonics of the topographic/isostatic induced potential. Accordingly, the harmonics of GEM-T2 [Marsh et al., 1990] up to degree 9 were augmented by the harmonics of a topographic/isostatic expansion designated "SET3" in the study by Pavlis and Rapp [1990, p. 373] from degree 10 to degree 50 to form a "combined" set of coefficients $\bar{C}nm$. A global set of 1° x 1° $\bar{\Delta}g^{TI}$ was then evaluated based on $\bar{C}nm$ as follows:

$$(\bar{\Delta}g^{TI})_{ij} = \frac{1}{\Delta\sigma_i}\frac{GM}{(r_i^E)^2}\sum_{n=2}^{50}(n-1)\left(\frac{a}{r_i^E}\right)^n\sum_{m=-n}^{n}\bar{C}nm\;\bar{IY}_{nm}^{ij} \tag{A3}$$

where i=0,1,...,179 and j=0,1,...,359. (Notation definitions can be found in [Pavlis, 1988]).

A merging process was performed next whereby a $\bar{\Delta}g^{TI}$ value was used to provide the mean anomaly estimate for a given 1° x 1° block if:

- The October 1990 estimate for the block originates from geophysical prediction, or,
- No estimate is available in the October 1990 database and the 1° x 1° mean elevation of the block is positive.

In this manner the resulting merged file (designated SETA) maintains the 45932 values of the October 1990 file, which originate from actual measurements, while in addition contains 8116 $\bar{\Delta}g^{TI}$ values (8.2% of the Earth's area) occupying land only blocks. The $\bar{\Delta}g^{TI}$ values in SETA were assigned standard deviation equal to 20 mgals, based on the accuracy assessment for these

values discussed by Pavlis and Rapp [1990]. Also, the minimum standard deviation for any anomaly in SETA regardless of source was set to 2 mgals, to avoid over optimistic accuracy estimates. In total, SETA contains 54048 anomalies covering 87.3% of the Earth's area. The geographic distribution of these anomalies is shown in Figure A.2.

The $\overline{\Delta g}^{C}$ of SETA represent surface mean free-air anomalies in the Molodensky sense. Their frequency content is not uniform worldwide but depends on factors such as the distribution of gravity measurements inside each 1° x 1° block and the averaging process used to estimate each mean value. In contrast, $\overline{\Delta g}^{TI}$ are formally interpreted as mean free-air anomalies continued to the surface of the reference ellipsoid, and their spectral content extends (by definition) only up to harmonic degree 50. Extensive analysis discussed by Pavlis [1988, section 5.2.5] has shown that the leakage of power from the higher-frequency component of $\overline{\Delta g}^{C}$, to the lower-frequency coefficients being solved for, from the **incomplete** set of discrete mean anomalies, can be minimized by removing the higher-frequency content of $\overline{\Delta g}^{C}$ (above degree 50) prior to the formation of the normal equations. The high-frequency component, $\overline{\delta g}_{HF}$, can be evaluated in terms of 1° x 1° mean values, based on an existing high-degree geopotential model such as OSU89B [Rapp and Pavlis, 1990]. In such procedure, two issues need careful consideration:

(1) The harmonic coefficients used to evaluate $\overline{\delta g}_{HF}$ should represent as precisely as possible the higher-frequency content of the data which will be used in the normal equations.

(2) $\overline{\delta g}_{HF}$ must be evaluated at the same level at which $\overline{\Delta g}^{C}$ refers (the topographic surface of the Earth).

The first requirement was satisfied in this analysis by developing a modified "OSU89B" type of model (complete to degree 360) that accounts for the additional land values in SETA, which were not available when OSU89B was developed. The specific procedure used to develop this modified model (designated 89B) is described in [Rapp, Wang and Pavlis, 1991]. To satisfy the second requirement, two alternative techniques were implemented and tested. Briefly described, the first technique "upward" continues $\overline{\delta g}_{HF}$ from the ellipsoid to the topographic surface (where $\overline{\Delta g}^{C}$ refers), while in the second technique $\overline{\Delta g}^{C}$ is "downward" continued to the ellipsoid and $\overline{\delta g}_{HF}$ is subsequently removed from the downward continued values. Both techniques require the analytic continuation terms g_1 [Wang, 1988], but the use of these terms in the implementation of each technique is different. Details on these aspects can be found in [Rapp, Wang and Pavlis, 1991]. Normal equations to degree 50 were formed considering both alternatives, and although in theory the two continuation procedures are equivalent, comparisons described in [ibid] indicated that the second method yields slightly better results. Hence, the second procedure will only be considered next, where the 1° x 1° mean anomalies input to the least-squares adjustment constitute a file designated SET2. These anomalies, denoted $\overline{\Delta g}_{ij}^{(2)}$, were defined by:

$$\overline{\Delta g}_{ij}^{(2)} = \begin{cases} \overline{\Delta g}_{ij}^{C} + (\overline{g}_1 - \overline{\delta g}_{HF})_{ij} \\ \overline{\Delta g}_{ij}^{TI} \end{cases} \qquad \text{(A4)}$$

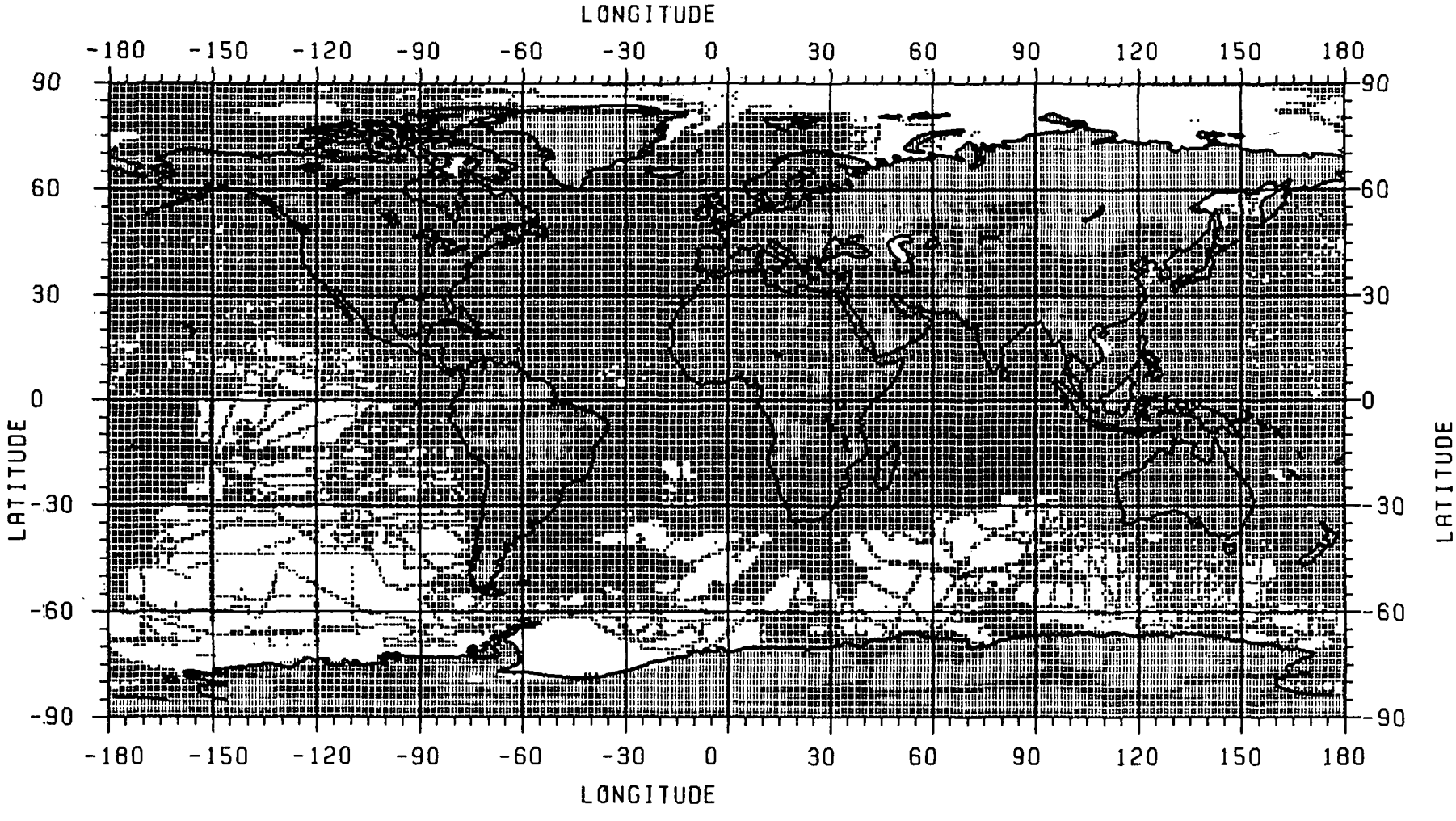

Figure A.2. Geographic Distribution of the 54048 1 x 1 Mean Free-Air Anomalies in SET A. "x" Identifies Values Originating From Gravity Measurements (45932) and "1" $\overline{\Delta}g^{TI}$ Values (8116).

depending on whether they originate from actual gravity measurements or from topographic/isostatic information. In equation (A4), $\overline{g}_1$ denotes 1° x 1° average of the analytic continuation term, and $\overline{\delta g}_{HF}$ is evaluated based on the 89B coefficients by:

$$(\overline{\delta g}_{HF})_{ij} = \frac{1}{\Delta\sigma_i} \frac{GM}{(r_i^E)^2} \sum_{n=51}^{360} (n-1) \left(\frac{a}{r_i^E}\right)^n \sum_{m=-n}^{n} \overline{C}_{nm}^{89B'} \overline{IY}_{nm}^{ij} \qquad \text{(A5)}$$

In Table A.2, statistics related to the anomalies of SET2 are given. The distribution of the data in SET2 is obviously identical to that of SETA shown in Figure A.2.

Table A.2. Statistics of the 1° x 1° Mean Anomalies in File SET2 Used in the Normal Equations Formed[1]

Number of values	54048
Percentage of area	87.3
Minimum value	-199.4
Maximum value	141.2
Mean value	-0.1
RMS value	19.2
RMS standard deviation	13.0

[1] Gravity anomaly units are mgals; mean and RMS values are weighted by the area of each 1° x 1° block.

Estimation of Geopotential Coefficients From Surface Gravity Data

The anomalies $\overline{\Delta g}_{ij}^{(2)}$ defined in equation (A4) lead to the following observation equation for the geopotential coefficients:

$$v_{ij}^{(2)} = \frac{1}{\Delta\sigma_i} \frac{GM}{(r_i^E)^2} \sum_{n=0}^{50}{}' (n-1) \left(\frac{a}{r_i^E}\right)^n \sum_{m=-n}^{n} \overline{C}_{nm}^{T} \overline{IY}_{nm}^{ij} - \overline{\Delta g}_{ij}^{(2)} \qquad \text{(A6)}$$

where $v_{ij}^{(2)}$ is the residual associated with the observation $\overline{\Delta g}_{ij}^{(2)}$ and $\overline{C}_{nm}^{T}$ represent the adjusted geopotential coefficients obtained on the basis of surface gravity data alone (even zonal harmonic coefficients are remainders after subtraction of the coefficients of the normal potential). The anomalies $\overline{\Delta g}_{ij}^{(2)}$ refer to the surface of the reference ellipsoid and r_i^E is the distance from the geocenter to the point on the ellipsoid at the mid latitude of the (i,j)-th block (and thus possesses equatorial symmetry). The prime of the summation in equation (A6) indicates absence of the first-degree terms. The inclusion of the zeroeth-degree term is necessitated by the fact that the incomplete set of discrete area-mean values used, gives rise to covariances between the $\overline{C}_{oo}^{T}$ and the rest of the coefficients, which must be taken into account [Pavlis, 1988]. The totality of observation equations of the form (A6) for all available $\overline{\Delta g}_{ij}^{(2)}$, is written in matrix form as:

$$V = A\hat{X} - L_b \qquad \text{(A7)}$$

where A is the design matrix, $\hat{X}$ is the vector containing $\overline{C}_{nm}^{T}$, L_b the vector of observations $\overline{\Delta g}_{ij}^{(2)}$ and V the vector of residuals $v_{ij}^{(2)}$. Minimization of the weighted norm of the residuals (V^TPV), under the condition (A7), yields the normal equation system:

$$(A^TPA)\ \hat{X} = A^TPL_b \tag{A8}$$

where P is the weight matrix defined by:

$$P = \sigma_o^2 \sum_{Lb}^{-1} \tag{A9}$$

with σ_o^2 being the a-priori variance of unit weight (taken to be 1) and $\sum_{L_b}$ the variance-covariance matrix of observations. The least-squares estimate $\hat{X}$ is given by:

$$\hat{X} = (A^TPA)^{-1}A^TPL_b \tag{A10}$$

The a-posteriori variance of unit weight is:

$$\hat{\sigma}_o^2 = \frac{V^TPV}{(d.f.)} \tag{A11}$$

where (d.f.) are the degrees of freedom, while the error covariance matrix of the estimates $\hat{X}$ is:

$$\sum_x = \sigma_o^2 (A^TPA)^{-1} \tag{A12}$$

For the purpose of combining the normal equations obtained here with corresponding normals obtained from the analysis of satellite perturbations, as well as with normals from altimeter data, it is critical that $\sum_{L_b}$ properly reflects the accuracy of the surface gravity data. At present, it is not possible to accurately estimate the full error covariance matrix of the gravity anomalies, while in addition, even simplistic error covariance models would make the formation of normal equations practically impossible (for degrees of expansion equal to 50 or higher), due to computational limitations. Accordingly, following previous experiences [Rapp and Pavlis, 1990], a diagonal $\sum_{L_b}$ matrix was used, but the original error estimates of the anomalies were modified in an attempt to compensate for the neglected error covariances. Denoting by $\sigma_{ij}{}^o$ the standard deviations of the anomalies in SET2 and by $\sigma_{ij}{}^m$ the modified values used to form $\sum_{L_b}$, the following relationship was imposed:

$$\max\ (8, 2\sigma_{ij}{}^o) \le \sigma_{ij}{}^m \le \min\ (16, 2\sigma_{ij}{}^o) \tag{A13}$$

This modification yields a ratio 4:1 between maximum and minimum weights and corresponds (approximately) to the weighting scheme used by Rapp and Pavlis [ibid] for the 30'x 30' mean anomalies. The RMS modified standard deviation is 13.7 mgals. According to the above, normal equations were formed, and the corresponding terrestrial-only solution was obtained. This solution is designated V2. In Table A.3, statistics related to this solution are given.

Table A.3. Statistics Related to the Terrestrial-Only Gravity Solution V2

Number of Anomalies	54048
Number of Coefficients	2598
Degrees of Freedom	51450
Minimum Residual (mgal)	-117.7
Maximum Residual (mgal)	187.5
Mean Residual (mgal)	0.0
RMS Residual (mgal)	7.3
∂_o^2	0.303
Number of |resid| > 7 mgal	11118

In Figure A.3 the locations of the 11118 residuals from V2 which exceed in magnitude 7 mgals are shown. It is clear that the solution fits well the input data over well surveyed (gravimetrically) continental areas (North America, Australia, Europe and most of Africa), while most of the large residuals occur over oceanic areas. This is primarily due to the incompatibility between the high-frequency component of the surface anomalies over the ocean, with the corresponding component of the altimetry-derived anomalies that are used in the evaluation of the "modified OSU89B" coefficients (see also [Pavlis, 1988]). It should be emphasized here that the residuals from the surface gravity solution, provide mostly a "goodness-of-fit" measure of the estimated coefficients to the input data. Long-wavelength errors that may be present in the surface anomalies cannot be detected without the incorporation of superior independent information from satellite-derived normals.

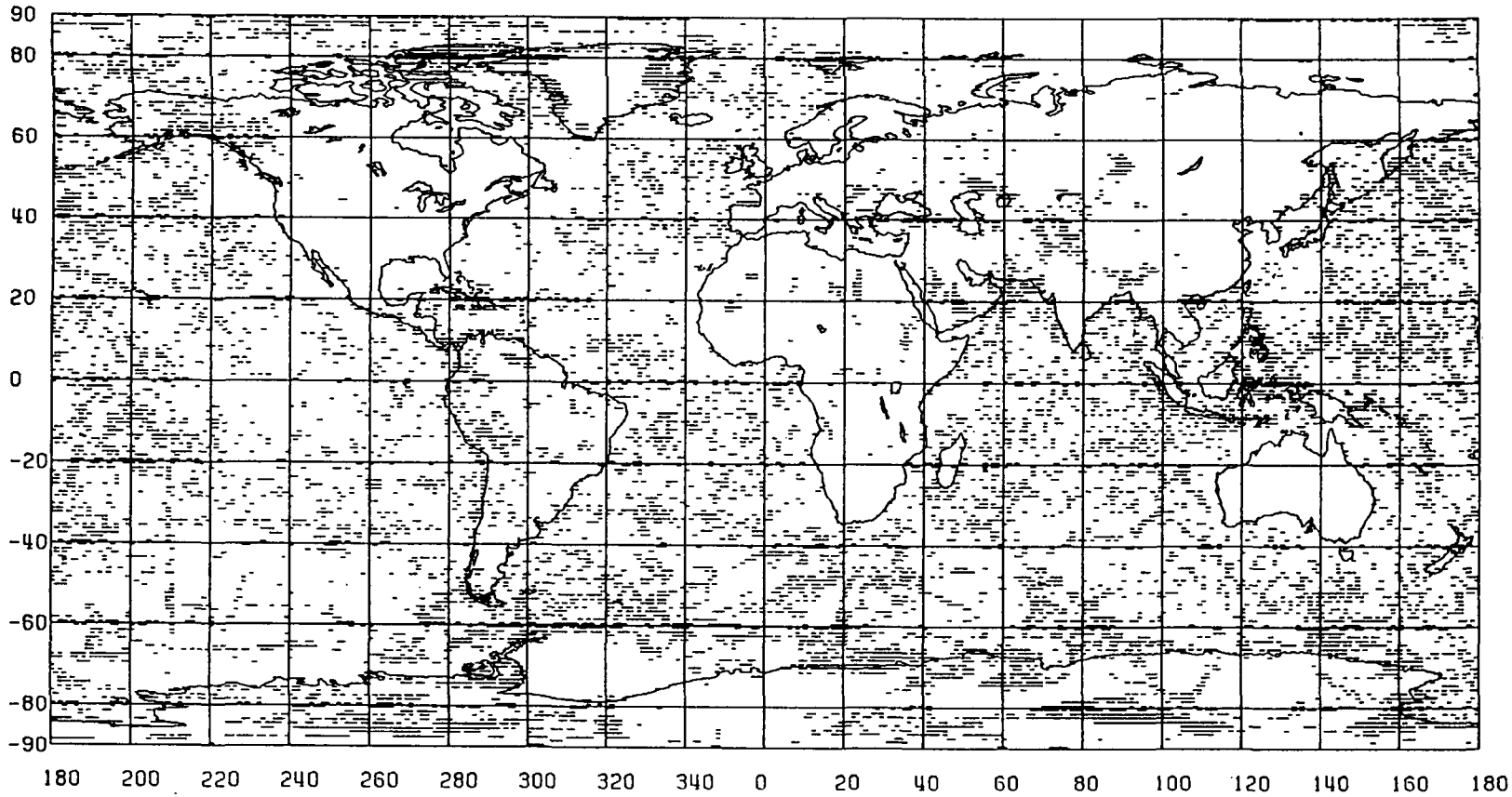

Figure A.3. Location of 11118 Residuals From the Solution V2 Whose Magnitude Exceeds 7 mgals.

Acknowledgements

The research described in this Appendix was supported through NASA Grant No. NAG-5-781 with the Ohio State University Research Foundation, Project No. 718266. This grant is administered through NASA/Goddard Space Flight Center with Barbara Putney as Technical Officer.

The computations described were carried out at the Ohio State University using the computer facilities of Academic Computing Services and the Ohio Supercomputer Center.

References

Despotakis, V., "The Development of the June 1986 1° x 1° and the August 1986 30' x 30' Terrestrial Mean Free-Air Anomaly Data Bases," Internal Report, Dep. of Geod. Sci. and Surv., Ohio State Univ., Columbus, 1986.

Kim, J., and R. Rapp, "The Development of the July 1989 1° x 1° and 30' x 30' Terrestrial Mean Free-Air Anomaly Data Bases," *Rep. 403*, Dep. of Geod. Sci. and Surv., Ohio State Univ., Columbus, 1990.

Marsh, J.G., F. J. Lerch, B. H. Putney, T. L. Felsentreger, B. V. Sanchez, S. M. Klosko, E. C. Pavlis, G. B. Patel, J. W. Robbins, R. G. Williamson, T. L. Engelis, W. F. Eddy, N. L. Chandler, K. E. Rachlin, S. Kapoor, L. E. Braatz, and D. S. Chinn, "The GEM-T2 Gravitational Model," *J. Geophys. Res.*, 95, B13, 22-043-22,071, 1990

Pavlis, N. K., "Modeling and Estimation of a Low Degree Geopotential Model from Terrestrial Gravity Data," *Rep. 386*, Dep. of Geod. Sci. and Surv., Ohio State Univ., Columbus, 1988.

Pavlis, N. K., and R. H. Rapp, "The Development of an Isostatic Gravitational Model to Degree 360 and Its Use in Global Gravity Modeling," *Geophys. J. Int., 100*, 369-378, 1990.

Rapp, R. H., and N. K. Pavlis, "The Development and Analysis of Geopotential Coefficient Models to Spherical Harmonic Degree 360," *J. Geophys Res.*, 95, B13, 21, 885-21, 911, 1990.

Rapp, R. H., Y. M. Wang, and N. K. Pavlis, "The Ohio State 1991 Geopotential and Seas Surface Topography Harmonic Coefficient Models," Report 410, Dep. of Geod. Sci. and Surv., Ohio State Univ., Columbus, August 1991.

Yi, Y., and R. H. Rapp, "The October 1990 1° x 1° Mean Anomaly File Including an Analysis of Gravity Information from China," Internal Report, Dep. of Geod. Sci. and Surv., Ohio State Univ., Columbus, February 1991.

Wang, Y. M., "Downward Continuation of the Free-Air Gravity Anomalies to the Ellipsoid Using the Gradient Solution, Poisson's Integral and Terrain Correction: Numerical Comparison and the Computations," *Rep. 393*, Dep. of Geod. Sci. and Surv., Ohio State Univ., Columbus, 1988.

REPORT DOCUMENTATION PAGE

Form Approved
OMB No. 0704-0188

1. AGENCY USE ONLY *(Leave blank)*	2. REPORT DATE	3. REPORT TYPE AND DATES COVERED
	January 1992	Technical Memorandum

4. TITLE AND SUBTITLE
Geopotential Models of the Earth From Satellite Tracking, Altimeter and Surface Gravity Observations: GEM-T3 and GEM-T3S

5. FUNDING NUMBERS

6. AUTHOR(S)
F.J. Lerch, R.S. Nerem, B.H. Putney, T.L. Felsentreger, B.V. Sanchez, S.M. Klosko, G.B. Patel, R.G. Williamson, D.S. Chinn, J.C. Chan, K.E. Rachlin, N.L. Chandler, J.J. McCarthy, J.A. Marshall, S.B. Luthcke, D.W. Pavlis, J.W. Robbins, S. Kapoor, E.C. Pavlis

7. PERFORMING ORGANIZATION NAME(S) AND ADDRESS(ES)
NASA-Goddard Space Flight Center
Greenbelt, Maryland 20771

8. PERFORMING ORGANIZATION REPORT NUMBER
92B00037

9. SPONSORING/MONITORING AGENCY NAME(S) AND ADDRESS(ES)
National Aeronautics and Space Administration
Washington, D.C. 20546-0001

10. SPONSORING/MONITORING AGENCY REPORT NUMBER
TM 104555

11. SUPPLEMENTARY NOTES
Authors Lerch, Nerem, Putney, Felsentreger, Sanchez: NASA/GSFC, Greenbelt, Maryland 20771. Authors Klosko, Patel, Williamson, Chinn, Chan, Rachlin, Chandler, McCarthy, Marshall, Luthcke, D.W. Pavlis, Robbins, and Kapoor: Hughes STX, Lanham, Maryland, 20706. Author E.C. Pavlis: University of Maryland, Department of Astronomy, College Park, Maryland 20740.

12a. DISTRIBUTION/AVAILABILITY STATEMENT
Unclassified - Unlimited
Subject Category 46

12b. DISTRIBUTION CODE

13. ABSTRACT *(Maximum 200 words)*

Improved models of the Earth's gravitational field have been developed from conventional tracking data (GEM-T3S) and from a combination of satellite tracking, satellite altimeter and surface gravimetric data (GEM-T3). This combination model represents a significant improvement in the modeling of the gravity field at half-wavelengths of 300 km and longer. Both models are complete to degree and order 50. The GEM-T3 model provides more accurate computation of satellite orbital effects as well as giving superior geoidal representation from that achieved in any previous Goddard Earth Model. A description of the models, their development and an assessment of their accuracy is presented. The GEM-T3 model used altimeter data from GEOS-3 (1975-76), Seasat (1978) and Geosat (1986-87) in estimating the orbits, geoid and dynamic height fields. Other satellite tracking data are largely the same as was used to develop GEM-T2, but contain certain important improvements in data treatment and expanded laser tracking coverage. Over 1300 arcs of tracking data from 31 different satellites have been used in the solution. Reliable estimates of the model uncertainties via error calibration and optimal data weighting techniques are discussed.

14. SUBJECT TERMS
Geodesy, Gravity, Sea Surface Topography, Satellite Orbits

15. NUMBER OF PAGES
128

16. PRICE CODE

17. SECURITY CLASSIFICATION OF REPORT	18. SECURITY CLASSIFICATION OF THIS PAGE	19. SECURITY CLASSIFICATION OF ABSTRACT	20. LIMITATION OF ABSTRACT
Unclassified	Unclassified	Unclassified	